New Applications for Real-Time Three-Dimensional Echocardiography

Ashraf Mohammed Anwar Ali

ISBN : 978-0-615-32933-8
Cover : Ashraf Mohammed Anwar Ali
Lay out : Ashraf Mohammed Anwar Ali
Illustrations : Ashraf Mohammed Anwar Ali

Printed by Multichoice Est.

New Applications for Real-Time Three-Dimensional Echocardiography

Nieuwe toepassingen van 3D echocardiografie

Thesis

to obtain the degree of Doctor from the
Erasmus University Rotterdam
by command of the
Rector Magnificus

Prof.dr. H.G. Schmidt

and in accordance with the decision of the Doctorate Board

The public defence shall be held on

Wednesday, November 25 2009 at 15.30 h.

By

Ashraf Mohammed Anwar Ali
born at El-Minia, Egypt

Doctoral Committee

Promoter: Prof.dr. M.L. Simoons.

Other members: Prof.dr. N. de Jong
Prof.dr.ir. H. Boersma
Prof.dr. A.C. van Rossum

Copromoter: Dr. F.J. ten Cate

Financial support by the Netherlands Heart Foundation for the publication of this thesis is gratefully acknowledged.

To

Soul of My Parents

Who were:

- The Source Of Morals And Goodness
- The Lovely Heart
- The River Of Kindness And Mercy

My Pray To Be Together In Paradise

****

Table of Contents

CHAPTER 1

GENERAL INTRODUCTION AND OUTLINE OF THE THESIS

Ashraf M. Anwar; MD, MSC

Department of Cardiology, Thoraxcenter,
Erasmus University Medical Center, Rotterdam, The Netherlands
Department of Cardiology, Al-Hussein University Hospital, Al-Azhar University, Cairo, Egypt

Background

Conventional two-dimensional echocardiography (2DE) has been established as the most widely diagnostic tool in clinical cardiology practice. Its application helps in morphological and functional assessment of cardiac chambers and valves. The advancement in technology of echo machines and its software analysis minimized many difficulties and limitations. However, 2DE application still carries many limitations. It requires mental conceptualization of a series of multiple orthogonal planer or tomographic images into an imaginary multidimensional reconstruction for better understanding of complex intracardiac structures and their spatial relation with surroundings [(1)]. Many of 2DE formula used for volume quantification and ejection fraction calculation especially for left ventricle are based on geometric assumption that may not true providing varied results in the setting of chamber dilatation or distortion and in the presence of regional wall motion abnormalities [(2)]. Interobserver variability for 2DE images interpretation is still due to different ways of data interpolation especially for measurement of mitral and aortic valve orifice area [(3,4)]. These limitations encourage numerous investigators to obviate it by the attempt to obtain three-dimensional images. Three-dimensional echocardiography was developed since more than 15 years provide more accurate assessment of ventricular volume, mass and function and provide a more complete view of the valves. Despite these advantages, it remained a research tool due to many limitations like electrocardiographic and respiratory gating, motion artifacts, time consuming offline analysis and reconstruction. Over the last few years, the advances in transducer and computer software technology led to enhancement of real-time three-dimensional echocardiography (RT3DE) to be applied for clinical utility. The recently developed matrix array transducer consists of approximately 3,000 firing elements improved the contrast resolution and penetration. By this transducer, the entire heart image could be obtained by a pyramidal full-volume acquisition of four cardiac cycles. The development in software made the data off-line analysis faster and easier.

Clinical Application

Numerous application of RT3DE have been proposed and well studied. It allows accurate assessment of ventricular volume and ejection fraction comparable to angiography, CT and MRI [(5-7)]. It was also applied for accurate and feasible evaluation of left ventricular mass among patients with a broad range of cardiac diseases [(8,9)]. Many studies showed feasibility of RT3DE for assessment of right ventricular volume and function [(10,11)]. The other major area in which RT3DE has been used for anatomical assessment is in congenital heart disease with considerable evidence of the superiority of it over 2DE [(12,13)]. Through RT3DE imaging planes and projections of the interatrial septum, accurate assessment of atrial septal defect including localization, number, size and rims could be obtained [(14)]. This assessment helps in selection of therapeutic strategy either surgical or transcatheter closure [(15)]. RT3DE application for assessment of ventricular septal defect is encouraging [(16,17)]. RT3DE application in valvular heart disease became standard due to its more feasibility and accuracy than 2DE especially for mitral valve assessment. By its enface views, full anatomical description of the mitral valve annulus, subvlvular apparatus, leaflet surface, tethering distances and tenting volumes could be obtained [(18-20)]. It helps in accurate calculation of mitral valve area comparable to catheterization with low interobserver and intraobserver variability [(21,22)]. The qualitative and quantitative assessment of RT3DE expands its use before and after mitral valvuloplasty and before surgical treatment [(23).]

Outline of this thesis

The aim of this thesis was to expand the use of RT3DE for anatomical and functional assessment of other important cardiac structures little or not studied before. It also discussed the feasibility and clinical applicability of RT3DE assessment of these structures.

Chapter 2. The study provided the actual description of the tricuspid valve annulus morphology as seen by RT3DE. Its shape was evident as an oval-shaped and not completely circular. Measurement of tricuspid annular diameter by 2DE was nearly matched with the minor diameter by RT3DE and significantly smaller than the major diameter. Through the ability to study the cyclic changes of the annulus area and diameter during systole and diastole, the annular function could be evaluated by fractional area change and fractional shortening.

Chapter 3. The study compared the measurement of tricuspid annulus area and diameter by RT3DE and MRI. Both techniques were well correlated and comparable. It was concluded that 2DE measurement of tricuspid annuls diameter could not be relied on due to underestimation compared to MRI and RT3DE. Annular function was correlated with the right ventricular systolic function, and thus it can be used as a marker of right ventricular function.

Chapter 4. The study described the use of RT3DE for evaluation of rheumatic tricuspid valve stenosis and assessment of its severity. Through RT3DE enface view, a detailed morphological assessment of mobility, thickness and calcification of all tricuspid valve leaflets. The unique RT3DE functional assessment of the valve could also be obtained through measurement of valve orifice area, and the three commissural widths.

Chapter 5. The study aimed to apply RT3DE for quantitative and qualitative assessment of the normal tricuspid valve and to standardize the normal values. The qualitative assessment included morphologic description of the three leaflets shape, position and their relation to each other and to the surrounding structures. The quantative assessment included measurements of tricuspid valve area, commissural width, tricuspid annular area and diameter. This paper described inconsistent findings in the echocardiographic textbooks on TV leaflet identification and set a new gold standard regarding the identification of each leaflet in each 2DE views.

Chapter 6. The study explained the feasibility and reliability of RT3DE for assessment of the true mitral annulus area and diameter. Its shape was seen as D-shaped and not completely circular. MRI measurements of mitral annulus were used as a gold standard to compare between 2DE and RT3DE measurements. It showed underestimation of 2DE while RT3DE was superior to it and comparable to MRI. The accuracy of RT3DE measurements was obtained with good interobserver and intraobserver agreements

Chapter 7. The morphological and functional changes of mitral annulus in both dilated and hypertrophic cardiomyopathy were described compared to normal subjects. The annulus increased in size and became flat due to over stretching in both types. Assessment of mitral annulus function by RT3DE calculation of fractional area changes and fractional shortening showed augmented function in hypertrophic cardiomyopathy and impaired in dilated cardiomyopathy. RT3DE measurements were comparable with MRI measurements with good interobserver agreement.

Chapter 8. The study was designed to apply a new RT3DE score for evaluation of mitral valve stenosis. By this score, each part of the two leaflets could be assessed separately regarding mobility, thickness, and calcification if any. Subvalvular apparatus affection was included in the score by assessment of chordal mobility, thickness nd separation at three levels. The study described the value of this score application for patients before percutaneous mitral valvuloplasty compared it with the standard 2DE Wilkins' score. The new RT3DE score is simple, less subjective with less interobserver variability. Its application added more valuable information needed before valvuloplasty and could predict the outcome (results and complications).

Chapter 9. The study clarified the role of RT3DE for anatomic description of right ventricular outflow tract and pulmonary valve. The morphologic assessment of outflow tract, pulmonary valve annulus, pulmonary valve, and proximal pulmonary artery was achieved in a considerable number of patients. RT3DE measurements of the outflow tract and pulmonary valve annulus diameter were higher than that obtained by 2DE. Measurement of area of both right ventricular outflow tract and pulmonary annulus may aid in selection of therapeutic strategy.

Chapter 10. The study described feasibility and reliability of RT3DE for assessment of left atrial volume and function. Functional assessment included both active and passive left atrial function through the volumetric changes during the cardiac cycle. RT3DE assessment of left atrial volume does not rely on assumption and thus depict the actual left atrial shape. RT3DE measurements were compared with 2DE measurements. It is so difficult by 2D planimetry to exclude left atrial appendage and pulmonary veins totally during volume calculation. This can explain the higher value of left atrial volume measurements by 2DE than that obtained by RT3DE.

Chapter 11. Assessment of left atrial volume at three phases of cardiac cycle (maximum volume, minimum volume, and pre-atrial contraction volume) was obtained by RT3DE. RT3DE assessment of cyclic changes of left atrial volume and indices of passive and active function may help in understanding the left atrial physiology. The existence of left atrial Frank-Starling mechanism was described through RT3DE measurement and evidenced by an increase in left atrial contractility in response to an increase in preload up to a certain point, beyond which the left atrial contractility decreased.

Chapter 12. The study assessed the calculation of left atrial ejection force in hypertrophic cardiomyopathy patients. This assessment depends on a standard formula used the mitral orifice (annulus or valve) area, transmitral velocity and blood viscosity. The calculation of ejection force by the formula used RT3DE measurement of mitral annulus diameter showed that hypertrophic cardiomyopathy is associated with higher ejection force than normal, and higher in obstructive HCM than non-obstructive indicating a higher atrial workload. The study concluded that ejection force should be determined in HCM patients by annulus area-derived formula instead of valve area-derived formula due to annular dilatation. So, RT3DE measurement of atrial ejection force through annuls area is recommended as a better indicator for left atrial work in HCM because it is more accurate and logic than 2DE measurement

References

1. Kasliwal RR, Chouhan NS, Sinha A, Gupta P, Tandon S, Trehan N. real-time three-dimensional transthoracic echocardiography. Indian Heart J 2005;57:128-137.
2. Sugeng L, Weinert L, Lang RM. Left ventricular assessment using real-time three-dimensional echocardiography. Heart 2003;89 (Suppl 3):29iii.
3. Binder TM, Rosenhek R, Porenta G, Maurer G, Baumgartner H. improved assessment of miral valve stenosis by volumetric real-time three-dimensional echocardiography. J Am Coll Cardiol 2000;36(4):1355-1361.
4. Houck R, Cooke J, Gill EA. Live 3D echocardiography: A replacement for traditional 2D echocardiography? Am J Roentgenol 2006;187:1092-1106.
5. Hibberd MG, Chuang ML, Beaudin RA, Riley MF, Mooney MG, Fearnside JT, Manning WJ, Douglas PS. Accuracy of three-dimensional echocardiography with unrestricted selection of imaging planes for measurement of left ventricular volumes and ejection fraction. Am Heart J. 2000;140:469-75
6. Sugeng L, Mor-Avi V, Weinert L, Niel J, Ebner C, Steringer-Mascherbauer R, Schmidt F, Galuschky C, Schummers G, Lang RM, Nesser HJ. Quantitative asessment of left ventricular size and function: Side-by-side comparison of real-time three-dimensional echocardiography and computed tomography with magnetic resonance reference. Circulation. 2006;114:654-661.
7. Jenkins C, Bricknell K, Hanekom L, Marwick TH. Reproducibilty and accuracy of echocardiographic assessment of left ventricular parameters using real-time three-dimensional echocardiography. J Am Coll Cardiol. 2004;44:878-886.
8. Mor-Avi V, Sugeng L, Weinert L, MacEneaney P, Caiani EG, Koch R, Salgo IS, Lang RM. Fast measurement of left ventricular mass with real-time three-dimensional echocardiography: comparison with magnetic resonance imaging. Circulation. 2004;110:1814-1818.
9. van den Bosch AE, Robbers-Visser D, Krenning BJ, McGhie JS, Helbing WA, Meijboom FJ, Roos-Hesselink JW. Comparison of real-time three-dimensional echocardiography to magnetic resonance imaging for assessment of left ventricular mass. Am J Cardiol. 2006;97(1):113-117.
10. Chen G, Sun K, Huang G. In vitro validation of right ventricular volume and mass measurement by real-time three-dimensional echocardiography. Echocardiogr. 2006;23(5):395-399.
11. Wang J, Wang X, Xie M, Yang Y, V QL, Yang Y, Wang L. Evaluation of right ventricular volume and systolic function by real-time three-dimensional echocardiography. J Huazhong Univ Sci Technolog Med Sci 2005;25(1):94-99.
12. Chan KL, Liu X, Ascah KJ, Beauchesne LM, Burwash IG. Comparison of real-ime 3-dimensional echocardiography with conventional 2-dimensional echocardiography in the assessment of structural heart disease. J Am Soc Echocardiogr 2004;17:976-980.
13. Seliem MA, Fedec A, Cohen MS, Ewing S, Farrell PE Jr, Rychik J, Schultz AH, Gaynor Jw, Spray TL. Real-time three-dimensional echocardiographic imaging of congenital heart disease using matrix-array technology: freehand real-time scanning adds instant morphologic details not well delineated by conventional 2-dimensional imaging. J Am Soc Echocardiogr 2006;19(2):121-129.

14. van den Bosch AE, ten Harkel DJ, McGhie JS, Roos-Hesselink JW, Simoons ML, Bogers AJJC, Meijboom FJ. Characterization of atrial septal defect assessed by real-time three-dimensional echocardiography. J Am Soc Echocardiogr 2006; 19(1): 7-13.
15. Cheng TO, Xie MX, Wang XF, Wang Y, Lu Q. Real-time three-dimensional echocardiography in assessing atrial and ventricular septal defects: an echocardiographic-surgical correlative study. Am Heart J 2004;148:1091-1095.
16. Mercer-Rosa L, Seliem MA, Fedec A, Rome J, Rychik J, Gaynor JW. Illustration of the additional value of real-time 3-dimensional echocardiography to conventional transthoracic and transesophageal 2-dimensional echocardiography in imaging muscular ventricular septal defects; does this have any impact on individual patient treatment?. van den Bosch AE, ten Harkel DJ, McGhie JS, Roos-Hesselink JW, Simoons ML, Bogers AJJC, Meijboom FJ. Characterization of atrial septal defect assessed by real-time three-dimensional echocardiography. J Am Soc Echocardiogr 2006;19(12) :1511-1519.
17. van den Bosch AE, ten Harkel DJ, McGhie JS, Roos-Hesselink JW, Simoons ML, Bogers AJJC, Meijboom FJ. Feasibility and accuracy of real-time three-dimensional echocardiographic assessment of ventricular septal defects. J Am Soc Echocardiogr 2006;19(1):7-13.
18. Sugeng L, Coon P, Weinert L, Jolly N, Lammertin G, bednarz JE, Thiele K, Lang RM. Use of Real-time three-dimensional transthoracic echocardiography in evaluation of mitral valve disease. J Am Soc Echocardiogr 2006;19:413-421.
19. Binder TM, Rosenhek R, Porenta G, Maurer G, Baumgartner H. Improved assessment of mitral valve stenosis by volumetric real-time three-dimensional echocardiography. J Am Coll Cardiol 2000;36:1355-61.
20. Watanabe N, Ogasawara Y, Yamaura Y, Kawamoto T, Toyota E, Akasaka T, Yoshida K. Quantification of mitral valve tenting in ischemic mitral regurgitation by transthoracic real-time three-dimensional echocardiography. J Am Coll Cardiol 2005;45:763-769.
21. Zamorano J, Cordeiro P, Sugeng L, Perez de Isla L, Weinert L, Macaya C, Rodrigo JL, Lang RM. Real-time three-dimensional echocardiography for rheumatic mitral valve stenosis evaluation: an accurate and novel approach. J Am Coll Cardiol 2004;43:2091-2096.
22. Sugeng L, Weinert L, Lammertin G, P Thomas P, KT Spencer KT, JM Decara JM, V Mor-Avi, D Huo, T Feldman, and RM Lang. Accuracy of mitral valve area measurements using transthoracic rapid freehand 3-dimensional scanning: comparison with non-invasive and invasive methods. J Am Soc Echocardiogr 2003;16:1292-1300.
23. Zamorano J, Perez de Isla L, Sugeng L, Cordeiro P, Rodrigo JL, Almeria C, Weinert L, Feldman T, Macaya C, Lang RM, Hernandez Antolin R. Non-invasive assessment of mitral valve area during percutaneous balloon mitral valvuloplasty: role of real-time 3D echocardiography. Eur Heart J 2004;25:2086-91.

CHAPTER 2

Assessment of Tricuspid Valve Annulus Size, Shape and function using Real-Time Three-Dimensional Echocardiography

Ashraf M. Anwar[1,2], Marcel L. Geleijnse[1], Folkert J. ten Cate[1] and Folkert J Meijboom[1]

[1]Department of Cardiology, Thoraxcenter, Erasmus University Medical Center, Rotterdam, The Netherlands
[2]Department of Cardiology, Al-Hussein University Hospital, Al-Azhar University, Cairo, Egypt

Interactive Cardiovascular and Thoracic Surgery Journal 2006;5:683-687

ABSTRACT

Tricuspid annulus (TA) evaluation continues to be a major problem in the surgical decision-making process. Obviously, 2-dimensional transthoracic echocardiography (2D TTE) is limited in TA visualization due to its complex 3D shape. The study aimed to determine TA morphology, size and function with real-time three-dimensional echocardiography (RT3DE) in 40 patients divided into two equal groups (I: normal TA and II: Dilated). 2D TTE measurements included TA diameter (TAD) at apical 4 chamber (AP4CH) and parasternal short axis (PSAX) views. RT3DE measurements included TA area (TAA), major TAD and minor TAD. TA fractional shortening (TAFS), and TA fractional area change (TAFAC) were calculated from End-systolic and end-diastolic measurements. RT3DE allowed visualization and measurement of the entire oval-shaped TA in all patients irrespective of its size (normal or dilated). 2D TTE measurement of TAD at both AP4CH and at PSAX views was significantly smaller than the major TAD measured by RT3DE (P <0.0001) and nearly matched with the minor TAD in all patients. Calculation of TAFS was comparable with both techniques. TAFAC was significantly higher than TAFS (P <0.0001). So, RT3DE could be relied on more accurately than 2D TTE in the assessment of TA size and function which may aid in decision-making and selection of proper surgical procedure when indicated.

INTRODUCTION

The tricuspid valve (TV) is composed of three leaflets (anterior, posterior and septal) attached to a fibrous annulus[1]. The three-dimensional (3D) shape of this tricuspid annulus (TA) is complex and does not conform to a flat ring[2]. Tricuspid regurgitation (TR) is the most common pathology affecting the TV. An understanding of the pathological process underlying TR is necessary to determine the optimal management strategy. Usually, TR is secondary to left-sided valvular pathology (mostly mitral valve disease) with pulmonary hypertension and right ventricular dilatation [3],[4]. Because the TA is a component of the right ventricle it will dilate also. However, since the septal leaflet is fixed between the fibrous trigones, the TA can only lengthen and dilate along the attachment of the anterior and posterior leaflets [5-7]. Unfortunately, TV evaluation continues to be a major problem in the surgical decision-making process [8]. Guidelines for TV repair include TA assessment (indexed TA size >2.1cm/m^2 and TA fractional shortening <25%)[3] . At the time of surgery the decision to repair the TV may be changed due to discrepant TA diameter (TAD) findings between pre-operative two-dimensional transthoracic (or transesophageal) echocardiography (2D TTE) and direct surgical visualization[3]. Obviously, 2D TTE is limited in visualizing the complete TA. Since real-time 3D echocardiography (RT3DE), has become available for clinical practice, it is now possible to examine the TV more completely [9]. The present study aimed to determine actual TA morphology, size and function with RT3DE and to compare the results with standard 2D TTE findings.

SUBJECTS AND METHODS

The study included forty consecutive patients with good image 2D TTE quality in whom also RT3DE was performed. Indications for echocardiography included follow-up for adult congenital heart disease (n = 12), valvular heart disease (n = 10), cardiomyopathy (n = 8), and analysis of shortness of breath (n = 10).

2D TTE Examination

2D TTE was done with a Sonos 7500 ultrasound system attached to a S3 transducer (Philips, Best, The Netherlands). The TV was imaged from apical and parasternal views with the patient in the left lateral decubitus position. In each patient, the following variables were measured by two blinded observers: (1) TAD, obtained from the apical 4-chamber (AP4CH) and parasternal short axis (PSAX) views at an end-diastolic and end-systolic still frame, and (2) TA fraction shortening (TAFS) defined as (end-diastolic TAD - end-systolic TAD) / end-diastolic TAD obtained from the AP4CH and PSAX.

RT3DE Examination

RT3DE was done with the same ultrasound system attached to a X4 matrix array transducer capable of providing real-time B-mode images. A full volume 3D data set was collected within approximately 5-10 seconds of breath holding in full volume mode from an apical window. The 3D data set was transferred for off-line analysis with TomTec software (Unterschleissheim, Munich, Germany). Data were stored digitally and subsequently evaluated by two blinded observers (AMA, OIIS). Data analysis of 3D images was based on a 2D approach relying on images obtained initially from the apical view. The TA was sliced between two narrow lines to exclude other tissues on the 2D image leading to clarification of annulus by a 3D image. This image was viewed and traced from the ventricular aspect, in 6 patients (15%) the atrial aspect was used because of better quality. Manual tracing of the inner border of the tricuspid annulus was done from the atrial aspect and once this is completed the surface area was automatically calculated and could be visualized from different points of views. Manual modification was made to correct any inconsistence.

The following RT3DE variables were obtained from both an end-diastolic and end-systolic still frame: (1) TA area (TAA_{3D}), (2) major TAD_{3D} defined as the widest TAD_{3D} (see Figure 1), and (3) minor TAD_{3D} defined as the smallest TAD_{3D} (see Figure 1). Subsequently, $TAFS_{3D}$ was calculated from major TAD_{3D} data and TA fractional area change ($TAFAC_{3D}$) was calculated from systolic and diastolic TAA_{3D}.

STATISTICAL ANALYSES

All data obtained by 2D TTE and RT3DE are presented as mean ± SD. A paired t-test was performed for comparing means of variables. The level of significance was set to $P < 0.05$. A SPSS statistical package was used (SPSS, version 12.1, SPSS Inc, Chicago). Interobserver agreement for 2D TTE and RT3DE measurements was assessed according to the Bland and Altman principle [10].

RESULTS

In Table 1, the clinical and echocardiographic parameters of all patients are displayed. Patients were classified into two groups; group I included 20 patients with normal end-diastolic $TAD_{2D\text{-}AP4CH}$ (<35mm) and group II included 20 patients with dilated end-diastolic $TAD_{2D\text{-}AP4CH}$ (≥35mm). There were no significant differences in clinical variables (age, gender) between the two groups. All echocardiographic parameters were significantly higher in group II patients (all $P < 0.0001$).

RT3DE acquisition

Acquisition and post-processing of RT3DE data was performed successfully in all patients in a reasonable time (approximately 1 minute for acquisition and 5 minutes for data analysis). The TA was clearly delineated in all patients and, as seen in Figure 1, its shape was not circular but oval, both in normal sized and in dilated TA (Figure 2).

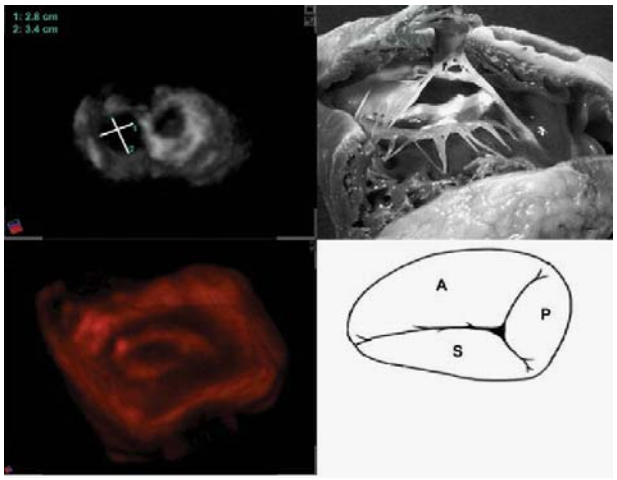

Fig (1): (a) Tricuspid annulus with two lines inside, line 1 is TAD by 2DE in AP4CH and line 2 is major TAD by RT3DE, with large difference in measurements, (b) surgical view of tricuspid annulus and leaflets, (c) tricuspid annulus and leaflets as seen by RT3DE, and (d) simple diagram of tricuspid annulus and the three leaflets of the valve

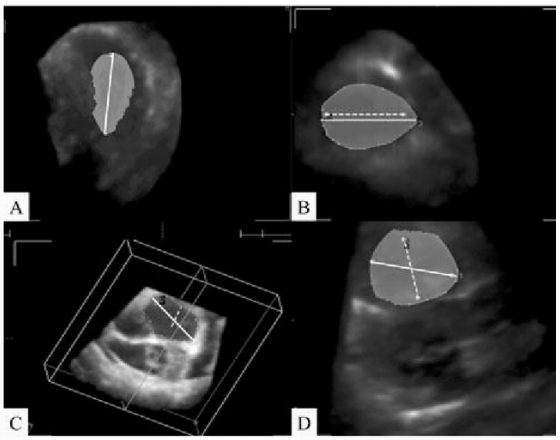

Fig (2): Real time 3D echo showed the morphology of the normal tricuspid annulus (A) and dilated annulus (B) as visualized from the ventricular aspect with delineation of its inner border. Both tricuspid annuli appeared as oval in shape. The horizontal line inside is the major tricuspid annular diameter (TAD) and vertical line is the minor TAD as measured by RT3DE. (C): Tricuspid annulus with the line measured at apical 4 chamber by 2DE inside it, which appeared away from the true diameter. (D): Tricuspid annulus with the line measured at parasternal short axis by 2DE inside it, which appeared away from the true diameter.

Comparison between 2D and 3D measurements

Diastolic value

There was a good correlation between end-diastolic $TAD_{2D\text{-}AP4CH}$ and $TAD_{2D\text{-}PSAX}$ (R = 0.79, *P* <0.0001). Major TAD_{3D} was well correlated with end-diastolic $TAD_{2D\text{-}AP4CH}$ and $TAD_{2D\text{-}PSAX}$ (R = 0.74, *P* <0.0001 and R = 0.75, *P* <0.0001, respectively). As seen in Table 1 and Figure 2, major TAD_{3D} measurements in both patients groups were significantly larger than end-diastolic $TAD_{2D\text{-}AP4CH}$ and $TAD_{2D\text{-}PSAX}$. Also when the largest TAD_{2D} was compared to TAD_{3D}, 3D measurements were significantly larger (44.9 ± 11.3 and 39.0 ± 10.3 mm, P <0.001). After reclassification of the patients according to major TAD_{3D} findings only 10 patients could be classified as normal (major TAD_{3D} <35mm). In these 10 patients actual $TAD_{2D\text{-}AP4CH}$ and $TAD_{2D\text{-}PSAX}$

values were 30.6 ± 6.0 and 29.1 ± 6.4 mm, respectively. Importantly, in patients with normal TAD_{2D}, 65% of them had grade 1-2 TR (see Table 1) whereas in normal TAD_{3D} only 30% of patients had grade 1-2 TR.

Systolic values

There was an excellent correlation between end-systolic $TAD_{2D\text{-}AP4CH}$ and $TAD_{2D\text{-}PSAX}$ (R = 0.89, *P* <0.0001). Major systolic TAD_{3D} measurements correlated well with end-systolic $TAD_{2D\text{-}AP4CH}$ and $TAD_{2D\text{-}PSAX}$ (R = 0.80, *P* <0.0001 and R = 0.66, *P* <0.05, respectively). As seen in Table 1, major systolic TAD_{3D} measurements were in both patients groups significantly greater than end-systolic $TAD_{2D\text{-}AP4CH}$ and $TAD_{2D\text{-}PSAX}$.

Fractional shortening

There were no significant differences between $TAFS_{2D\text{-}AP4CH}$ (14.2 ± 7.1%), $TAFS_{2D\text{-}PSAX}$ (14.6 ± 9.2%), and $TAFS_{3D}$ (17.8 ± 13.2%). $TAFAC_{3D}$ was significantly higher than the aforementioned $TAFS_{2D}$ or $TAFS_{3D}$ measurements (26.6 ± 12.7 %; *P* <0.0001).

Minor TAD

No significant differences were detected between end-systolic and end-diastolic minor TAD_{3D} versus $TAD_{2D\text{-}AP4CH}$ and $TAD_{2D\text{-}PSAX}$ in both groups (Table 1).

Table 1. Clinical and echocardiographic data of all patients.

	All patients (n = 40)	**Group I (n = 20)**	**Group II (n = 20)**
Clinical characteristics			
Age (yr)	29.8 ± 11	26.3 ± 9	33.1 ± 14
Male gender (%)	17 (43%)	10 (50%)	7 (35%)
Diastolic echo values			
$TAD_{2D\text{-}AP4CH}$ (mm)	37.7 ± 10.2	29.1 ± 3.2*	45.4 ± 7.9 **
$TAD_{2D\text{-}PSAX}$ (mm)	35.7 ± 9.1	29.6 ± 6.1*	41.2 ± 8.0*
Major TAD_{3D} (mm)	45.0 ± 11.3	38.6 ± 9.3	50.7 ± 10
Minor TAD_{3D} (mm)	37.3 ± 11.6	30.7 ± 9.2	43.7 ± 10.0
TAA_{3D} (mm^2)	159.7 ± 84.3	105.8 ± 67.5	208.3 ± 81.7
Systolic echo values			
$TAD_{2D\text{-}AP4CH}$ (mm)	32.4 ± 9.5	25.4 ± 3.9 **	38.3 ± 7.1***
$TAD_{2D\text{-}PSAX}$ (mm)	30.2 ± 7.8	24.9 ± 3.5*	34.4 ± 6.7*
Major TAD_{3D} (mm)	36.0 ± 9.5	25.4 ± 5.3	41.7 ± 8.5
Minor TAD_{3D} (mm)	30.5 ± 8.5	25.4 ± 5.3	35.6 ± 8.1
TAA_{3D} (mm^2)	117.9 ± 66.9	81.4 ± 44.2	150.8 ± 67.5
Fractional shortening			
TAFS2D-AP4CH	14.2 ± 7.1	13.5 ± 5.7	15.0 ± 8.2
TAFS2D-PSAX	14.8 ± 9.2	14.6 ± 8.8	15.1 ± 8.8
TAFS3D major TAD	17.8 ± 13.2	18.5 ± 14.3	16.6 ± 10.4
TAFAC3D	26.2 ± 12.9	23.7 ± 13.4	27.9 ± 12.2
Tricuspid regurgitation			
None	7 (17%)	7 (35%)	0 (0%)
Grade 1-2	23 (58%)	13 (65%)	10 (50%)
Grade 3-4	10 (25%)	0 (0%)	10 (50%)

Group I included patients with normal tricuspid annulus diameter, Group II included patients with dilated (>35mm) tricuspid annulus diameter. AP4CH: apical 4-chamber view, FS: fractional shortening, PSSAX: parasternal short axis view, TAA: tricuspid annular area, TAD: tricuspid annular diameter, TAFAC: tricuspid annular fractional area change. * *P* <0.001 compared to RT3DE; ** *P* <0.01 compared to RT3DE, *** *P* <0.05 compared to RT3DE

Interobserver agreement

As seen in Figure 3, the limits of interobserver agreement for major TAD_{3D} (mean difference -0.5 ± 1.7 mm, agreement –3.9 to 2.9) were comparable to end-diastolic $TAD_{2D\text{-}AP4CH}$ (mean difference 0.1 ± 2.0 mm, agreement –3.9 to 4.1). The limits of interobserver agreement for $TAD_{2D\text{-}PSAX}$ (mean difference 1.0 ± 4.8 mm, agreement –3.8 to 5.8) were worse, in particular for lower TAD values.

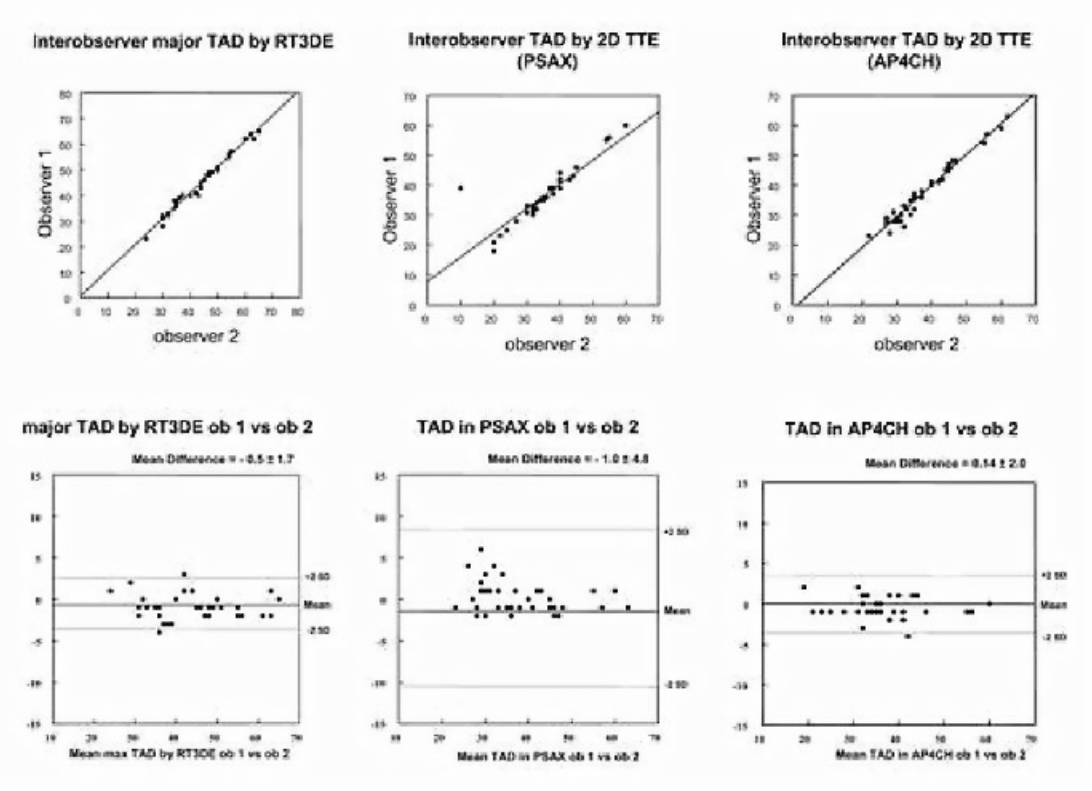

Fig (3): Interobserver correlation and agreement according to Bland and Altman principle for measuring tricuspid annular diameter (TAD), A)**:** TAD in apical 4-chamber (P4CH) by two dimensional echocardiography (2DE), B): TAD in parasternal short axis (PSAX) by 2DE, C): Major TAD by real time three dimensional echocardiography (RT3DE).

DISCUSSION

In the present study, the morphological and functional aspects of the TA were assessed by RT3DE. The main findings of our study are (1) TA shape was not circular but oval, both in normal sized and in dilated TA, (2) TAD is underestimated by 2D TTE, and (3) TAFS measurements are comparable for 2D TTE and RT3DE.

TAD measurements are of critical importance in the TV surgical decision-making process [11-13]. Absence of TR or the presence of only mild TR does not mean that the TV is free of any abnormality such as TA dilatation. At a given time, even considerable TA dilatation may not always result in significant TR [(11,12)]. Not only the selection of patients undergoing surgery for TR is dependent on echocardiographic TAD assessment [(11)], but also the type of surgical technique (valve plication or ring placement) is influenced by measurements of TA function and TAD [3,14].

Although 2D TTE is helpful to assess TV function and to detect TR severity it has important limitations in describing TV morphological details, such as TAD [(13,14)]. It is well known that after mitral valve surgery patients may clinically deteriorate due to underestimated TV pathology and significant residual or developing TR [15-]. RT3DE may yield more detailed anatomical information. In the present study, the TA was visualized well in all subjects allowing even measurements of its area, both at end-systole and end-diastole. This is in accordance with a 3D study by Schnabel *et al.* [(9)] in which TA visualization was well or at least sufficiently in over 90% of patients. When TAD_{2D} measurements were compared with the TAD_{3D} measurements, 2D measurements were significantly smaller than the major TAD_{3D} measurements (diameter measured from the antero-septal to the antero-posterior commissure). In fact, TAD_{2D} measurements corresponded more with the minor TAD_{3D} measurements. In 2D TTE studies it was shown that the normal value for TAD is <35mm[14]. However, in our study half of the patients with a normal TAD_{2D} had an actual TAD (measured with 3D) larger than 35mm. So, 2D TTE cannot be relied on defining TAD as normal. It seems necessary to re-establish normal TAD values with 3D imaging. Importantly, interobserver agreement for TAD_{3D} measurements was comparable to $TAD_{2D\text{-}AP4CH}$ measurements and better than $TAD_{2D\text{-}PSAX}$ measurements. If 2D TTE is the only available assessment tool for TAD, the apical 4-chamber view seems preferred because of better interobserver agreement compared to $TAD_{2D\text{-}PSAX}$ and more alignment with TAD_{3D} measurements.

Like other cardiac structures, cyclic changes occur in TAD during systole and diastole [(3,11,15)]. Calculation of TAFS from systolic and diastolic TAD showed no difference between 2D TTE and RT3DE. This is because end-systolic and end-diastolic TAD_{3D} values are to an equal extent increased compared with 2D values.

Calculation of TA function by $TAFAC_{3D}$ was significantly higher than that measured by diameter changes either in 2D TTE or RT3DE. This could be explained by the accuracy of global function by area percent changes than single distance percent changes especially when more lengthening occur.

In accordance with previous study [12] that reported no relation between presence and severity of TR and degree of TA dilatation when 2D TTE was relied on as 65% of normal TAD_{2D} had grade 1-2 TR. but with normal major TAD_{3DE}, the percentage decreased to 30%.

STUDY LIMITATION

The main limitation of this study is that RT3DE data were not compared with a "gold standard" such as magnetic resonance imaging or surgical findings. Nevertheless, our main findings (oval shape of the TA, larger TAD_{3D}) were consistently found in the large majority of patients. Also, RT3DE images more critically depend on image quality than 2D TTE images and the value of RT3DE should be assessed in a more non-selected (image quality) population.

CONCLUSION

The TA is an oval structure with a major and a minor diameter. 2D TTE underestimates TAD, regardless whether it is measured from the apical 4-chamber or parasternal short axis view. This may have important implications in the TV surgical decision-making processes.

REFERENECES

1. Silver MD, Lam JH, Ranganathan N, Wigle ED. Morphology of the human tricuspid valve. *Circulation* 1971;43:333-48.
2. Yacoub MH, Cohn LH. Novel approaches to cardiac valve repair: from structure to function: Part II. *Circulation* 2004;109:1064-72.
3. Colombo T, Russo C, Ciliberto GR, Lanfranconi M, Bruschi G, Agati S, Vitali E. Tricuspid regurgitation secondary to mitral valve disease: tricuspid annulus function as guide to tricuspid valve repair. *Cardiovasc Surg* 2001;9:369-77.
4. Cohn LH. Tricuspid regurgitation secondary to mitral valve disease: when and how to repair. *J Card Surg* 1994;9:237-41.
5. Tei C, Pilgrim JP, Shah PM, Ormiston JA, Wong M. The tricuspid valve annulus: study of size and motion in normal subjects and in patients with tricuspid regurgitation. *Circulation* 1982;66:665-71.
6. Ubago JL, Figueroa A, Ochoteco A, Colman T, Duran RM, Duran CG. Analysis of the amount of tricuspid valve anular dilatation required to produce functional tricuspid regurgitation. *Am J Cardiol* 1983;52:155-8.
7. Shemin R. tricuspid valve disease In: Cohn LH, Edmunds LH jr eds. cardiac surgery in the adults. New York: McGraw-Hill 2003.
8. McGrath LB G-lL, Bailey BM. Tricuspid valve operation in 530 patients. Twenty-five-year assessment of early and late phase events. *Journal of thoracic and cardiovascular surgery* 1990;99:124-133.
9. Schnabel R, Khaw AV, von Bardeleben RS, Strasser C, Kramm T, Meyer J, Mohr-Kahaly S. Assessment of the tricuspid valve morphology by transthoracic real-time-3D-echocardiography. *Echocardiography* 2005;22:15-23.
10. Bland JM, Altman DG. Statistical methods for assessing agreement between two methods of clinical measurement. *Lancet* 1986;1:307-10.
11. Goldman ME, Guarino T, Fuster V, Mindich B. The necessity for tricuspid valve repair can be determined intraoperatively by two-dimensional echocardiography. *J Thorac Cardiovasc Surg* 1987;94:542-50.
12. Chopra HK, Nanda NC, Fan P, Kapur KK, Goyal R, Daruwalla D, Pacifico A. Can two-dimensional echocardiography and Doppler color flow mapping identify the need for tricuspid valve repair? *J Am Coll Cardiol* 1989;14:1266-74.
13. De Simone R, Lange R, Tanzeem A, Gams E, Hagl S. Adjustable tricuspid valve annuloplasty assisted by intraoperative transesophageal color Doppler echocardiography. *Am J Cardiol* 1993;71:926-31.
14. Dreyfus GD, Corbi PJ, Chan KM, Bahrami T. Secondary tricuspid regurgitation or dilatation: which should be the criteria for surgical repair? *Ann Thorac Surg* 2005;79:127-32.
15. Tager R, Skudicky D, Mueller U, Essop R, Hammond G, Sareli P. Long-term follow-up of rheumatic patients undergoing left-sided valve replacement with tricuspid annuloplasty--validity of preoperative echocardiographic criteria in the decision to perform tricuspid annuloplasty. *Am J Cardiol* 1998;81:1013-6.

CHAPTER 3

Value of Assessment of Tricuspid Annulus: Real-Time Three-Dimensional Echocardiography and Magnetic Resonance Imaging

Ashraf M. Anwar[1,2], Osama I.I. Soliman[1,2], Attila Nemes[1,4], Robert-Jan van Geuns[2,3], Marcel L. Geleijnse[1], and Folkert J. ten Cate[1]

[1]Department of Cardiology, Thoraxcenter, Erasmus University Medical Center, Rotterdam, The Netherlands

[2]Department of Cardiology, Al-Hussein University Hospital, Al-Azhar University, Cairo, Egypt

[3]Department of Radiology, Erasmus University Medical Center, Rotterdam, the Netherlands

[4]Second Department of Medicine and Cardiology Center, University of Szeged, Szeged, Hungary

International Journal of Cardiovascular Imaging 2008;

ABSTRACT

Aim: To detect the accuracy of real-time three-dimensional echocardiography (RT3DE) and two-dimensional echocardiography (2DE) for tricuspid annulus (TA) assessment compared with magenetic resonance imaging (MRI).

Methods: Thirty patients (mean age 34 ± 13 years, 60% males) in sinus rhythm were examined by MRI, RT3DE, and 2DE for TA assessment. End-diastolic and end-systolic TA diameter (TAD) and TA fractional shortening (TAFS) were measured by RT3DE, 2DE, and MRI. c TA area (TAA) and TA fractional area changes (TAFAC) were measured by RT3DE and MRI. End-diastolic and end-systolic right ventricular (RV) volumes and ejection fraction (RV-EF) were measured by MRI.

Results

The TA was clearly delineated in all patients and visualized as an oval-shaped by RT3DE and MRI. There was a good correlation between TADMRI and TAD3D ($r = 0.75$, $P = 0.001$), while TAD2D was fairly correlated with TAD3D and TADMRI ($r = 0.5$, $P = 0.01$ for both). There were no significant differences between RT3DE and MRI in TAD, TAA, TAFS, and TAFAC measurements, while TAD2D and TAFS2D were significantly underestimated ($P < 0.001$). TAFS2D was not correlated with RV-EF, while TAFS3D and TAFAC3D were fairly correlated with RV-EF ($r = 0.49$, $P = 0.01$, and $r = 0.47$, $P = 0.02$ respectively).

Conclusion

RT3DE helps in accurate assessment of TA comparable to MRI and may have an important implication in the TV surgical decision making processes. RT3DE analysis of TA function could be used as a marker of RV function.

INTRODUCTION

Evaluation of tricuspid annulus (TA) continues to be a major problem in the surgical decision-making process due to its complex three-dimensional shape[1-3]. Accurate assessment of TA has many values in clinical application. For example, the decision of tricuspid valve repair may change due to discrepancy between pre-operative measurement of TA diameter (TAD) by two-dimensional transthoracic (or transesophageal) echocardiography (2DE) and direct surgical visualization[4]. Several studies described a strong correlation between TA motion and right ventricular (RV) function [5-8]. Analysis of TA velocity by tissue Doppler imaging has been found useful for RV functional assessment[9,10]. In these studies, the assessment of TA motion was relied on 2DE, M-mode and tissue Doppler recording. Since RT3DE has become available for clinical practice, it is now possible to examine the TV more completely[11]. This study aimed to use RT3DE in evaluation of TA morphology, size and cyclic changes during cardiac cycle. It also aimed to correlate TA function with RV function that was assessed by magnetic resonance imaging (MRI).

SUBJECTS and METHODS

The study included 30 patients (mean age 34 ± 13 years, 60% were males) who were scheduled for routine MRI examination for evaluation of right ventricular function (10 patients with congenital heart disease, five with chronic pulmonary disease, five with multivalvular affection, and 10 normals). 2DE and RT3DE were performed at the same day of MRI examination after their informal consent for assessment of TA. The inclusion criteria for selection were good 2D image quality, sinus rhythm and mild to moderate tricuspid regurgitation.

MRI Examination

MRI studies were performed with a 1.5 T MRI (General Electric, Milwaukee WI; Signa 1.5 T MRI) equipped with a four-element torso coil. A cardiac-triggered, steady-state, free-precession sequence (FIESTA; temporal resolution and time of echo of 3.5 and 1.3 ms, respectively, flip angle of 45 degrees) was used for quantitative analysis. 10 cine short axis slices were acquired (slice thickness 10 mm, gap 0 mm). Additional imaging parameters were a field of view of 320 to 380 mm and a matrix of 160 X 128. These series of high quality images encompassing the right ventricle (RV) produced a three-dimensional data set with sharp edge between the blood pool and myocardium. Quantitative

analysis was performed using standardized software (MassPlus, Medis Inc., Leiden, NL). By this software, manual tracing was done for TA and right ventricular (RV) endocardial border on all images (end-diastolic and end-systolic). The following measures were obtained at end-diastolic and end-systolic: (1) TA area (TAA_{MRI}), (2) TAD_{MRI}, (3) RV volume, (4) RV ejection fraction (RV-EF) was calculated as (RV end-diastolic volume- RV end-systolic volume/RV end-diastolic volume) · 100%, (5) TAfractional shortening (TAFSMRI) defined as (enddiastolic TADMRI–end-systolic TADMRI)/enddiastolic

TADMRI · 100% and (6) TA fractional area changes (TAFACMRI) defined as (end-diastolic TAAMRI–end-systolic TAAMRI)/end-diastolic TAAMRI · 100%.

Transthoracic 2DE

2DE was done with a Sonos 7500 ultrasound system attached to a S3 transducer (Philips, Best, The Netherlands). The TV was imaged from apical 4-chamber view with the patient in the left lateral decubitus position. The following measures were obtained: (1) TAD_{2D} was defined as the distance between the insertion sites of septal and anterior TV leaflets and obtained at an end-diastolic and end-systolic still frame and (2) TA fraction shortening (TAFS2D) defined as (end-diastolic TAD2D–end-systolic TAD2D)/enddiastolic TAD2D · 100%

Transthoracic RT3DE

RT3DE was done with the same ultrasound system attached to a X4 matrix array transducer capable of providing real-time B-mode images. A full volume 3D data set was collected within approximately 5-10 seconds of breath holding in full volume mode from an apical window. The 3D data set was transferred for off-line analysis with TomTec software (Unterschleissheim, Munich, Germany). Data were stored digitally and subsequently evaluated by two blinded observers (AMA, OIIS). Data analysis of 3D images was based on a 2D approach relying on images obtained initially from the apical view. The TA was sliced between two narrow lines to exclude other tissues on the 2D image leading to clarification of annulus by a 3D image. TA was viewed and traced manually from the atrial aspect and once this is completed the surface area was automatically calculated and could be visualized from different points of views. Manual modification was made to correct any inconsistence. The following RT3DE variables were obtained from both an end-diastolic and end-systolic still frame: (1) TA area (TAA_{3D}), and (2) TAD_{3D} defined as the widest TAD (see Figure 1), Subsequently, $TAFS_{3D}$ and TA fractional area changes ($TAFAC_{3D}$) (%) were calculated by the same formula used in 2DE.

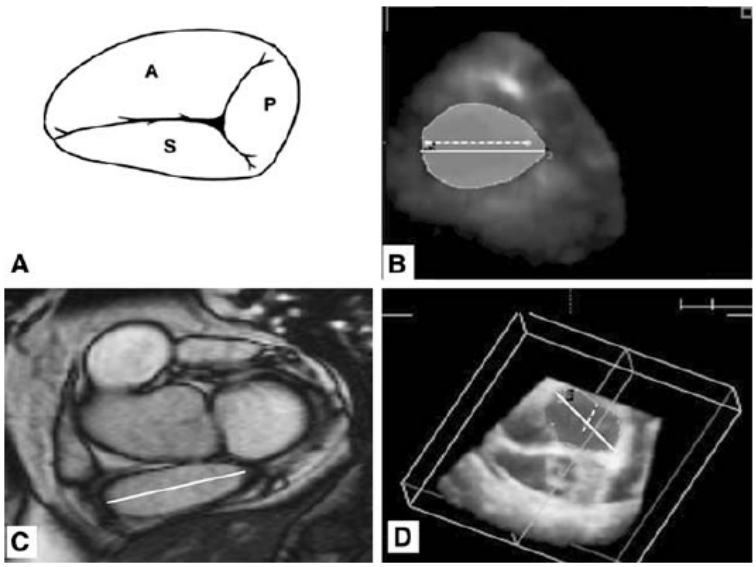

Fig. 1 Tricuspid annulus oval shape as seen by graphic representation (**A**), real-time three-dimensional echocardiography (**B**), magnetic resonance imaging (**C**), and tricuspid annulus with 2 lines inside, the larger is the TAD by real-time three-dimensional echocardiography and the smaller is the TAD by two-dimensional echocardiography with large difference in measurements

STATISTICAL ANALYSES

All data obtained by MRI, 2DE and RT3DE are presented as mean ± SD. A paired *t*-test and was performed for comparing means of variables. The level of significance was set to $P < 0.05$. A SPSS statistical package was used (SPSS, version 12.1, SPSS Inc, Chicago). Pearson's coefficient was used for correlation between RT3DE and MRI data. Interobserver agreement for RT3DE measurements was assessed according to the Bland and Altman principle[12].

RESULTS

Acquisition of RT3DE data was performed in all patients in a reasonable time (approximately 1 minute for acquisition and 5 minutes for data analysis). The TA was clearly delineated in all patients. An oval shaped TA (not circular) was visualized by RT3DE and MRI (Figure 1). TAD3D was obtained with very good interobserver agreement (mean difference – 0.4 ± 1.5 mm, agreement –3.4–2.6). There was a good correlation between TADMRI and TAD3D (R = 0.75, $P = 0.001$), while TAD2D was fairly correlated with TAD3D and TADMRI (R = 0.5, $P = 0.01$ for both). There were no significant differences between RT3DE and MRI in TAD, TAA, TAFS, and TAFAC measurements, while TAD2D and TAFS2D were significantly underestimated ($P < 0.001$) (Table 1). TAFS2D was not correlated with RV-EF, while TAFS3D and TAFAC3D were fairly correlated with RV-EF (r = 0.49, $P = 0.01$, and r = 0.47, $P = 0.02$ respectively).

Table 1 Comparison between measurements of TA size and function by 2DE, RT3DE and MRI

	2DE	RT3DE	MRI
End-diastolic TAD (mm)	33.0 ± 8.5	43.2 ± 10.0	44.1 ± 9.2
End-diastolic TAA (mm^2)	—-	1835 ± 425	1869 ± 392
End-systolic TAD (mm)	27.0 ± 7.8	32.0 ± 8.7	32.5 ± 8.2
End-systolic TAA (mm^2)	—	1120 ± 307	1137 ± 288
TAFS (%)	18.7 ± 4.0	26.3 ± 5.9	26.7 ± 5.7
TAFAC (%)	—	39.3 ± 4.9	39.5 ± 4.7

TAD: Tricuspid annular diameter, TAA: Tricuspid annular area, TAFS: Tricuspid annulus fractional shortening and TAFAC: tricuspid annular fractional area change

DISCUSSION

In the present study, the morphological and functional aspects of TA were assessed by MRI and RT3DE. The main findings of our study are (1) TA shape was not circular but oval, (2) TAD measurement by RT3DE is more accurate than by 2DE, and (3) TA function was fairly correlated with RV function.

TAD measurements have an important role in the TV surgical decision-making process not only for the selection of patients undergoing surgery, but also the type of surgical technique (valve plication or ring placement)[13-15]. Although 2DE is helpful to assess TV function and to detect TR severity it has important limitations in describing TV morphological details, such as TAD[14,15]. RT3DE may yield more detailed anatomical description of TA morphology and function [16, 17]. In the present study, the TA was visualized well in all subjects allowing even measurements of its area. This is in accordance with Schnabel et al. [11] who reported well or at least sufficient TA visualization in over 90% of patients. The measurements of TAD by RT3DE and MRI showed good correlation without significant difference between both techniques. When TAD2D measurements were compared with the TAD3D and TADMRI measurements, 2D measurements were significantly underestimated. Analysis of TA motion by M-mode, 2DE and tissue Doppler imaging has been studied as a feasible marker for RV function reflecting the longitudinal RV shortening and lengthening. All these analyses described the physiological behavior of TA plane systolic motion towards the apex along the RV long axis [5–10]. The TA plane systolic displacement is not influenced by its complex structure and asymmetrical shape [18]. In the present study TA circumferential and horizontal motion along the RV short axis was assessed by RT3DE. TA motion along the RV short axis, which was fairly correlated with RV function that was assessed by MRI as a standard method for assessing RV ejection fraction. Fair and not good correlation may be explained by the meridional motion of the muscles and other structures of the RV inflow region. Furthermore, the myocytes are disposed longitudinally in the inflow region and more sensitive

to meridional stress [19]. Despite this fair correlation, the summation of TA motion along both RV long and short axes increases the accuracy and correlation values for estimation of RV function [20].

Study Limitations

The main limitation of this study is that RT3DE images more critically depend on image quality than 2DE images and the value of RT3DE should be assessed in a more non-selected (image quality). Due to the high cost of MRI, a small number of patients were included.

CONCLUSION

RT3DE helps in accurate assessment of TA comparable to MRI, while 2DE could not be relied on due to underestimation. This may have important implications in the TV surgical decision-making processes. RT3DE analysis of TA function could be used as a marker of RV function.

REFERENCES

1. Silver MD, Lam JH, Ranganathan N, Wigle ED. Morphology of the human tricuspid valve. Circulation 1971;43:333-48.

2. Yacoub MH, Cohn LH. Novel approaches to cardiac valve repair: from structure to function: Part II. Circulation 2004;109:1064-72.

3. McGrath LB, Gonzalez-Lavin L, Bailey BM, Grunkemeier GL, Fernandez J, Laub GW. Tricuspid valve operations in 530 patients. Twenty-five-year assessment of early and late phase events. J Thorac Cardiovasc Surg 1990;99:124-33.

4. Colombo T, Russo C, Ciliberto GR, Lanfranconi M, Bruschi G, Agati S, Vitali E. Tricuspid regurgitation secondary to mitral valve disease: tricuspid annulus function as guide to tricuspid valve repair. Cardiovasc Surg 2001;9:369-77.

5. Alam M, Samad BA. Detection of exercise-induced reversible right ventricular wall motion abnormalities using echocardiographic determined tricuspid annular motion. Am J Cardiol 1999;83:103-5, A8.

6. Shah AR, Grodman R, Salazar MF, Rehman NU, Coppola J, Braff R. Assessment of acute right ventricular dysfunction induced by right coronary artery occlusion using echocardiographic atrioventricular plane displacement. Echocardiography 2000;17:513-9.

7. Therrien J, Henein MY, Li W, Somerville J, Rigby M. Right ventricular long axis function in adults and children with Ebstein's malformation. Int J Cardiol 2000;73:243-9.

8. Ghio S, Recusani F, Klersy C, Sebastiani R, Laudisa ML, Campana C, Gavazzi A, Tavazzi L. Prognostic usefulness of the tricuspid annular plane systolic excursion in patients with congestive heart failure secondary to idiopathic or ischemic dilated cardiomyopathy. Am J Cardiol 2000;85:837-42.

9. Alam M, Wardell J, Andersson E, Samad BA, Nordlander R. Characteristics of mitral and tricuspid annular velocities determined by pulsed wave Doppler tissue imaging in healthy subjects. J Am Soc Echocardiogr 1999;12:618-28.

10. Alam M, Wardell J, Andersson E, Samad BA, Nordlander R. Right ventricular function in patients with first inferior myocardial infarction: assessment by tricuspid annular motion and tricuspid annular velocity. Am Heart J 2000;139:710-5.

11. Schnabel R, Khaw AV, von Bardeleben RS, Strasser C, Kramm T, Meyer J, Mohr-Kahaly S. Assessment of the tricuspid valve morphology by transthoracic real-time-3D-echocardiography. Echocardiography 2005;22:15-23.

12. Bland JM, Altman DG. Statistical methods for assessing agreement between two methods of clinical measurement. Lancet 1986;1:307-10.

13. Goldman ME, Guarino T, Fuster V, Mindich B. The necessity for tricuspid valve repair can be determined intraoperatively by two-dimensional echocardiography. J Thorac Cardiovasc Surg 1987;94:542-50.

14. De Simone R, Lange R, Tanzeem A, Gams E, Hagl S. Adjustable tricuspid valve annuloplasty assisted by intraoperative transesophageal color Doppler echocardiography. Am J Cardiol 1993;71:926-31.

15. Dreyfus GD, Corbi PJ, Chan KM, Bahrami T. Secondary tricuspid regurgitation or dilatation: which should be the criteria for surgical repair? Ann Thorac Surg 2005;79:127-32.

16. Fukuda S, Saracino G, Matsumura Y, Daimon M, Tran H, greenberg NL, Hozumi T, Yoshikawa J, Thomas JD, Shiota T (2006) Three-dimensional geometry of the tricuspid annulus in healthy subjects and in patients with functional tricuspid regurgitation. Circulation 114(suppl I):492–498

17. Anwar AM, Geleijnse ML, ten Cate FJ, Meijboom FJ Assessment of tricuspid valve annulus size, shape
and function using real-time three-dimensional echocardiography. Interactive CardioVascular and Thoracic Surgery 2006; 10.1510/icvts.2006.132381

18. Ueti OM, Camargo EE, Ueti A de A, de Lima-Filho EC, Nogueira (2002) Assessment of right ventricular function with Doppler echocardiographic indices derived from tricuspid annular motion: comparison with radionuvleide angiography. Heart 88:244–248

19. Squara P, Journois D, Estagnasie P (1997) Elastic energy an index of right ventricular filling. Chest 11:351–358

20. Smith JL, Bolson EL, wang SP, Hubka M, Sheehan FH (2003) Three-dimensional assessment of two-dimensional
technique for evaluation of right ventricular function by tricuspid annulus motion. Int J Cardiovasc Imaging 19(3):189–197

CHAPTER 4

Evaluation of Rheumatic Tricuspid Valve Stenosis by Real-Time Three-Dimensional Echocardiography

Ashraf M. Anwar[1,2], Marcel L. Geleijnse[1], Osama I.I. Soliman[1,2], Jackie S Mcghie[1], Attila Nemes[1,3], and Folkert J. ten Cate[1]

[1]Department of Cardiology, Thoraxcenter, Erasmus University Medical Center, Rotterdam, The Netherlands
[2]Department of Cardiology, Al-Hussein University Hospital, Al-Azhar University, Cairo, Egypt
[3]Second Department of Medicine and Cardiology Center, University of Szeged, Szeged, Hungary

Heart 2007;93:363-364

INTRODUCTION

Rheumatic heart disease causes tricuspid valve (TV) stenosis in up to 8% of patients [1]. Unfortunately, TV stenosis is easily missed at clinical examination except in advanced cases when a high degree of clinical suspicion exists [2]. Undetected and thus uncorrected TV stenosis may lead to postoperative low cardiac output despite successful relief of left sided valve disease and carries a high mortality and morbidity [3]. Two-dimensional echocardiography (2DE) can detect thickened TV leaflets and a reduced TV orifice diameter, and continuous-wave Doppler allows estimation of the tricuspid transvalvular pressure gradient [4]. However, in most patients it is not possible to visualize all three TV leaflets simultaneously with 2DE [5]. Transthoracic real-time three-dimensional echocardiography (RT3DE) may be a valuable imaging modality for the examination of stenotic TV valves because all leaflets can be seen simultaneously and studied from both atrial and ventricular aspects. This study aimed to apply RT3DE for TV assessment in patients with rheumatic TV heart disease.

PATIENTS AND METHODS

Five patients (mean (SD) age 33 (7) years, four men) with an established diagnosis of rheumatic TV disease were examined by 2DE (Philips Sonos 7500 with S3 probe, Best, The Netherlands) and RT3DE (same system with X4 probe). These patients were compared to eight patients (mean (SD) age 35 (4) years, five men) with rheumatic heart disease without relevant TV involvement and 13 controls (mean (SD) age 31 (6) years, eight men) without rheumatic heart disease. With 2DE, the TV was assessed from the apical 4-chamber and parasternal short axis views. 2DE data obtained were: (1) TV leaflet separation (TV-LS_{2D}) defined as the distance between the TV tips at maximal opening obtained from an apical 4-chamber (TV-$LS_{2D\text{-}AP4CH}$) and parasternal short-axis window (TV-$LS_{2D\text{-}PSAX}$), (2) tricuspid annular diameter (TAD_{2D}) obtained from an apical 4-chamber ($TAD_{2D\text{-}AP4CH}$) and parasternal short-axis ($TAD_{2D\text{-}PSAX}$) view at an end-diastolic still-frame, and (3) descriptive morphology of the TV leaflets including thickness, mobility and calcification. Each descriptor was graded as mild when less than one whole TV leaflet was involved, moderate when a one or two whole TV leaflets were involved and severe when all three TV leaflets were involved.

The apical recorded full volume three-dimensional data set was analysed with TomTec software (Unterschleissheim, Munich, Germany). RT3DE data obtained were: (1) TAD_{3D} defined as the widest TAD that could be measured from an end-diastolic still frame, (2) maximal tricuspid annulus

area (TAA_{3D}) obtained from an end-diastolic still frame and measured by manual planimetry, (3) TV area (TVA_{3D}) defined as the narrowest part of the TV at the time of maximal TV opening and measured by manual planimetry, (4) descriptive TV morphology as described before in the 2DE section but now separately scored for each TV leaflet, and (5) commissural width for each TV commissure (antero-septal, antero-posterior, and postero-septal), obtained from an end-diastolic still frame.

RESULTS

$TV\text{-}LS_{2D\text{-}AP4CH}$ and $TV\text{-}LS_{2D\text{-}PSAX}$ were well correlated (r = 0.89, P <0.05) with comparable mean (SD) values for $TV\text{-}LS_{2D\text{-}AP4CH}$ and $TV\text{-}LS_{2D\text{-}PSAX}$ (11.8 (2.6) vs. 11.8 (3.4) mm, respectively). As Table 1 shows mean $TV\text{-}LS_{2D}$ values were not significantly different in the three studied groups.

Acquisition and post-processing of RT3DE data was successfully performed in all patients. TAD_{3D} was larger than TAD_{2D} in all TV stenosis patients, regardless of the 2DE view used (mean values were 46 mm for TAD_{3D}, 38 mm for $TAD_{2D\text{-}AP4CH}$, and 35 mm for $TAD_{2D\text{-}PSAX}$). Mean (SD) TVA_{3D} in the patients with significant TV stenosis was 216 (61) mm^2, correlated well with mean $TV\text{-}LS_{2D}$ (r = 0.95, P <0.01). Due to the small number of patients, TVA_{3D} was not significantly related to the transtricuspid mean pressure gradient (r = -0.76).

RT3DE and morphological description (including thickness, mobility, calcification, and position) was possible for each separate TV leaflet. The grade of TV leaflet affection scored with 2DE and RT3DE were similar in terms of thickness, mobility, and calcification. However, RT3DE could also assess individual TV leaflet position (relative to other TV leaflets) and the extent of TV affection. In addition, all three commissures could be adequately evaluated with RT3DE including assessment of commissural width during maximal TV opening. As seen in the Table, patients with TV stenosis had significantly smaller commissural width.

Table 1. Comparison of patients with rheumatic heart disease with tricuspid valve stenosis, without significant tricuspid valve stenosis, and controls.

	Rheumatic HD TV with stenosis (n = 5)	**Rheumatic HD TV without stenosis (n = 8)**	**Controls (n = 13)**
Male sex, n (%)	4 (80)	5 (63)	8 (62)
Age (years)	33 (7)	35 (4)	31 (6)
$TV\text{-}LS_{2D}$ (mm)	11.8 (2.9)	12.0 (4.8)	15.0 (3.3)
TVA_{3D} (mm^2)	216 (61)*	381 (92)	518 (207)
3D commissural width (mm)	2.6 (0.2)*	4.1 (0.5)	5.9 (1.6)

2D, two-dimensional; 3D, three dimensional; HD, heart disease; LS, leaflet separation; TV, tricuspid valve; TVA, tricuspid valve area.
Values are represented as mean (SD) unless otherwise specified.
*P <0.005 versus patients with rheumatic HD without significant TV involvement and $P < 0.0001$ versus controls.

DISCUSSION

Rheumatic TV inflammation causes scarring and fibrosis of TV leaflets with fusion of its commissures resulting in TV stenosis. Estimation of the transtricuspid pressure gradient is usually only performed when a morphologically abnormal TV is seen. Therefore, good morphological imaging and description of the TV is essential to identify TV stenosis. With RT3DE, each separate TV leaflet can be assessed with regard to thickness, mobility, calcification, and its relation to other TV leaflets. In addition, RT3DE provides unique TV measurements such as TVA_{3D} and commissural width at the time of maximal TV opening. This distance between the TV commissures during diastole may be a new indicator of TV stenosis severity. Although the TV leaflets can sometimes be visualised simultaneously by 2DE from an angulated subcostal view, measurement of TVA is only rarely possible because even when all leaflets are visualised simultaneously the image cross section will not be at the correct TVA level. Unfortunately, from all other 2DE views, including the atypical parasternal projection [5], only two TV leaflets can be visualized simultaneously. In our study, TVA_{3D} had better discriminative value than $TV\text{-}LS_{2D}$ for the separation of rheumatic heart disease patients with TV involvement versus rheumatic heart disease patients without TV involvement or normal control subjects (see Table). Importantly, in rheumatic TV involvement TVA_{3D} best correlated to the mean transtricuspid pressure gradient than mean $TV\text{-}LS_{2D}$. Obviously, our findings should be confirmed in larger studies and some of our findings should be validated using a gold standard such as magnetic resonance imaging. By combining all information obtained by RT3DE the diagnostic and therapeutic decision-making process regarding the TV may be facilitated.

REFERENCES

1. Hauck AJ, Freeman DP, Ackermann DM, Danielson GK, Edwards WD. Surgical pathology of the tricuspid valve: a study of 363 cases spanning 25 years. *Mayo Clin Proc* 1988; 63(9): 851-63.
2. Parris TM, Panidis JP, Ross J, Mintz GS. Doppler echocardiographic findings in rheumatic tricuspid stenosis. *Am J Cardiol* 1987; 60(16): 1414-6.
3. Fisher EA and Goldman ME. Simple, rapid method for quantification of tricuspid regurgitation by two-dimensional echocardiography. *Am J Cardiol* 1989; 63(18): 1375-8.
4. Pearlman AS. Role of echocardiography in the diagnosis and evaluation of severity of mitral and tricuspid stenosis. *Circulation* 1991; 84 (3 Suppl): I193-7.
5. Schnabel R, Khaw AV, von Bardeleben RS, Strasser C, Kramm T, Meyer J, Mohr-Kahaly S. Assessment of the tricuspid valve morphology by transthoracic real-time-3D-echocardiography. *Echocardiography* 2005; 22(1): 15-23.

CHAPTER 5

Assessment of Normal Tricuspid Valve Anatomy by Real-Time Three-Dimensional Echocardiography

Ashraf M. Anwar[1,2], Marcel L. Geleijnse[1], Osama I.I. Soliman[1,2], Jackie S McGhie[1], Rene Frowijn[1], Attila Nemes[1,3], Annemien E van den Bosch[1], Tjebbe W. Galema[1], and Folkert J. ten Cate[1]

[1]Department of Cardiology, Thoraxcenter, Erasmus University Medical Center, Rotterdam, The Netherlands
[2]Department of Cardiology, Al-Hussein University Hospital, Al-Azhar University, Cairo, Egypt
[3]Second Department of Medicine and Cardiology Center, University of Szeged, Szeged, Hungary

International Journal of Cardiovascular Imaging 2008;

ABSTRACT

Background: The tricuspid valve (TV) is a complex structure. Unlike the aortic and mitral valve it is not possible to visualize all TV leaflets simultaneously in one cross-sectional view by standard two-dimensional echocardiography (2DE) either transthoracic or transesophageal due to the position of TV in the far field.

Aim: Quantitative and qualitative assessment of the normal TV using real-time 3-dimensional echocardiography (RT3DE).

Methods: RT3DE was performed for 100 normal adults (mean age 30 ± 9 years, 65% males). RT3DE visualization was evaluated by 4-point score (1: not visualized, 2: inadequate, 3: sufficient, and 4: excellent). Measurements included TV annulus diameters (TAD), TV area (TVA), and commissural width.

Results: In 90% of patients with good 2DE image quality, it was possible to analyse TV anatomy by RT3DE. A detailed anatomical structure including unique description and measurement of tricuspid annulus shape and size, TV leaflets shape, and mobility, and TV commissural width were obtained in majority of patients. Identification of each TV leaflet as seen in the routine 2DE views was obtained.

Conclusion: RT3DE of the TV is feasible in a large number of patients. RT3DE may add to functional 2DE data in description of TV anatomy and providing highly reproducible and actual reality (anatomical and functional) measurements

INTRODUCTION

The tricuspid valve (TV) is a multi-component complex structure [1]. In classic anatomic studies the anterior, septal and posterior TV cusps were described [2,3]. Unlike the aortic and mitral valve it is not possible to visualize all TV cusps simultaneously in one cross-sectional view by standard two-dimensional transthoracic echocardiography (2DE)[4]. During transesophageal two-dimensional echocardiography small changes in transducer angle, probe position and rotation may bring to light some additional TV details [5,6]. However, because of the position of the TV in the far field, transesophageal echocardiography can still only provide limited information and can also not visualize all TV cusps simultaneously. In three-dimensional (3D) transesophageal image reconstruction and intracardiac echocardiography studies this goal could be achieved but at the cost of some procedural risks and an increase in procedural duration [7,8]. Real-time three-dimensional echocardiography (RT3DE) can visualize the atrio-ventricular valves from both the ventricular and atrial side in detail without these limitations [9]. This study aimed to apply RT3DE for quantitative and qualitative assessment of normal TV anatomy.

SUBJECTS AND METHODS

In one hundred patients (mean age 30 ± 9 years, 65% males) the TV was examined by transthoracic RT3DE after an informed consent. All patients had sinus rhythm and normal right-sided heart (normal right ventricular dimensions and function, normal right atrial dimension, trivial or absent tricuspid regurgitation and normal tricuspid valve function). Patients with good 2DE image quality only were included.

Transthoracic RT3DE

RT3DE was done with a commercially available ultrasound system (Philips Sonos 7500, Best, The Netherlands) attached to a X4 matrix array transducer capable of providing real-time B-mode images. The 3D data set was collected within approximately 5-10 seconds of breath holding in full volume mode from an apical window and transferred for off-line analysis with TomTec software (Unterschleissheim, Munich, Germany). Data analysis of 3D images was based on a two-dimensional approach relying on images obtained initially from the apical 4-chamber view. The images were adjusted to put the TV in the center of interest. To exclude non-relevant tissue, the TV was sliced between the two narrowest lines by which all parts of the TV leaflets were still in between. The TomTec software allows in this way visualization of the short-axis TV view in a 3D display (see Figure 1). RT3DE gain and brightness were adjusted to improve delineation of anatomic structures. The following points were checked for visualization: 1) tricuspid annulus diameter and area, 2) TV leaflets (number, mobility,

thickness and relation to each other), 3) TV area, and 4) TV commissures (antero-septal, antero-posterior, and postero-septal) including the position of their closure lines. All these structures were classified according to a subjective 4-point scale for image quality (1 = not visualized, 2 = inadequate, 3 = sufficient and 4 = good).

For quantitative assessment of TV the following RT3DE data were obtained: 1) TV annulus diameter defined as the widest diameter that could be measured from an end-diastolic still frame, 2) maximal TV annulus area obtained from an end-diastolic still frame and measured by manual planimetry, 3) TV area defined as the narrowest part of the TV at the time of maximal opening and measured by manual planimetry, and 4) TV commissural width obtained from a late-diastolic still frame using zoom function to avoid underestimation. The images were optimized for each commissure along its plane to measure the maximal width of the angle formed by the to adjacent TV leaflets.

To identify the TV leaflets visualized by the standard 2DE images the TomTec quad screen display was used. As seen in Figure 1, this screen contains four images; the upper two images are two-dimensional echocardiographic images perpendicular to each other, the lower two images are a short-axis two-dimensional echocardiographic image and a RT3DE image. From the properly chosen two-dimensional image a mid-diastolic frame was selected to visualize the TV leaflets just separated from each other. Each leaflet was defined by a marker, after which this marker position was compared with the RT3DE image to detect which leaflet was shown in the 2DE images. Analysis of images was done by two experienced echocardiographers (AMA, JSM) independently. Each one dealt with the full volume image as acquired from echo machine and the selection of cut plane, angulation and gain setting adjustment were dependable on his experience.

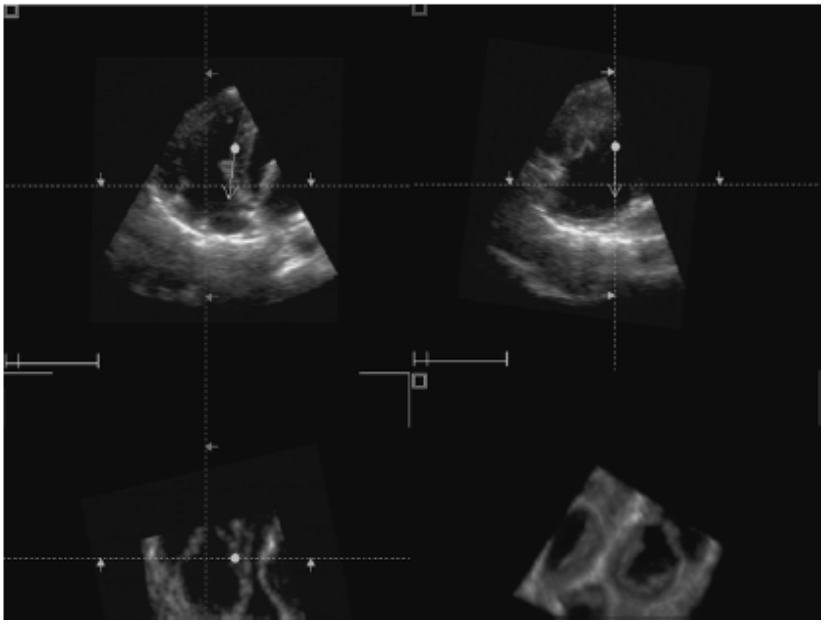

Fig. 1 TomTec quadri screen display of the tricuspid valve. The upper two images represent two-dimensional views created from the 3D data set (4-chamber, left and orthogonal view, right). The lower left image represents a two-dimensional short axis view and the lower right image represents the 3D image

STATISTICAL ANALYSES

All data obtained by RT3DE were presented as mean ± SD. Interobserver agreement for the visualization score was estimated using kappa values for each morphologic feature and classified as poor (kappa <0.4), moderate (kappa 0.4 to 0.7), or good (kappa >0.7). Interobserver variability for RT3DE measurements was assessed according to the Bland and Altman method in a randomly selected group of 50 patients [10].

RESULTS

Acquisition and analysis of the RT3DE data was performed in approximately 10 minutes per patient. The TV could be visualized in 90% of patients enface from both ventricular and atrial aspects in relation to adjacent cardiac structures. In these 90 patients detailed analysis of the TV was performed including tricuspid annulus shape and size, TV leaflets shape, size, and mobility, and commissural width.

Tricuspid annulus

Tricuspid annulus visualization was good in 54 patients (60%), sufficient in 27 patients (30%), and inadequate in 9 patients (10%). As seen in Figure 2, tricuspid annulus shape appeared as oval rather than circular. Tricuspid annulus diameter and area could be measured in 63 patients (70%), normal values were 4.0 ± 0.7 cm and 10.0 ± 2.9 cm^2, respectively.

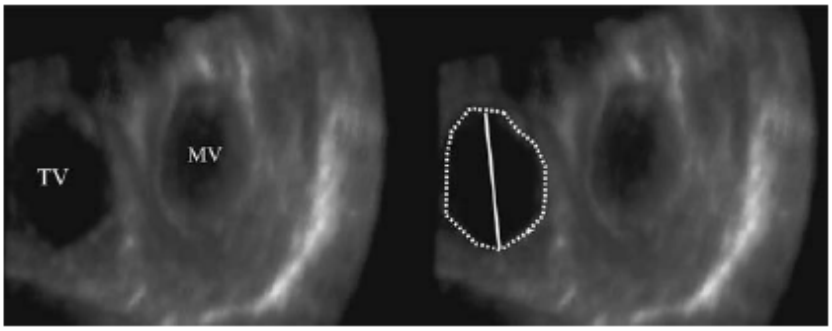

Fig. 2 Oval-shaped Tricuspid annulus (the line represent the tricuspid annulus diameter, the dots demark the area)

Tricuspid valve leaflets

Visualization of the three TV leaflets (in motion) was good visualized in 72 patients (80%), sufficient in 9 patients (10%), and inadequate in another 9 patients (10%). The anterior leaflet was the largest and most mobile of the three leaflets and had a nearly semicircular shape. The septal leaflet was the least mobile and had a semi-oval shape. Its position was parallel to the interventricular septum. The posterior leaflet was the smallest one with variable shape. It was clearly separated from the septal leaflet in all patients but in 10% of patients it was hard to discriminate the posterior leaflet from the anterior leaflet even during maximal TV opening.

From the RT3DE data set all standard two-dimensional TV cross-sections (apical 4-chamber, parasternal short-axis and parasternal long-axis right ventricular inflow) were simulated. As seen in Figure 3, in the apical 4-chamber view in all patients the septal leaflet was seen adjacent to the septum and the anterior leaflet was seen adjacent to the right ventricular free wall. In the parasternal short-axis view, the posterior leaflet was seen adjacent to the right ventricular free wall in 92% of patients and in the remaining 8% no leaflet could be obtained although modification of the cut plane downward could identify this leaflet. In this view the leaflet adjacent to the aorta was the anterior in 52% and the septal leaflet in 48%. In the parasternal right ventricular inflow view the leaflets seen were identical to the apical 4-chamber view with in all patients the septal leaflet seen adjacent to the septum and the anterior leaflet seen adjacent to the right ventricular free wall.

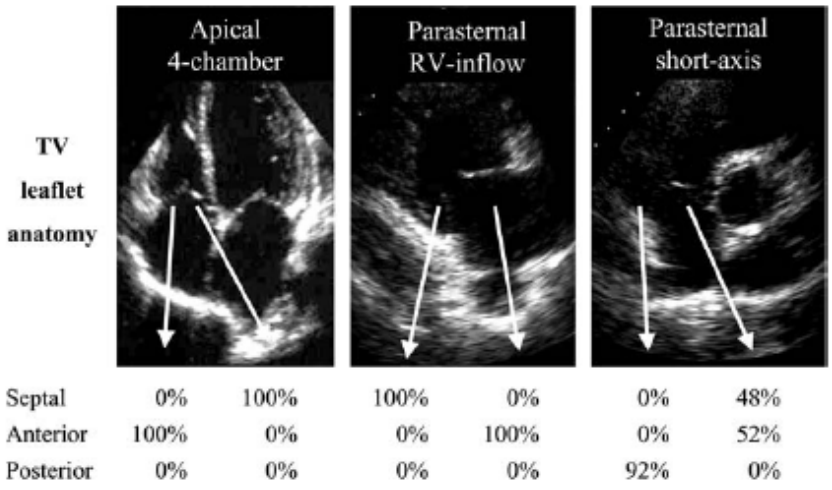

Fig. 3 Identification of the tricuspid valve leaflets seen on two-dimensional imaging. Below the 2D images, percentage of leaflet identification in each standard view depending the RT3DE images

Tricuspid valve area

Visualization of the triangular shaped TV area was visualized good in 50 patients (55%), sufficient in 27 patients (30%), and inadequate in 13 patients (15%). As seen in Figure 4, the anterior and septal leaflets formed the TV area's angle and the small posterior leaflet formed its base. TV area could be measured in 77 patients (86%) and mean TV area in these patients was 4.8 ± 1.6 cm^2.

Tricuspid valve commissures

As seen in Figure 4, the three TV leaflets were separated from each other by three commissures. The commissures and the direction of closure lines were good visualized in 45 patients (50%), sufficient in 18 patients (20%), inadequate in 18 patients (20%), and not visualized in 9 patients (10%). TV commissural width could be obtained in 63 patients (70%), mean commissural width in these patients was 5.4 ± 1.5 mm for the antero-septal commissure, 5.2 ± 1.5 mm for the postero-septal commissure, and 5.1 ± 1.1 mm for the antero-posterior commissure, respectively. Visualization and measurement of commissures was relatively easy for the

antero-septal commissure and most difficult for the antero-posterior commissure. All measurements are listed in Table 2 as absolute value and indexed to body surface area.

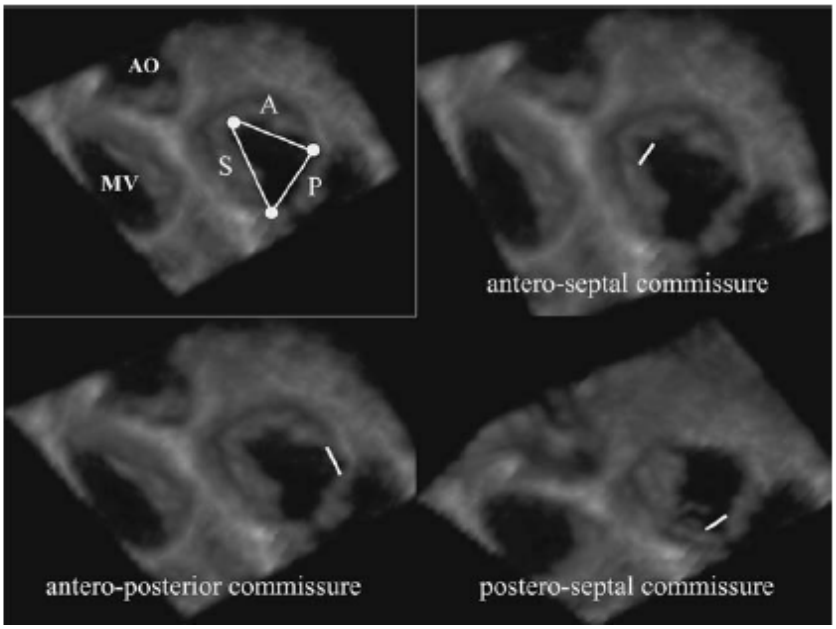

Fig. 4 Triangular shape TV area and commissural views

Table 1: Scores for real-time three-dimensional echocardiography visualization of TV structures.

Score	TV Annulus	TV Leaflets	TV area	TV commissures
Good (4)	60%	80%	55%	50%
Sufficient (3)	30%	10%	30%	20%
Inadequate (2)	10%	10%	15%	20%
Not visualized (1)	0%	0%	0%	10%
Mean score	3.5 ± 0.7	3.7 ± 0.6	3.4 ± 0.7	3.1 ± 1.0
Median score	3.0	3.0	3.0	2.5

Abbreviations: TV = tricuspid valve

Table 2: Normal (absolute and index) values of TV annulus (diameter and area), TV area, and the width of the 3 TV commissures.

Parameter	Absolute value	Index Value
Tricuspid annulus diameter	4.0 ± 0.7 (cm)	2.2 ± 0.4 (cm/m^2)
Tricuspid annulus area	10.0 ± 2.9 (cm^2)	5.5 ± 1.6 (cm^2/m^2)
Tricuspid valve area	4.8 ± 1.6 (cm^2)	2.7 ± 0.9 (cm^2/m^2)
Antero-septal commissure	5.4 ± 1.5 (mm)	2.9 ± 0.8 (mm/m^2)
Postero-septal commissure	5.2 ± 1.5 (mm)	2.9 ± 0.7 (mm/m^2)
Antero-posterior commissure	5.1 ± 1.1 (mm)	2.9 ± 0.6 (mm/m^2)

Interobserver variability

The visualization score between two observers was good for the TV annulus (kappa value 0.91) and TV leaflets (kappa value 0.71) and moderate for the TV commissures (kappa value 0.59). As seen in Figure 5, good

interobserver correlations were found for measurement of TV annulus (r = 0.98, P <0.0001) and TV area (r = 0.95, P <0.0001) and fair correlation was found for TV commissural width (r = 0.51, P <0.001). In the same Figure, the interobserver agreement for TV annulus diameter (mean difference - 0.28 ± 1.20 mm, agreement: 2.12, - 2.68), for TV area (mean difference: 0.17 ± 0.52 cm^2, agreement: 1.21, - 0.87), and for TV commissural width (mean difference: 0.01 ± 0.62 mm, agreement: 1.25, - 1.24) is displayed.

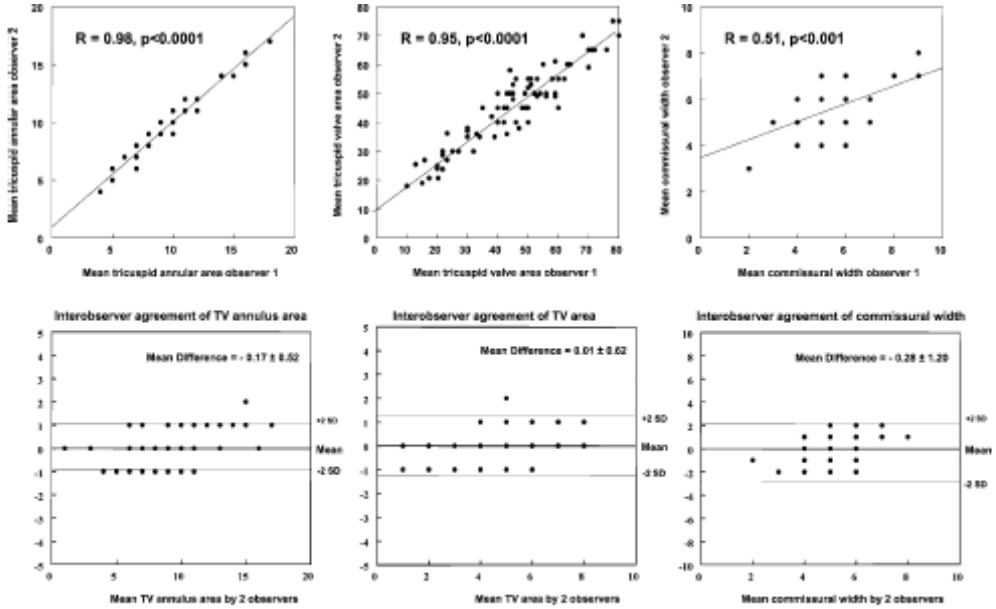

Fig. 5 Interobserver correlations (top) and Bland–Altman analysis (bottom) of TV annulus, leaflets, and commissures

DISCUSSION

Two-dimensional echocardiography is a valuable imaging modality for the functional assessment of TV [11-13]. However, with 2DE it is not possible to visualize all TV cusps simultaneously in one cross-sectional view nor can detailed anatomical information of the TV annulus, leaflets, and commissures be provided. Previous studies and case reports described visualization of TV by RT3DE [9,14] in abnormal states, while this study applied RT3DE for the morphological assessment of the normal TV anatomy. RT3DE allowed analysis of TV annulus, leaflets and commissures in the majority of patients. Beside this morphologic description, quantitative assessment could be obtained. However, it should be noticed that only patients with good 2DE image quality underwent RT3DE. In our experience these patients represent over 50% of the total number of patients referred to our echocardiographic laboratory. Nevertheless, RT3DE allowed TV analysis to a level quite comparable to that recently reported by others for the mitral valve leaflets [15].

One of the salient findings in our study was the identification of the TV leaflets as seen in the routine 2DE views. It is still a matter of controversy in echocardiographic textbooks. In one well known echocardiographic textbook [16], the leaflet seen in the apical 4-chamber view adjacent to the right ventricular free wall was described as being the anterior or posterior leaflet depending on the exact rotation and angulation of the image plane. However, in our study this leaflet was consistently found to be the anterior leaflet (see Figure 6 for explanation), as described in another textbook [17]. Also, in both these echocardiographic textbooks [16,17] in the parasternal short-axis view the leaflet adjacent to the right ventricular free wall was described as being the anterior. However, as shown in Figure 3 and explained in Figure 6, in all patients in whom a leaflet could be identified in our study it was the posterior one.

In our study tricuspid annulus diameter (and area) could be reliably obtained with RT3DE. Tricuspid annulus measurement is of critical importance in the TV surgical decision-making process if a patient is operated for mitral valve disease and has concomitant TV regurgitation [18,19]. In addition, TV area could be reliably obtained and this may have important implications for the diagnosis of tricuspid stenosis [20,21]. Visualization of commissures and measurement of its width were obtained with difficulty, in particular for the antero-posterior commissure. Commissural width also showed weak interobserver correlation. This may be due to differences in the commissural levels and tissue dropout. For proper assessment of the three commissures, more cut planes with different angles are needed. However, assessment of commissural width may also be a valuable tool for the diagnosis, follow up, and selection of therapeutic strategy of tricuspid stenosis. All our RT3DE measurements were consistent with the measurements described in anatomical studies [2,3]. Our data may potentially take RT3DE a step further into clinical routine (providing accurate TV measurements) and may enhance the understanding of TV valve morphology.

Limitation of Study

The main limitation of this study is that RT3DE data were not compared with a “gold standard” such as magnetic resonance imaging, autopsy or surgical findings. Also, RT3DE images more critically depend on 2DE image quality.

CONCLUSION

Three-dimensional imaging of the TV is feasible in a large number of patients. RT3DE may add to functional 2DE data in description of TV anatomy and providing highly reproducible and actual reality (anatomic and functional) measurements.

REFERENCES

1 Lamers WH, Viragh S, Wessels A, et al. Formation of the tricuspid valve in the human heart. Circulation 1995; 91:111-121

2 Silver MD, Lam JH, Ranganathan N, et al. Morphology of the human tricuspid valve. Circulation 1971; 43:333-348

3 Wafae N, Hayashi H, Gerola LR, et al. Anatomical study of the human tricuspid valve. Surg Radiol Anat 1990; 12:37-41

4 Maslow AD, Schwartz C, Singh AK. Assessment of the tricuspid valve: a comparison of four transesophageal echocardiographic windows. J Cardiothorac Vasc Anesth 2004; 18:719-724

5 Pandian NG, Hsu TL, Schwartz SL, et al. Multiplane transesophageal echocardiography. Imaging planes, echocardiographic anatomy, and clinical experience with a prototype phased array OmniPlane probe. Echocardiography 1992; 9:649-666

6 Zaroff JG, Picard MH. Transesophageal echocardiographic (TEE) evaluation of the mitral and tricuspid valves. Cardiol Clin 2000; 18:731-750

7 Light ED, Idriss SF, Wolf PD, et al. Real-time three-dimensional intracardiac echocardiography. Ultrasound Med Biol 2001; 27:1177-1183

8 Nekkanti R, Nanda NC, Ahmed S, et al. Transesophageal three-dimensional echocardiographic demonstration of clefts in the anterior tricuspid valve leaflet. Am J Geriatr Cardiol 2002; 11:329-330

9 Schnabel R, Khaw AV, von Bardeleben RS, et al. Assessment of the tricuspid valve morphology by transthoracic real-time-3D-echocardiography. Echocardiography 2005; 22:15-23

10 Bland JM, Altman DG. Statistical methods for assessing agreement between two methods of clinical measurement. Lancet 1986; 1:307-310

11 Colombo T, Russo C, Ciliberto GR, et al. Tricuspid regurgitation secondary to mitral valve disease: tricuspid annulus function as guide to tricuspid valve repair. Cardiovasc Surg 2001; 9:369-377

12 Tunon J, Cordoba M, Rey M, et al. Assessment of chronic tricuspid regurgitation by colour Doppler echocardiography: a comparison with angiography in the catheterization room. Eur Heart J 1994; 15:1074-1084

13 Rivera JM, Mele D, Vandervoort PM, et al. Effective regurgitant orifice area in tricuspid regurgitation: clinical implementation and follow-up study. Am Heart J 1994; 128:927-933

14 Faletra F, Marchesina U La, Bragato R, Chiara F De. Three dimensional transthoracic echocardiography images of tricuspid stenosis. Heart 2005; 91: 499.

15 Sugeng L, Coon P, Weinert L, et al. Use of real-time 3-dimensional transthoracic echocardiography in the evaluation of mitral valve disease. J Am Soc Echocardiogr 2006; 19:413-421

16 Otto C. Textbook of clinical echocardiography. 3rd ed: El-sevier Saunders, 2004

17 Feigenbaum H. Feigenbaum's Echocardiography. 6th ed. Philadelphia, USA: Lippincott, Williams & Wilkins, 2005

18 Goldman ME, Guarino T, Fuster V, et al. The necessity for tricuspid valve repair can be determined intraoperatively by two-dimensional echocardiography. J Thorac Cardiovasc Surg 1987; 94:542-550

19 De Simone R, Lange R, Tanzeem A, et al. Adjustable tricuspid valve annuloplasty assisted by intraoperative transesophageal color Doppler echocardiography. Am J Cardiol 1993; 71:926-931

20 Ribeiro PA, al Zaibag M, Idris MT. Percutaneous double balloon tricuspid valvotomy for severe tricuspid stenosis: 3-year follow-up study. Eur Heart J 1990; 11:1109-1112

21 Sharma S, Loya YS, Desai DM, et al. Percutaneous double-valve balloon valvotomy for multivalve stenosis: immediate results and intermediate-term follow-up. Am Heart J 1997; 133:64-70

CHAPTER 6

True Mitral Annulus Diameter is Underestimated by Two-dimensional Echocardiography as Evidenced by Real-Time Three-dimensional Echocardiography and Magnetic Resonance Imaging

Ashraf M. Anwar MD[1,2], Osama I.I. Soliman MD[1], Folkert J. ten Cate MD[1], Attila Nemes MD[1,4], Jackie S. McGhie MSc[1], Boudewijn J. Krenning MD[1], Robert-Jan van Geuns MD[1,3], Tjebbe W. Galema MD[1], Marcel L. Geleijnse MD[1]

[1]Department of Cardiology, Thoraxcenter, Erasmus University Medical Center, Rotterdam, The Netherlands
[2]Department of Cardiology, Al-Hussein University Hospital, Al-Azhar University, Cairo, Egypt
[3]Department of Radiology, Erasmus University Medical Center, Rotterdam, The Netherlands
[4]Second Department of Medicine and Cardiology Center, University of Szeged, Szeged, Hungary

International Journal of Cardiovascular Imaging 2007;

ABSTRACT

Background: Mitral annulus assessment is of great importance for the diagnosis and treatment of mitral valve disease. The present study sought to assess the value of real-time three-dimensional echocardiography for the assessment of true mitral annulus diameter (MAD).

Methods: One hundred and fifty patients (mean age 38 ± 18 years) with adequate two-dimensional (2D) echocardiographic image quality underwent assessment of MAD_{2D} and MAD_{3D} (with real-time three-dimensional echocardiography). In a subgroup of 30 patients true MAD was validated with magnetic resonance imaging (MRI).

Results: There was a good interobserver agreement for MAD_{2D} (mean difference = - 0.25 ± 2.90 mm, agreement: - 3.16, 2.66) and MAD_{3D} (mean difference = 0.29 ± 2.03, agreement = - 1.74, 2.32). Measurements of MAD_{2D} and MAD_{3D} were well correlated (R = 0.81; p <0.0001). However, MAD_{3D} was significantly larger than MAD_{2D} (3.7 ± 0.9 vs. 3.3 ± 0.8 cm, p <0.0001). In the subgroup of 30 patients with MRI validation, MAD_{3D} and MAD_{MRI} were significantly larger than MAD_{2D} (3.3 ± 0.5 and 3.4 ± 0.5 cm vs. 2.9 ± 0.4 cm, both p <0.001). There was no significant difference between MAD_{MRI} and MAD_{3D}.

Conclusion: MAD_{3D} can be reliably measured and is superior to MAD_{2D} in the assessment of true mitral annular size.

INTRODUCTION

The mitral annulus (MA) is a vital component of the mitral valve apparatus and plays a crucial role in left ventricular and left atrial function [1]. The MA marking the hinge line of the mitral valve leaflets is more D-shaped than circular as portrayed by prosthetic rings. The straight border accommodates the aortic valve allowing this valve to be wedged between the interventricular septum and the mitral valve. Although the term annulus implies a solid ring-like fibrous cord to which the leaflets are attached, this is not the case [2]. Therefore, some authors used the term "aortoventricular membrane" instead of MA, to emphasize that there is an extension of this fibrous cord into the subvalvular region [3]. MA assessment is of great importance for the diagnosis and treatment of mitral valve disease. MA dilatation is one of the main mechanisms for development of mitral regurgitation and selection of the optimal individual therapy for mitral regurgitation depends on MA size and function [4,5]. This has been studied in both animals and humans using echocardiography, sonomicrometry and magnetic resonance imaging (MRI) [6-11]. The present study aimed to assess true MA diameter (MAD) by comparing two-dimensional echocardiography (2DE), real-time three-dimensional echocardiography (RT3DE), and MRI as gold standard.

METHODS

The study included 150 patients (Table 1) randomly selected from our 3D database that included relatively young patients (mean age 38 ± 18 years) with adequate 2DE image quality. Age, gender, weight and height of all patients were recorded and body surface area was calculated by the standard formula (weight 0.425 in kilograms x height 0.725 in centimeters x 0.007184). In all patients, 2DE and RT3DE were performed.

Table1: Clinical categorization of patients (n = 150)

Category	**N (%)**
Normal	52 (34%)
Congenital Heart Disease	48 (32%)
Ischemic Heart Disease	20 (14%)
Valvular Disease	20 (14%)
Cardiomyopathy	10 (6%)

Transthoracic 2DE

2DE was undertaken with the patient lying in the left lateral decubitus position using both apical and parasternal views. 2DE studies were performed using a 3.5 MHZ probe and a commercially available

ultrasound system (Philips Sonos 7500, Best, The Netherlands). The following measures were obtained: (1) MA diameter (MAD_{2D}) obtained from an apical 4-chamber view at end-diastole (Just before mitral valve closure), and (2) MAD index ($MADI_{2D}$) calculated as MAD_{2D} / body surface area.

Transthoracic RT3DE

RT3DE was done with the same ultrasound system attached to a X4 matrix array transducer capable of providing real-time B-mode images. A full volume 3D data set was collected within approximately 5-10 seconds of breath holding in full volume mode from an apical window. The 3D data set was stored digitally and transferred for off-line analysis with TomTec software (Unterschleissheim, Munich, Germany). Two blinded observers (AMA, OIIS) subsequently evaluated all data. Data analysis of 3D images was based on a 2D approach relying on images obtained initially from the apical view. The MA was sliced between two narrow lines to exclude other tissue on the 2D image leading to clarification of the MA in the 3D image. The 3D image of the MA was viewed and traced from the ventricular aspect. Manual tracing of the inner border of the MA was done and once this was completed the surface area was automatically delineated and could be visualized from different points of views. The following RT3DE data were obtained: (1) end-diastolic MAD_{3D} defined as the perpendicular line drawn from the top of the MA curvature to the middle of the straight MA border (see Figure 1), (2) end-diastolic MA area (MAA_{3D}), (3) MAD_{3D} index ($MADI_{3D}$) calculated as MAD_{3D} / body surface area, and (4) MAA_{3D} index ($MAAI_{3D}$) calculated as MAA_{3D} / body surface area.

Normal values for MAD_{2D}, MAD_{3D}, $MADI_{3D}$, MAA_{3D}, and $MAAI_{3D}$ were established in 25 patients without apparent left-sided heart disease (defined as normal left atrial and ventricular dimension and function with normal mitral valve function).

Magnetic resonance imaging

In a non-selected group of 30 patients, MRI was performed with a 1.5 T MRI (General Electric, Signa 1.5 T MRI, Milwaukee WI) equipped with a for-element cardio coil. An ECG-triggered, steady state, free-precession sequence (FIESTA; repetition time and time of echo of 3.5 and 1.4 ms, respectively, 12 shots, temporal resolution of 42 ms, flip angle of 45 degrees) was used for quantitative analysis. Ten cine short axis slices were acquired (slice thickness 8 mm, gap 2 mm) covering the heart from the base to the apex. Additional imaging parameters were a field of view of 320 to 380 mm and a matrix of 160 X 128. Quantitative measurements were performed using standardized Dicom viewing software on the

basal slice demonstrating the mitral valve annulus in end-diastole. MAD_{MRI} was defined as described before in the RT3DE section (see Figure 1).

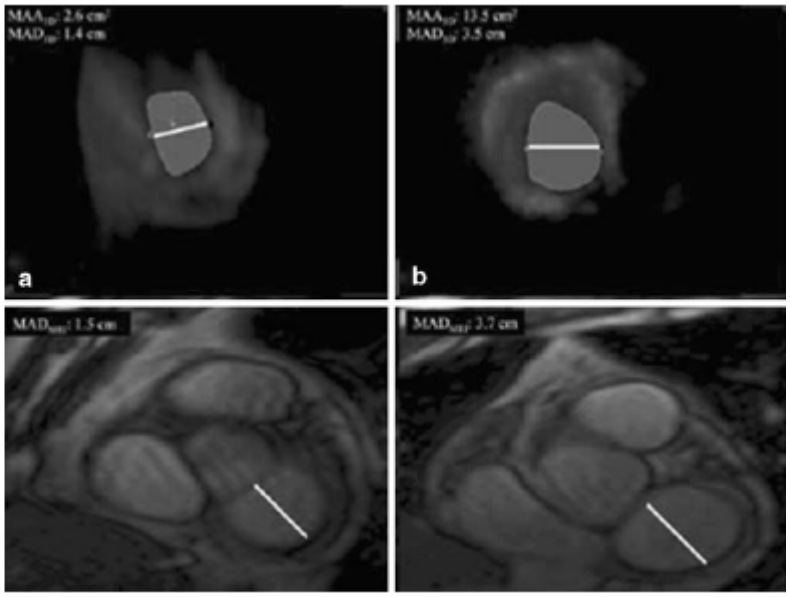

Fig. 1 Real-time three-dimensional echocardiographic images from the ventricular aspect of normal (**A**, top left) and dilated (**B**, top right) mitral annulus morphology. The D-shaped morphology can be clearly appreciated, as confirmed by the magnetic resonance images (**C**, **D** bottom) the straight border of **D** is anterior and the curvature is posterior. In all figures the white line indicates mitral annular diameter

STATISTICAL ANALYSES

All data obtained by 2DE, RT3DE, and MRI were presented as mean ± SD. Data analyses were performed using statistical software (SPSS, version 12.1, SPSS Inc, Chicago). A paired sample t-test was performed to compare between means of variables of techniques. The difference in values was considered statistically significant with the level of $P < 0.05$. Pearson's coefficient was used for correlation between variables. Interobserver and intraobserver agreements were assessed for MAD_{2D} and MAD_{3D} in the first 100 patients and expressed according to the Bland and Altman method [12].

RESULTS

Acquisition and post-processing of RT3DE data were performed successfully in all patients within a reasonable time (approximately 1 minute for acquisition and 5 minutes for data analysis). The MA was clearly delineated in all patients and, as seen in Figure 1, its shape was not circular but D-shaped, both in normal sized and in dilated MA. As seen in Figure 2, in the total group of 150 patients, measurements of MAD_{2D} and MAD_{3D} were well correlated ($R = 0.81$; $p < 0.0001$). However, MAD_{3D} was significantly larger than MAD_{2D} (3.7 ± 0.9 vs. 3.3 ± 0.8 cm, $P < 0.0001$).

Surgical validation: In three patients referred for mitral valve repair, MAD_{3D} matched with MAD measured by surgeon (blinded with MAD_{3D} measurement) while MAD_{2D} by preoperative transthoracic 2DE and intraoperative transesophageal echo was smaller than the surgical measurement.

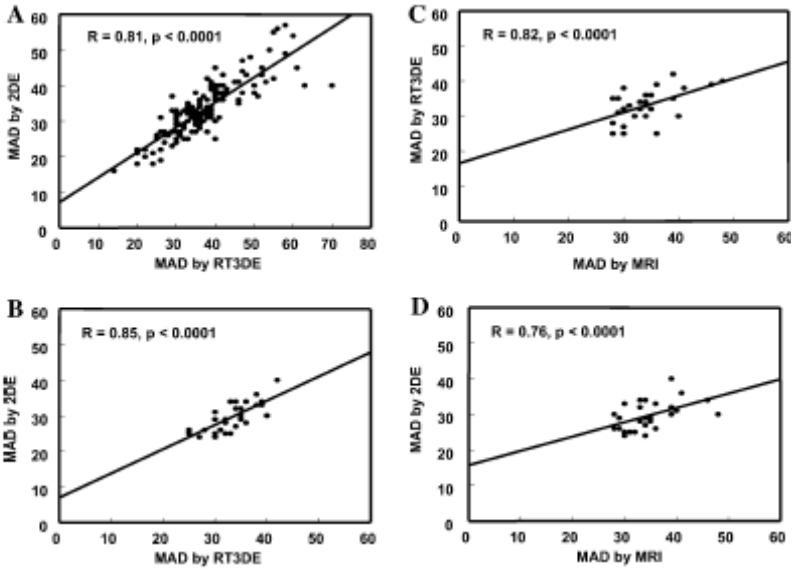

Fig. 2 Correlation between two-dimensional and three-dimensional echocardiographic mitral annulus diameter measurements in 150 patients (A), and in subgroup of 30 patients (B–D) that underwent magnetic resonance imaging

MRI validation: In the subgroup of 30 patients who underwent 2DE, RT3DE, and MRI, the D-shaped MA was confirmed by the MRI images (Figure 1d). As seen in Figure 3, MAD_{2D}, MAD_{3D}, and MAD_{MRI} were well correlated. MAD_{3D} and MAD_{MRI} were significantly larger than MAD_{2D} (3.3 ± 0.5 and 3.4 ± 0.5 cm vs. 2.9 ± 0.4 cm, both $P < 0.001$). There was no significant difference between MAD_{MRI} and MAD_{3D}. Also, there was no significant difference between MAA_{3D} and MAA_{MRI} (Table 2).

Table 2: Comparison between RT3DE and MRI measurements

	RT3DE	**MRI**
Diastolic MAA (cm^2)	8.7 ± 2.9	9.0 ± 2.3
Diastolic MAAI (cm^2/m^2)	4.7 ± 1.8	4.8 ± 2.0
Diastolic MAD (cm)	3.3 ± 0.5	3.4 ± 0.5
Diastolic MADI (cm/m^2)	1.8 ± 0.5	1.8 ± 0.7

Abbreviation: MAA: mitral annulus area, MAAI: mitral annulus area index, MAD: mitral annulus diameter, MADI: mitral annulus diameter index

Normal RT3DE values: Normal values assessed in patients without apparent left-sided heart disease were 2.5 ± 0.5 cm for MAD_{2D}, 2.8 ± 0.6 cm for MAD_{3D} , 1.5 ± 0.3 cm/m^2 for $MADI_{3D}$, 8.1 ± 2.4 cm^2 for MAA_{3D}, and 4.3 ± 0.8 cm^2/m^2 for $MAAI_{3D}$.

Interobserver and intraobserver agreements: As seen in Fig. 3, there was a good interobserver agreement for MAD_{2D} (mean difference = - 0.25 ± 2.90 mm, agreement: - 3.16, 2.66) and MAD_{3D} (mean difference = 0.29 ± 2.03mm, agreement = - 1.74, 2.32). Likewise, there was a good intraobserver agreement for MAD_{2D} (mean difference = - 0.23 ± 2.28mm, agreement = -2.51, 2.05) and MAD_{3D} (mean difference = - 0.10 ± 3.00mm, agreement = - 3.10, 2.92).

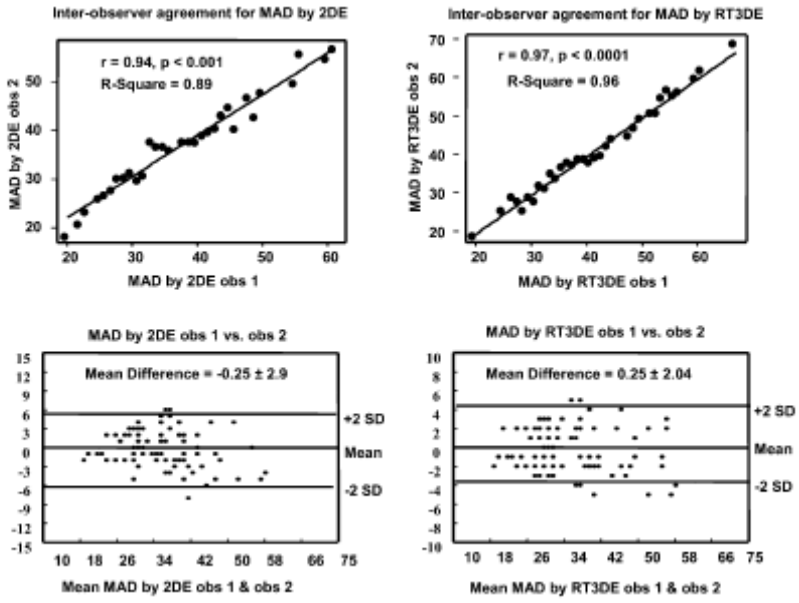

Fig. 3 Correlations and interobserver agreements of mitral annulus diameter as measured by two-dimensional and three-dimensional echocardiography

DISCUSSION

Assessment of MA size is an important issue in patients with mitral valve disease. An increase in MAD results in reduced mitral valve leaflet coaptation and thus an increase in the incidence and severity of mitral regurgitation [13,14]. Reduction in MAD is an essential element in mitral valve repair and prevention of regurgitation not only in organic mitral valve disease, but also in ischemic mitral regurgitation [15,16]. Accurate assessment of MAD is crucial for the selection of a proper sized prosthetic ring, percutaneous annuloplasty device or stented valve implantation [17-19]. The current study showed that in patients with adequate 2DE image quality, the MA could be well visualized from the ventricular (and atrial) aspect with RT3DE. MAD_{3D} could be reliably measured with excellent inter- and intraobserver agreements.

The main finding in our study was a significant underestimation of true MAD by MAD_{2D} as evidenced by MAD_{3D} and MAD_{MRI} measurements. Because of the relatively fixed MA trigone, changes in MAD size (regardless whether these are due to cyclic changes in the heart cycle or to a pathological process such as left ventricular dilatation) [7] occur mainly along the axis represented by the perpendicular line drawn from the top of the MA curvature to the middle of the straight MA. As seen in Figure 4, it is this MAD that we measure with RT3DE, whereas with 2DE an underestimated MAD is measured. MAD_{3D} and MAD_{MRI} were well correlated with no significant difference in between these measurements. The underestimation of true MAD may explain the frequently encountered discrepancy between pre-operative MAD_{2D} assessment and implanted ring-prosthesis size [20].

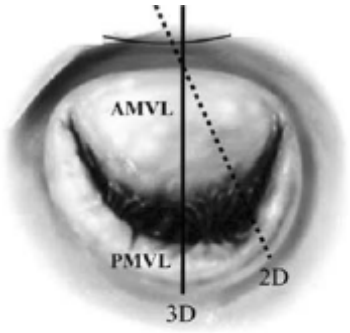

Fig. 4 RT3DE and 2DE (dashed line) measurement of mitral annulus diameter. AMVL—anterior mitral valve leaflet; PMVL—posterior mitral valve leaflet

Because of the limited information available in the literature we assessed normal MAD and MAA in patients without apparent left-sided heart disease. With variable methods available for MAA measurements, the definition of normal MAA is quite variable, probably caused by the complex geometry of the MA. MAA_{2D} measurements in other studies [9,21] ranged from 6.9 ± 0.8 to 12.2 ± 3.8 cm^2. In two recent very small studies (with 10 and 7 subjects, respectively) [7,22], normal transesophageal assessed MAA_{3D} values were 11.8 ± 2.5 cm^2 and normal MAA_{MRI} values were 9.5 ± 1.4 cm^2. MAA values in fresh human autopsy specimens[23] ranged from 6.4 to 8.2 cm^2. In our study, MAA_{3D} in normal subjects was 8.1 ± 2.4 cm^2 or (4.3 ± 0.8 cm^2/m^2) when corrected for body surface area.

Study Limitations

The study excluded patients with bad image quality and/ or in non-sinus rhythm because RT3DE is totally dependent on 2D images and the analysis of full volume mode will not be achieved with variable heart rate. The another limitation was that the surgical measurements of MAD were obtained only in three cases

CONCLUSION

MAD_{3D} can be reliably measured in patients with adequate image quality and is superior to MAD_{2D} in the assessment of true MA size. Normal values for MAD_{3D} are 2.8 ± 0.6 cm (or indexed for body surface area 1.5 ± 0.3 cm/m^2) and for MAA_{3D} 8.1 ± 2.4 cm^2 (or indexed for body surface area 4.3 ± 0.8 cm^2/m^2).

REFERENCES

1. Timek TA, Dagum P, Lai DT, Liang D, Daughters GT, Ingels NB, Jr., Miller DC. Pathogenesis of mitral regurgitation in tachycardia-induced cardiomyopathy. Circulation 2001;104:I47-53.
2. Ho SY. Anatomy of the mitral valve. Heart 2002;88 Suppl 4:iv5-10.
3. Boudoulas H, Wooley CF. Floppy Mitral Valve, Mitral Valve Prolapse, and Mitral Valvular Regurgitation. Curr Treat Options Cardiovasc Med 2001;3:15-24.
4. De Simone R, Wolf I, Mottl-Link S, Hoda R, Mikhail B, Sack FU, Meinzer HP, Hagl S. A clinical study of annular geometry and dynamics in patients with ischemic mitral regurgitation: new insights into asymmetrical ring annuloplasty. Eur J Cardiothorac Surg 2006;29:355-61.
5. Mihalatos DG, Mathew ST, Gopal AS, Joseph S, Grimson R, Reichek N. Relationship of mitral annular remodeling to severity of chronic mitral regurgitation. J Am Soc Echocardiogr 2006;19:76- 82.
6. Gorman JH, 3rd, Gupta KB, Streicher JT, Gorman RC, Jackson BM, Ratcliffe MB, Bogen DK, Edmunds LH, Jr. Dynamic three-dimensional imaging of the mitral valve and left ventricle by rapid sonomicrometry array localization. J Thorac Cardiovasc Surg 1996;112:712-26.
7. Komoda T, Hetzer R, Uyama C, Siniawski H, Maeta H, Rosendahl UP, Ozaki K. Mitral annular function assessed by 3D imaging for mitral valve surgery. J Heart Valve Dis 1994;3:483-90.
8. Cosgrove DM, 3rd, Arcidi JM, Rodriguez L, Stewart WJ, Powell K, Thomas JD. Initial experience with the Cosgrove-Edwards Annuloplasty System. Ann Thorac Surg 1995;60:499-503; discussion 503-4.
9. Pai RG, Tanimoto M, Jintapakorn W, Azevedo J, Pandian NG, Shah PM. Volume-rendered three-dimensional dynamic anatomy of the mitral annulus using a transesophageal echocardiographic technique. J Heart Valve Dis 1995;4:623-7.
10. Yamaura Y, Yoshikawa J, Yoshida K, Hozumi T, Akasaka T, Okada Y. Three-dimensional analysis of configuration and dynamics in patients with an annuloplasty ring by multiplane transesophageal echocardiography: comparison between flexible and rigid annuloplasty rings. J Heart Valve Dis 1995;4:618-22.
11. Kaji S, Nasu M, Yamamuro A, Tanabe K, Nagai K, Tani T, Tamita K, Shiratori K, Kinoshita M, Senda M, Okada Y, Morioka S. Annular geometry in patients with chronic ischemic mitral regurgitation: three-dimensional magnetic resonance imaging study. Circulation 2005;112:I409-14.
12. Bland JM, Altman DG. Statistical methods for assessing agreement between two methods of clinical measurement. Lancet 1986;1:307-10.
13. Enriquez-Sarano M, Basmadjian AJ, Rossi A, Bailey KR, Seward JB, Tajik AJ. Progression of mitral regurgitation: a prospective Doppler echocardiographic study. J Am Coll Cardiol 1999;34:1137-44.
14. Srichai MB, Grimm RA, Stillman AE, Gillinov AM, Rodriguez LL, Lieber ML, Lara A, Weaver JA, McCarthy PM, White RD. Ischemic mitral regurgitation: impact of the left ventricle and mitral valve in patients with left ventricular systolic dysfunction. Ann Thorac Surg 2005;80:170-8.
15. Czer LS, Maurer G, Bolger AF, DeRobertis M, Chaux A, Matloff JM. Revascularization alone or combined with suture annuloplasty for ischemic mitral regurgitation. Evaluation by color Doppler echocardiography. Tex Heart Inst J 1996;23:270-8.
16. Baba H, Okawa Y, Koike S, Hashimoto M, Matsumoto K. [The causes and management of ischemic mitral regurgitation]. Nippon Kyobu Geka Gakkai Zasshi 1997;45:543-9.
17. Maniu CV, Patel JB, Reuter DG, Meyer DM, Edwards WD, Rihal CS, Redfield MM. Acute and chronic reduction of functional mitral regurgitation in experimental heart failure by Percutaneous mitral annuloplasty. J Am Coll Cardiol 2004;44:1652-61.
18. Ma L, Tozzi P, Huber CH, Taub S, Gerelle G, von Segesser LK. Double-crowned valved stents for off-pump mitral valve replacement. Eur J Cardiothorac Surg 2005;28:194-8; discussion 198-9.
19. Webb JG, Harnek J, Munt BI, Kimblad PO, Chandavimol M, Thompson CR, Mayo JR, Solem JO. Percutaneous transvenous mitral annuloplasty: initial human experience with device implantation in the coronary sinus. Circulation 2006;113:851-5.

20. Ghosh P BN. Inaccuracy of prediction of mitral valve prosthesis size. Asian Cardiovasc Thorac Ann 1999;7:190.
21. Yiu SF, Enriquez-Sarano M, Tribouilloy C, Seward JB, Tajik AJ. Determinants of the degree of functional mitral regurgitation in patients with systolic left ventricular dysfunction: A quantitative clinical study. Circulation 2000;102:1400-6.
22. Flachskampf FA, Chandra S, Gaddipatti A, Levine RA, Weyman AE, Ameling W, Hanrath P, Thomas JD. Analysis of shape and motion of the mitral annulus in subjects with and without cardiomyopathy by echocardiographic 3-dimensional reconstruction. J Am Soc Echocardiogr 2000;13:277-87.
23. Timek TA, Miller DC. Experimental and clinical assessment of mitral annular area and dynamics: what are we actually measuring? Ann Thorac Surg 2001;72:966-74.

CHAPTER 7

Assessment of Mitral Annulus Size and Function by Real-Time Three-Dimensional Echocardiography in Cardiomyopathy: Comparison with Magnetic Resonance Imaging

Ashraf M. Anwar[1,2], Osama I.I. Soliman[1,2], Attila Nemes[1,3] , Tjeerd Germans[4], Boudewijn J. Krenning[1], Marcel L. Geleijnse[1], Albert C Van Rossum[4], and Folkert J. ten Cate[1]

[1]Department of Cardiology, Thoraxcenter, Erasmus University Medical Center, Rotterdam, The Netherlands
[2]Department of Cardiology, Al-Hussein University Hospital, Al-Azhar University, Cairo, Egypt
[3] Second Department of Medicine and Cardiology Center, University of Szeged, Szeged, Hungary
[4] Medical Center, Free University, amesterdam, the Netherlands

Journal of the American Society of Echocardiography 2007; 20:941-948

ABSTRACT

Objective: We sought to assess mitral annular (MA) size and function in hypertrophic (HCM) and dilated cardiomyopathy (DCM) using real-time 3-dimensional echocardiography (RT3DE).

Methods: The study included 30 patients with HCM, 20 patients with DCM, and 30 control subjects. RT3DE measurements included end-systolic and end-diastolic MA area (MAA_{3D}), MA diameter (MAD_{3D}), MA fractional area change (MAFAC), and MA fractional shortening. In subgroup of 50 patients, magnetic resonance imaging (MRI) was used for MAA_{MRI} and MAD_{MRI} measurement

Results: End-diastolic MAA_{3D} was larger in HCM than in control group (P <0.0001). Higher MAFAC and MAFS were present in HCM than in control group (P = 0.001 and P = 0.006 respectively). End-systolic and end-diastolic MAA_{3D} in DCM were higher than in HCM and control groups (P <0.0001). Lower MAFAC and MA fractional shortening were present in DCM than in HCM and control groups (P <0.0001). MAFAC correlated well with left ventricular function in control subjects (r = 0.94, P < 0.0001), whereas correlation was less in DCM (r = 0.53, P = 0.02) and HCM (r = 0.42, P < 0.01). RT3DE and MRI measurements were comparable.

Conclusion: RT3DE assessment of MA size and function in control subjects and patients with cardiomyopathy is accurate and well correlated with MRI.

INTRODUCTION

The mitral annulus (MA) is a vital component of the mitral valve apparatus and plays a crucial role in left ventricular (LV) and left atrial function [1]. The MA changes its shape from a saddle shape to a more flat structure and this leads to pronounced variations not only from heart to heart but also within the same heart [2]. The MA opposite the area of valvular fibrous continuity tends to be weaker because of lack of a well-formed fibrous cord. This area is susceptible to expand under hemodynamic stress, and therefore often involved in annulus dilatation. During systole, contraction of the surrounding LV muscle causes the annulus to contract. MA physiology assessment is important for diagnosis and treatment of mitral valve disease[3,4]. Several anatomic alterations of mitral valve apparatus are frequently presented in hypertrophic cardiomyopathy (HCM) and dilated cardiomyopathy (DCM) [5-8].Three-dimensional echocardiography (3DE) has the ability to analyse the shape and dynamics of normal and abnormal MA [9]. It can also assess the MA area (MAA) in short axis paraplanes [10,11]. The current study aimed to use real-time 3DE (RT3DE) in the assessment of MA size and function in patients with HCM and DCM compared with control subjects. To detect the accuracy of RT3DE measurement, the RT3DE data were compared to that obtained from magnetic resonance imaging (MRI).

METHODS

The study included 30 patients (mean age of 38 ± 15 years, 80% males) with established diagnosis of HCM[12], 20 patients (mean age 39 ± 12 years, 50% males) with established diagnosis of DCM[13] and 30 control subjects (mean age 40 ± 20, 66% males) with normal 2-dimensional echocardiography (2DE) study results. Depending on resting LV outflow tract (LVOT) gradient detected by continuous wave Doppler, the patients with HCM were classified into two subgroups: A) included 20 patients with non-obstructive HCM (LVOT gradient <50 mmHg) and B) included 10 patients with obstructive HCM (LVOT gradient >50 mmHg). All patients and control subjects were examined by 2DE and RT3DE. In a non-selected group of 50 patients (20 normal, 15 HCM patients, and 15 DCM patients), MRI studies were performed as gold standard technique for validation of RT3DE measurements.

2DE examination

The 2DE studies were performed using a 3.5 MHZ probe and a commercially available ultrasound system (Philips Sonos 7500, Best, The Netherlands). The 2DE examination was undertaken with the patient in the left lateral decubitus position using both apical and parasternal views The following data measures were obtained: (1) LV fractional Shortening ($LVFS_{2D}$) was defined as (end-diastolic dimension – end-systolic dimension) / end-diastolic dimension x 100% by M-mode, (2) LV ejection fraction ($LVEF_{2D}$) defined as (end-diastolic volume – end-systolic volume) / end-diastolic volume x 100 % using 2D biplane modified Simpson method, (3) Mitral regurgitation was defined by color Doppler and graded according to the maximum regurgitant jet area as mild (jet area< 4 cm^2), moderate (jet area 4-8 cm^2), and severe (jet area> 8 cm^2)[14]

RT3DE examination

RT3DE was performed using the same ultrasound system with (X 4 matrix) transducer capable of providing real-time B-mode and colour-Doppler. The 3D images were collected within 5 to 7 seconds of breath holding in full volume mode. The 3D data were transferred to an offline analysis system (Tom Tec, Munich, Germany). Data were stored digitally and subsequently evaluated by two expert echocardiographers. Data analysis of 3DE imaging had been based on a 2D approach relying on the echocardiographic images obtained from the apical views and on manual tracing of inner border of the mitral annulus. Once this is completed the surface area was automatically delineated and could be visualized from different points of view. Manual modification was done to correct any image if necessary. The following measures were obtained: (1) MAA_{3D} measured from atrial aspect at end-diastole (just before mitral valve closure) and at end-systole (just before mitral valve opening), (2) MA diameter (MAD_{3D}) defined as the perpendicular line drawn from the peak of annular area curvature to the middle of its straight annular border (aortic trigone) at the same frames selected for area measurement, and (3) MA fractional area changes ($MAFAC_{3D}$) (%) and $MAFS_{3D}$ (%): calculated by the formula used for $LVFS_{2D}$.

MRI examination

In a non-selected group of 50 patients (20 control subjects, 15 patients with HCM, and 15 patients with DCM), MRI studies were performed with a 1.5-T whole-body scanner (Sigma, General Electric, Milwaukee, Wis) and using a 4-channel phased-array body coil. A retro-triggered, steady state, free-

precession gradient echo-sequence was used for cine imaging. Image parameters were: repetition time of 3,5 milliseconds (ms), echo time 1.4 ms, temporal resolution of 42 ms, flip angle of 45 degrees, slice thickness of 8 mm with a slice gap of 2 mm, and an image resolution of 2.0 x 3.0 mm). First, cines with a 4-, 3-, and 2-chamber view were obtained. Then, a stack of 10 short axis slices was used for full coverage of the LV, planned on the 4-chamber view starting at the level of the mitral valve annulus, using the 2-chamber view as second localizer. Quantitative measurement was performed using standardized digital imaging and communication in medicine viewing software on the basal short axis slice, on which the mitral valve annulus was visualized in end-diastole. MAA_{MRI} and MAD_{MRI} were defined as described before in the RT3DE section (see Figure 1).

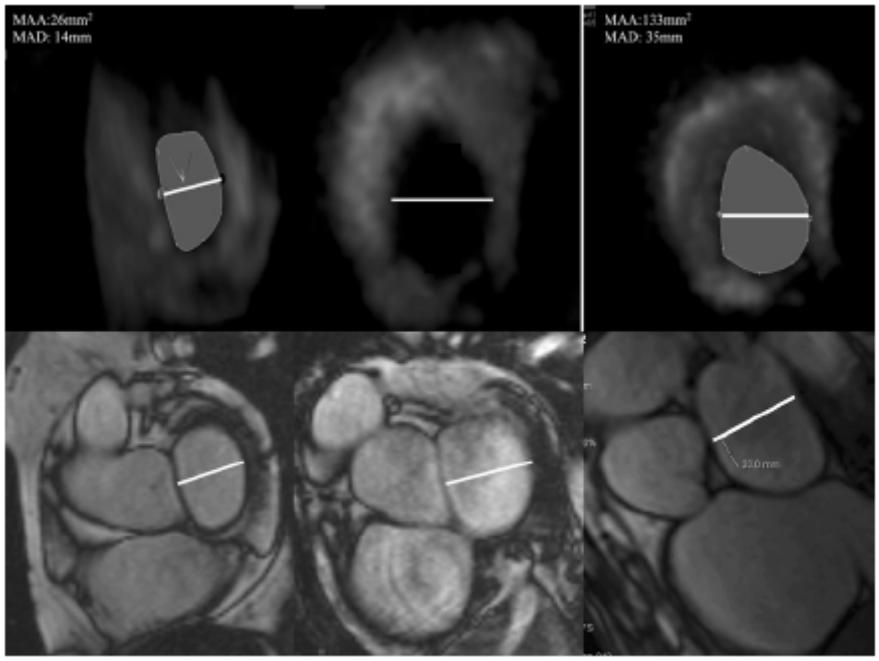

Figure 1: Morphology of mitral annulus in control subject (left), patient with hypertrophic cardiomyopathy (middle), and patients with dilated cardiomyopathy (right) as visualized by RT3DE (top) and MRI (bottom). Horizontal lines indicate the annulus diameter (MAD).

STATISTICAL ANALYSES

All data obtained by 2DE and RT3DE were presented as mean ± SD. Data analyses were performed using statistical software (SPSS, version 12.1, SPSS Inc, Chicago). Independent sample *t*-test and analysis of variance (ANOVA) test were used for comparison between the 3 groups for analysis of variance within each group and in-between. The level of significance was set to $P < 0.05$. Interobserver agreements for RT3DE measurements were expressed according to the method of Bland and Altman[15].

RESULTS

Echocardiographic data of all groups are shown in Table 1. There were no significant differences in age distribution. The highest $LVFS_{2D}$ and $LVEF_{2D}$ were present in patients with HCM (38.4 ± 9.6 and 71.1 ± 17.7% respectively), whereas the lowest $LVFS_{2D}$ and $LVEF_{2D}$ were present in patients with DCM (10.0 ± 2.2 and 18.4 ± 4.1 % respectively). The prevalence and severity of mitral regurgitation were comparable in HCM and DCM patient groups and higher than in control group (P <0.0001). Acquisition of RT3DE data set was performed successfully in all patients and control subjects (Figure 1).

MA in HCM

End-diastolic MAA_{3D} was significantly larger in HCM group than in control group (11.7 ± 2.8 vs. 8.7 ± 2.9 cm^2, P <0.0001), whereas end-systolic MAA_{3D} showed no significant difference. End-diastolic MAD_{3D} tended to be higher in patients with HCM than in control subjects but this was not statistically significant (P = 0.05). $MAFAC_{3D}$ and $MAFS_{3D}$ were larger in patients with HCM than in control subjects (51.2 ± 21.8% vs. 33.8 ± 13.8 %, P = 0.001 and 31.0 ± 17.6% vs. 20.1 ± 10.2%, P = 0.006 respectively). Age and sex were equally distributed within both HCM subgroups (I_A and I_B). LV end-diastolic diameter was comparable in both groups, whereas LV end-systolic diameter was lower in subgroup I_B (3.1 ± 0.7 vs. 2.3 ± 0.7 cm, P = 0.01). Thus, a higher $LVFS_{2D}$ was present in I_B than in I_A (48.0 ± 6 vs. 34.3 ± 8%, P = 0.001). The prevalence and severity of mitral regurgitation were comparable in both subgroups. All MA measurements by RT3DE showed no significant difference between the HCM subgroups.

MA in DCM

MAA_{3D} and MAD_{3D} were significantly larger in patients with DCM than in control subjects both at end-diastole and end-systole (all P < 0.0001) (Table 1). Compared with control subjects, patients with DCM had significantly lower $MAFAC_{3D}$ (23.2 ± 15.1 vs. 33.8 ± 13.8 %, P = 0.01) and $MAFS_{3D}$ (4.2 ± 7.9 vs. 20.1 ± 10.2%, P = 0.03).

DCM versus HCM

MAA_{3D} was significantly larger in DCM than in HCM both at end-diastole (15.5 ± 6.6 vs. 11.7 ± 2.8 cm^2, P = 0.01), and at end-systole (11.6 ± 5.4 vs. 5.6 ± 2.5 cm^2, P < 0.0001). End-systolic MAD_{3D} was significantly larger in DCM than in HCM (3.6 ± 0.8 vs. 2.7 ± 1.0 cm, P = 0.001), whereas no

significant differences in end-diastolic MAD_{3D} were found. $MAFAC_{3D}$ and $MAFS_{3D}$ were significantly lower in DCM than in HCM (all $P < 0.0001$) (Table 1).

Table 1: Clinical and echocardiographic data of all studied patient groups

	HCM (n = 30)	**DCM (n = 20)**	**Control (n = 30)**
Age (yr)	38 ± 15	39 ± 12	40 ± 20
Male gender (%)	24 (80%)	8 (40%)	18 (60%)
$LVFS_{2D}$ (%)	38.4 ± 9.6	10.0 ± 2.2	28.3 ± 5.4
$LVEF_{2D}$ (%)	71.1 ± 17.7	18.4 ± 4.1	52.4 ± 1.0
Mitral regurgitation			
No	8 (27%)	4 (20%)	24 (80 %)
Mild	15 (50%)	12 (60%)	6 (20%)
Moderate-severe	7 (23%)	4 (20%)	0 (0%)
Diastolic values			
MAA_{3D} ($cm^{2)}$	11.7 ± 2.8	15.5 ± 6.6	8.7 ± 2.9
MAD_{3D} (cm)	4.0 ± 1.6	4.3 ± 1.0	3.4 ± 0.5
Systolic values			
MAA_{3D} ($cm^{2)}$	5.6 ± 2.5	11.6 ± 5.4	5.6 ± 1.7
MAD_{3D} (cm)	2.7 ± 1.0	3.6 ± 0.8	2.7 ± 0.5
Systolic function			
$MAFAC_{3D}$ (%)	51.2 ± 21.8	23.2 ± 15.1	33.8 ± 13.8
$MAFS_{3D}$ (%)	31.0 ± 17.6	14.2 ± 7.9	20.1 ± 10.2

DCM, Dilated cardiomyopathy; *EF*, ejection fraction; *FAC*, fractional area change; *FS*, fractional shortening; *HCM*, hypertrophic cardiomyopathy; *LV*, left ventricular; *MA*, mitral annulus; *MAA*, MA area; *MAD*, MA diameter

MA function & LV function

$MAFS_{3D}$ did not correlate with $LVFS_{2D}$ and $LVEF_{2D}$ in all patients. $MAFAC_{3D}$ was strongly correlated with $LVEF_{2D}$ in control subjects ($r = 0.94$, $P < 0.0001$). However, this correlation decreased in DCM and HCM, ($r = 0.53$, $P = 0.01$ and $r = 0.42$, $P = 0.02$ respectively) (Figure 2).

MRI and RT3DE

In the subgroup of 50 patients who were investigated with both MRI and RT3DE, there was an excellent agreement between both imaging modalities in measurements of MAA ($r = 0.92$, $P < 0.0001$) and MAD ($r = 0.85$, $P < 0.0001$) (Figure 3). No significant differences were found between both imaging modalities for measurements of MAA and MAD (Table 2).

Table 2: Comparison between RT3DE and MRI measurements

	RT3DE	**MRI**
Diastolic MAA (cm^2)		
HCM patients	11.7 ± 2.8	11.3 ± 2.3
DCM patients	15.5 ± 6.6	16.4 ± 5.5
Normal control	8.7 ± 2.9	9.0 ± 2.3
Diastolic MAD (cm)		
HCM patients	4.0 ± 1.6	3.8 ± 0.7
DCM patients	4.3 ± 1.0	4.5 ± 0.9
Normal control	3.4 ± 0.5	3.3 ± 0.5

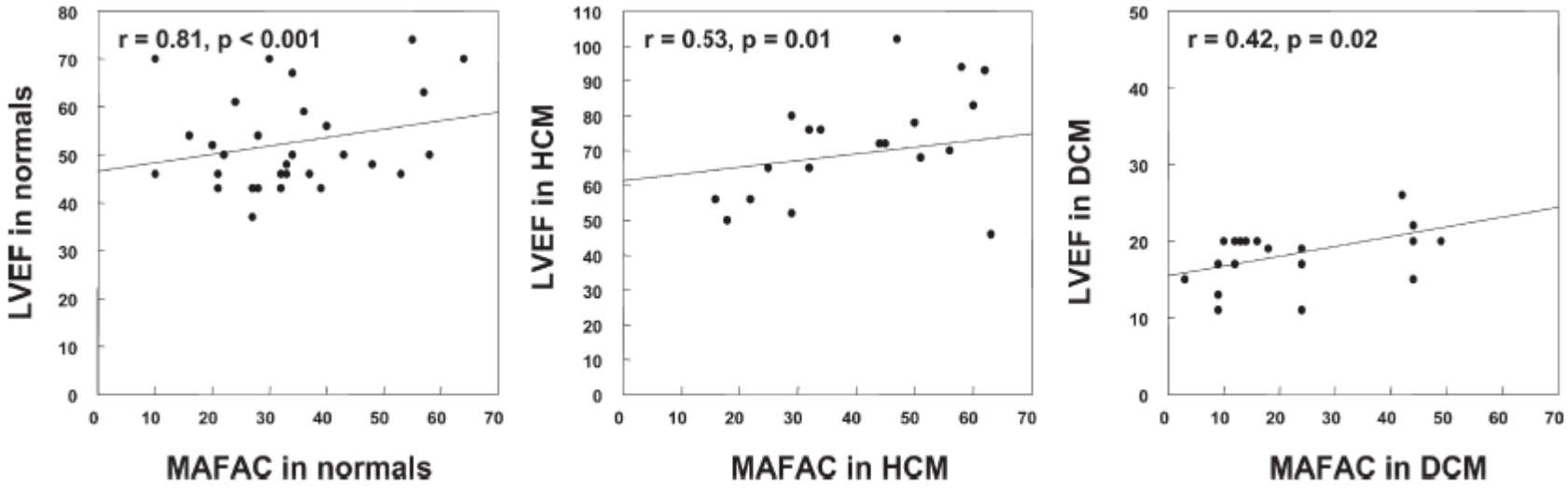

Figure 2 Correlation between mitral annulus fractional area change (*MAFAC*) and left ventricular ejection fraction (*LVEF*) in control subjects and in patients with hypertrophic cardiomyopathy (*HCM*) and dilated cardiomyopathy (*DCM*).

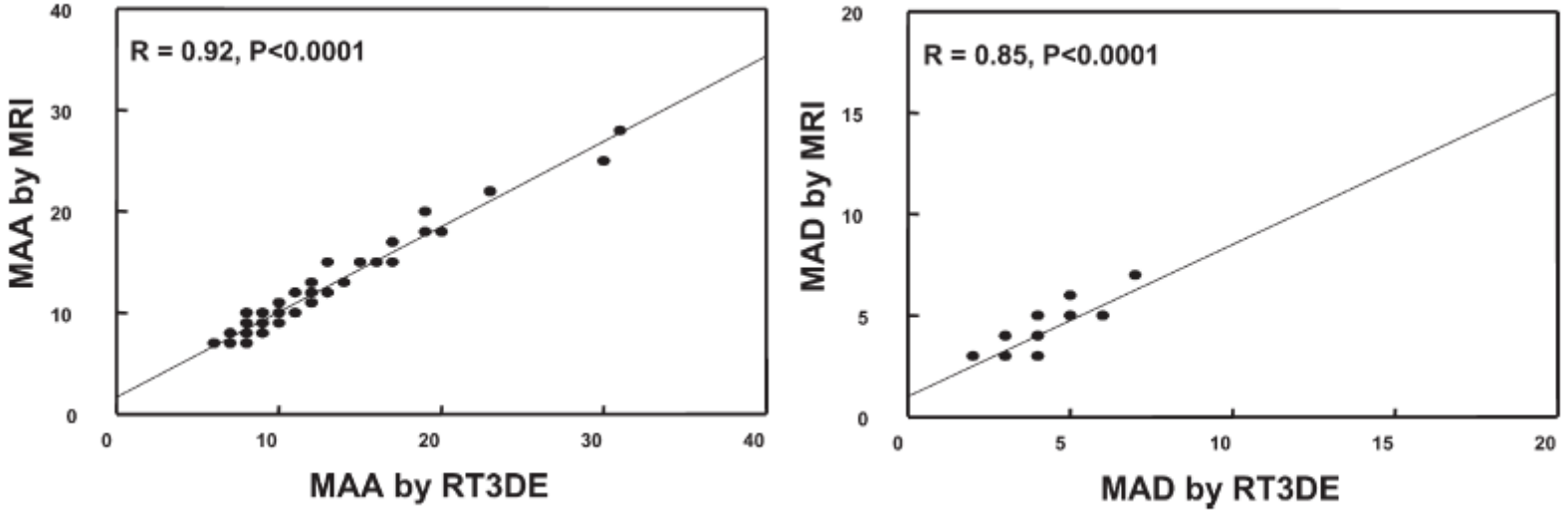

Figure 3 Correlation between mitral annulus (MA) diameter (*MAD*) measured by real-time 3-dimensional echocardiography (*RT3DE*) and magnetic resonance imaging (*MRI*). *MAA*, MA area.

Interobsever agreement

As shown in Figure 4, in the control group, interobserver agreement was good for MAA_{3D} (mean difference = - 0.1 ± 1.7, agreement = - 3.5, 3.3) and for MAD_{3D} (mean difference = - 0.1 ± 1.9, agreement = - 3.90, 3.70). In patients with HCM, agreement was also good for MAA_{3D} (mean difference = - 0.2 ± 1.3, agreement = - 2.8, 2.4), and for MAD_{3D} (mean difference = -0.1 ± 2.1, agreement = - 4.3, 4.1). In patients with DCM, agreement was also good for MAA_{3D} (mean difference = - 0.5 ± 2.3, agreement = - 5.1, 4.1), and for MAD_{3D} (mean difference = - 0.3 ± 2.2, agreement = - 4.7, 4.1).

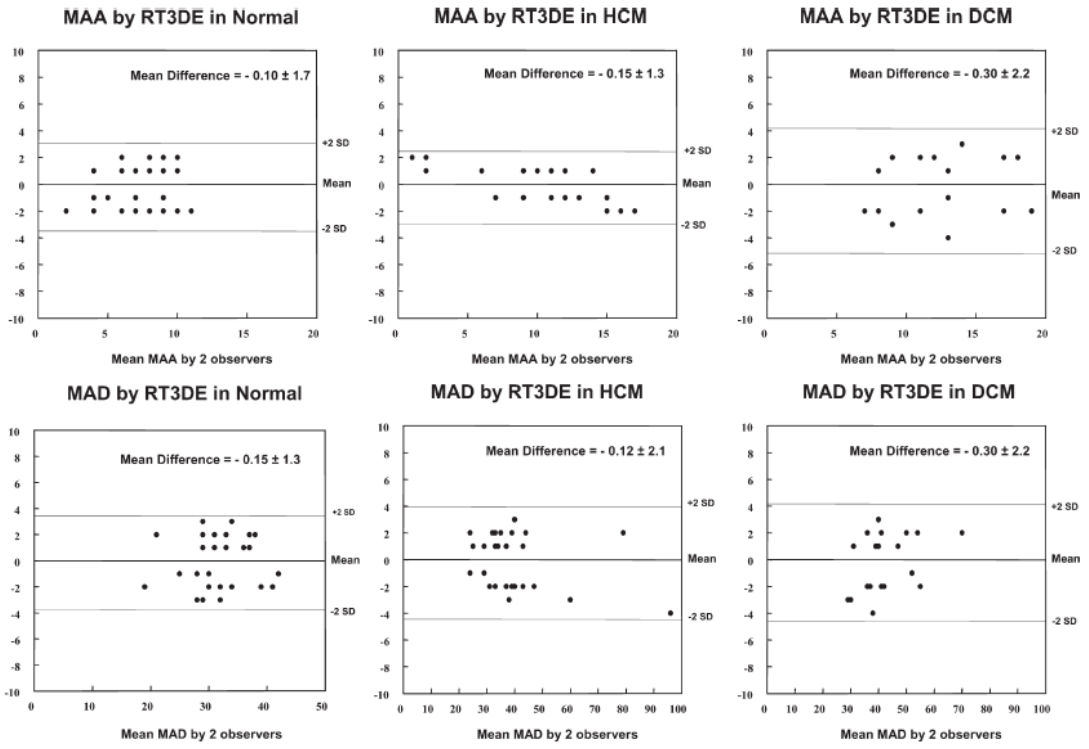

Figure 4: Interobsever agreement of mitral annuls (MA) area (MAA) and MA diameter (MAD) measurements by RT3DE in control group, and in patients with HCM and DCM.

DISCUSSION

In this study the morphological and functional aspects of the MA in HCM and DCM were assessed by RT3DE. MA shape was not completely circular but D-shaped in control subjects and in patients with cardiomyopathy. MAA_{3D} and MAD_{3D} correlated well with MAA_{MRI} and MAD_{MRI} in control subjects and in patients with cardiomyopathy. Despite MA dilatation in patients with HCM and DCM, MA function is augmented in patients with HCM and impaired in patients with DCM as assessed by $MAFAC_{3D}$ and $MAFS_{3D}$.

The importance of studying MA size and function in cardiomyopathy is to expand the understanding of the underlying patho-physiology of the occurrence of mitral regurgitation in several cardiomyopathies. Subsequently, it may also affect therapeutic decision-making in patients with significant functional mitral regurgitation, because accurate assessment of the MA is crucial for selection of prosthetic mitral valve rings, percutaneous annuloplasty devices and stented valve implantation [16-18]

In the current study, the MA could be well visualized with RT3DE from different points of view in both patients and control subjects. Tracings of the MA and calculation of its surface areas in systole and diastole were reproducible and discriminated normal from dilated MA. Larger end-diastolic MAA_{3D} in HCM and DCM were found (11.7 ± 2.8 and 15.5 ± 6.6 cm^2, respectively), which is in concordance with measurements from Flachskampf et al (10.2 ± 4.2 cm^2 in HCM and15.2 ± 4.2 cm^2in DCM)[19].

The MA acts as a sphincter facilitating ventricular filling by expansion and aids to competent mitral valve closure by contraction. In accordance with the previous studies, MA function was augmented in HCM and impaired in DCM[19,20]. This may be a result of stretching of MA that occurs along the left ventricular axis. The functional activity of the muscular part of MA along the left ventricular axis may play a role. Both types of HCM (obstructive and non-obstructive) showed no significant differences in parameters of MA size and function. This may be explained by the fact that MA stretching of MA occurs mainly along the muscular part and very little on the fibrous part. In HCM, MA dilatation occurs to a certain limit beyond which, more stretch will be prevented by the hyperactive muscular part even with significant mitral regurgitation. In both HCM types, the muscular part is hyperactive. In this study $MAFAC_{3D}$ in control subjects showed good correlation with $LVEF_{3D}$, but this correlation was less in both HCM and DCM groups. This discrepancy may be explained by the higher incidence of electromechanical dys-synchrony in HCM and DCM [21-23].

When MA dilates, the geometry changes due to flattening and stretching with loss of normal saddle shape, which may contribute to functional mitral regurgitation [24,25]. This may explains the direct correlation between mitral regurgitation severity and MA dilatation [26]. In addition, MA dilatation may underlie the high incidence of mitral regurgitation in patients with HCM irrespective to LVOT gradient [27]. The MA dilatation may also explain why significant mitral regurgitation persists after successful surgical myomectomy in obstructive HCM and disappears when the myomectomy is combined with

mitral valve repair [28,29]. It also partially explains why annuloplasty is preferred to mitral valve replacement with improvement of outcome after mitral annuloplasty in severe LV dysfunction [30,31].

CONCLUSION

RT3DE can be reliably used for accurate assessment of MA size and function in control subjects, patients with HCM, or patients with DCM and can be used to facilitate clinical decision making when surgical mitral valve repair is indicated. In addition, it may be used in the follow up studies of patients with cardiomyopathy.

REFERENCES

1. Timek TA, Miller DC. Experimental and clinical assessment of mitral annular area and dynamics: what are we actually measuring? *Ann Thorac Surg* 2001;72:966-74.
2. Yacoub MH, Cohn LH. Novel approaches to cardiac valve repair: from structure to function: Part II. *Circulation* 2004;109:1064-72.
3. Yamaura Y, Yoshikawa J, Yoshida K, Hozumi T, Akasaka T, Okada Y. Three-dimensional analysis of configuration and dynamics in patients with an annuloplasty ring by multiplane transesophageal echocardiography: comparison between flexible and rigid annuloplasty rings. *J Heart Valve Dis* 1995;4:618-22.
4. Komoda T, Hetzer R, Uyama C, Siniawski H, Maeta H, Rosendahl UP, Ozaki K. Mitral annular function assessed by 3D imaging for mitral valve surgery. *J Heart Valve Dis* 1994;3:483-90.
5. Klues HG, Maron BJ, Dollar AL, Roberts WC. Diversity of structural mitral valve alterations in hypertrophic cardiomyopathy. *Circulation* 1992;85:1651-60.
6. He S, Hopmeyer J, Lefebvre XP, Schwammenthal E, Yoganathan AP, Levine RA. Importance of leaflet elongation in causing systolic anterior motion of the mitral valve. *J Heart Valve Dis* 1997;6:149-59.
7. Yiu SF, Enriquez-Sarano M, Tribouilloy C, Seward JB, Tajik AJ. Determinants of the degree of functional mitral regurgitation in patients with systolic left ventricular dysfunction: A quantitative clinical study. *Circulation* 2000;102:1400-6.
8. Otsuji Y, Handschumacher MD, Schwammenthal E, Jiang L, Song JK, Guerrero JL, Vlahakes GJ, Levine RA. Insights from three-dimensional echocardiography into the mechanism of functional mitral regurgitation: direct in vivo demonstration of altered leaflet tethering geometry. *Circulation* 1997;96:1999-2008.
9. Kaplan SR, Bashein G, Sheehan FH, Legget ME, Munt B, Li XN, Sivarajan M, Bolson EL, Zeppa M, Arch MZ, Martin RW. Three-dimensional echocardiographic assessment of annular shape changes in the normal and regurgitant mitral valve. *Am Heart J* 2000;139:378-87.
10. Yamaura Y, Yoshida K, Hozumi T, Akasaka T, Okada Y, Yoshikawa J. Three-dimensional echocardiographic evaluation of configuration and dynamics of the mitral annulus in patients fitted with an annuloplasty ring. *J Heart Valve Dis* 1997;6:43-7.
11. Yamaura Y, Yoshida K, Hozumi T, Akasaka T, Morioka S, Yoshikawa J. Evaluation of the mitral annulus by extracted three-dimensional images in patients with an annuloplasty ring. *Am J Cardiol* 1998;82:534-6.
12. Rakowski H, Sasson Z, Wigle ED. Echocardiographic and Doppler assessment of hypertrophic cardiomyopathy. *J Am Soc Echocardiogr* 1988;1:31-47.
13. Corya B, Feigenbaum H, Rasmussen S, Black MJ. Echocardiographic features of congestive cardiomyopathy compared with normal subjects and patients with coronary artery disease. *Circulation* 1974;49:1153-9.
14. Spain MG, Smith MD, Grayburn PA, Harlamert EA, DeMaria AN. Quantitative assessment of mitral regurgitation by Doppler color flow imaging: angiographic and hemodynamic correlations. *J Am Coll Cardiol* 1989;13:585-90.
15. Bland JM, Altman DG. Statistical methods for assessing agreement between two methods of clinical measurement. *Lancet* 1986;1:307-10.
16. Maniu CV, Patel JB, Reuter DG, Meyer DM, Edwards WD, Rihal CS, Redfield MM. Acute and chronic reduction of functional mitral regurgitation in experimental heart failure by percutaneous mitral annuloplasty. *J Am Coll Cardiol* 2004;44:1652-61.
17. Ma L, Tozzi P, Huber CH, Taub S, Gerelle G, von Segesser LK. Double-crowned valved stents for off-pump mitral valve replacement. *Eur J Cardiothorac Surg* 2005;28:194-8; discussion 198-9.
18. Webb JG, Harnek J, Munt BI, Kimblad PO, Chandavimol M, Thompson CR, Mayo JR, Solem JO. Percutaneous transvenous mitral annuloplasty: initial human experience with device implantation in the coronary sinus. *Circulation* 2006;113:851-5.
19. Flachskampf FA, Chandra S, Gaddipatti A, Levine RA, Weyman AE, Ameling W, Hanrath P, Thomas JD. Analysis of shape and motion of the mitral annulus in subjects with and without cardiomyopathy by echocardiographic 3-dimensional reconstruction. *J Am Soc Echocardiogr* 2000;13:277-87.
20. Young AA, Kramer CM, Ferrari VA, Axel L, Reichek N. Three-dimensional left ventricular deformation in hypertrophic cardiomyopathy. *Circulation* 1994;90:854-67.
21. D'Andrea A, Caso P, Cuomo S, Salerno G, Scarafile R, Mita C, De Corato G, Sarubbi B, Scherillo M, Calabro R. Prognostic value of intra-left ventricular electromechanical asynchrony in patients with

mild hypertrophic cardiomyopathy compared with power athletes. *Br J Sports Med* 2006;40:244-50; discussion 244-50.
22. Ennezat PV, Marechaux S, Le Tourneau T, Lamblin N, Bauters C, Van Belle E, Gal B, Kacet S, Asseman P, Deklunder G, LeJemtel TH, de Groote P. Myocardial asynchronism is a determinant of changes in functional mitral regurgitation severity during dynamic exercise in patients with chronic heart failure due to severe left ventricular systolic dysfunction. *Eur Heart J* 2006;27:679-83.
23. Turner MS, Bleasdale RA, Vinereanu D, Mumford CE, Paul V, Fraser AG, Frenneaux MP. Electrical and mechanical components of dyssynchrony in heart failure patients with normal QRS duration and left bundle-branch block: impact of left and biventricular pacing. *Circulation* 2004;109:2544-9.
24. Kaji S, Nasu M, Yamamuro A, Tanabe K, Nagai K, Tani T, Tamita K, Shiratori K, Kinoshita M, Senda M, Okada Y, Morioka S. Annular geometry in patients with chronic ischemic mitral regurgitation: three-dimensional magnetic resonance imaging study. *Circulation* 2005;112:I409-14.
25. De Simone R, Wolf I, Mottl-Link S, Hoda R, Mikhail B, Sack FU, Meinzer HP, Hagl S. A clinical study of annular geometry and dynamics in patients with ischemic mitral regurgitation: new insights into asymmetrical ring annuloplasty. *Eur J Cardiothorac Surg* 2006;29:355-61.
26. Mihalatos DG, Mathew ST, Gopal AS, Joseph S, Grimson R, Reichek N. Relationship of mitral annular remodeling to severity of chronic mitral regurgitation. *J Am Soc Echocardiogr* 2006;19:76-82.
27. Manabe K, Oki T, Fukuda N, Iuchi A, Tabata T. [Transesophageal echocardiographic study on the mechanisms of mitral regurgitation in hypertrophic cardiomyopathy: comparison with sigmoid septum]. *J Cardiol* 1995;26:233-41.
28. Heric B, Lytle BW, Miller DP, Rosenkranz ER, Lever HM, Cosgrove DM. Surgical management of hypertrophic obstructive cardiomyopathy. Early and late results. *J Thorac Cardiovasc Surg* 1995;110:195-206; discussion 206-8.
29. Joyce FS, Lever HM, Cosgrove DM, 3rd. Treatment of hypertrophic cardiomyopathy by mitral valve repair and septal myectomy. *Ann Thorac Surg* 1994;57:1025-7.
30. Bishay ES, McCarthy PM, Cosgrove DM, Hoercher KJ, Smedira NG, Mukherjee D, White J, Blackstone EH. Mitral valve surgery in patients with severe left ventricular dysfunction. *Eur J Cardiothorac Surg* 2000;17:213-21.
31. Rothenburger M, Rukosujew A, Hammel D, Dorenkamp A, Schmidt C, Schmid C, Wichter T, Scheld HH. Mitral valve surgery in patients with poor left ventricular function. *Thorac Cardiovasc Surg* 2002;50:351-4.

CHAPTER 8

VALIDATION OF A NEW SCORE FOR THE ASSESSMENT OF MITRAL STENOSIS USING REAL-TIME THREE-DIMENSIONAL ECHOCARDIOGRAPHY

Ashraf M Anwar[1,2], Wael M Attia[2] , Osama I. I. Soliman[1,2], Mohammed A Mosad[2], Munir Othman[2], Marcel L. Geleijnse[1], Ali M El-Amin[2], and Folkert J. ten Cate[1]

[1]Department of Cardiology, Thoraxcenter, Erasmus University Medical Center, Rotterdam, The Netherlands
[2]Department of Cardiology, Al-Hussein University Hospital, Al-Azhar University, Cairo, Egypt

Submitted to Journal of American Society of Echocardiography

ABSTRACT

Objectives: Assessment of mitral valve (MV) morphology in mitral stenosis (MS) patients by a new real-time three-dimensional echocardiography (RT3DE) scoring system.

Methods: We conducted a two-staged study. The first stage was to study the feasibility, and reliability of the RT3DE score in 17 patients with MS. The second stage was a validation of the RT3DE score in 74 consecutive patients (mean age 33.4 ± 8.6 years, 65% females) who were candidate for percutaneous mitral valvuloplasty (PTMV). MV morphology was assessed by Wilkins' score and compared to the RT3DE score. RT3DE score was constructed by dividing each MV leaflet into 3 scallops and composed of 31 points (with increasing abnormality) including 6 points for thickness, 6 for mobility, 10 for calcification and 9 for subvalvular apparatus involvement. The total RT3DE score was assumed and defined for low (<8), mild (8-14) and high (≥15)..

Results: In the first stage, RT3DE score was easily applied to all patients with good interobserver and intraobserver agreements. In the second stage, RT3DE improved the MV morphological assessment for detection of extent and distribution of calcification, and commissural splitting. Both scores were correlated well for assessment of thickness and calcification ($r= 0.63$, $p<0.0001$ and $r= 0.44$, $p<0.0001$ respectively). Pre-PTMV predictors of optimal success were the low calcification and subvalvular apparatus Wilkins score and low mobility and subvalvular apparatus RT3DE score. Incidence and severity of mitral regurgitation were associated with high calcification RT3DE score.

Conclusions: The new RT3DE score is feasible and highly reproducible for the assessment of MV morphology in MS patients. In comparison with Wilkins score, RT3DE score added more valuable information before PTMV that may help in selection of patients and could predict the outcome.

INTRODUCTION

Rheumatic mitral valve (MV) disease still remains an important public health concern particularly in developing countries. In selection of the proper therapeutic strategy for mitral stenosis (MS), two-dimensional echocardiography (2DE) is of crucial importance [1]. Apart from estimation of the transmitral pressure gradient, 2DE can calculate MV area by planimetry and pressure half-time [2]. 2DE is essential in the selection of patients for percutaneous mitral valvuloplasty (PTMV) [3]. Of all available MV scoring systems, the Wilkins' score is the most commonly used [4-6]. This score evaluates MV thickness, mobility, leaflet calcification, and the degree of subvalvular apparatus thickening [6]. A favourable Wilkins' score (<8 points) is highly predictable of good outcome after PTMV [7]. More recently, it has been shown that other factors such as commissural fusion and calcification are also strong predictors of outcome after PTMV [8-10].

The introduction of real-time three-dimensional echocardiography (RT3DE) and advances in analysis software has improved MV orientation and evaluation[11]. Several studies have reported improved accuracy and superiority of RT3DE over 2DE for MV area (MVA) estimation [12-14]. RT3DE allows a unique "en-face" view and morphologic analysis of the entire MV apparatus including the MV annulus and subvalvular apparatus, also in relation to other nearby structures. We proposed a new RT3DE score for the quantitative and qualitative assessment of the MV in patients with mitral stenosis (MS) and compared it with Wilkins score in the prediction of PTMV outcome.

METHODS

The study was designed as two-stages. The first stage was for derivation of the RT3DE score and assessment of its applicability in 17 patients (mean age 30.6 ± 7.8 year, 70% females) with an established diagnosis of MS and good 2DE image quality. All 17 patients were in sinus rhythm. Once the score was developed, the second stage of the study was started for validation of this score in a prospective new sample of 74 consecutive patients (mean age 34.4 ± 5.9 year, 62% females). 67 patients (74 %) were in sinus rhythm, while 24 patients (26 %) were in atrial fibrillation. Finally, the RT3DE score was applied for the entire 91 patients (first and second stages) to assess its value. All patients were examined by 2DE and RT3DE. All data were analyzed by two independent expert echocardiographers (A. M. A & O, I. S in the first stage, A. M. A & W. M. A in the second stage). The analysis was done also by each one at two different days to assess the interobserver and intraobserver variabilities.

The study was designed as two-stages. The first stage was for derivation of the RT3DE score and assessment of its applicability in 17 patients (mean age 30.6 ± 7.8 year, 70% females) with an established diagnosis of MS and good 2DE image quality. All 17 patients were in sinus rhythm. Once the score was developed, the second stage of the study was started for validation of this score in a prospective new sample of 74 consecutive patients (mean age 34.4 ± 5.9 year, 62% females). 67 patients (74 %) were in sinus rhythm, while 24 patients (26 %) were in atrial fibrillation. Finally, the RT3DE score was applied for the entire 91 patients (first and second stages) to assess its value. All patients were examined by 2DE and RT3DE. All data were analyzed by two independent expert echocardiographers (A. M. A & O, I. S in the first stage, A. M. A & W. M. A in the second stage). The analysis was done also by each one at two different days to assess the interobserver and intraobserver variabilities.

Transthoracic 2DE examination

A complete 2DE study was performed 24 hours prior to PTMV using a 3.5 MHz (S3) probe and a commercially available ultrasound system (Philips Sonos 7500, Best, Netherlands). The morphology score according to Wilkins' score system was applied for evaluation of four factors: leaflet thickness, mobility, calcification and the degree of subvalvular thickening (Table 1). Each factor is given a score of 0 for normal, 1 for mild MV involvement, 2 for moderate and 3-4 for severe, yielding a summed score of 16 points. The higher the score, the greater the morphological abnormality of the MV Thus a score of less than 5 points defines mild MV involvement, 5-8 moderate involvement, and >8 severe MV involvement severity [6]**.** The following measurements were obtained: 1) MVA was defined as the narrowest orifice at the time of maximal mitral valve opening and measured by 2D planimetry in short axis view, 2) mean transmitral pressure gradient was calculated by continuous wave Doppler, 3) mitral regurgitation was graded according to vena contracta using color Doppler and graded as mild , moderate and severe [15], 4) left atrial diameter was measured in M-mode from parasternal long axis view at the level of aortic valve, 5) commissural splitting was defined as the terminal distance between the two MV leaflets and measured from parasternal short axis view at the mitral valve level at an end-diastolic still frame for each commissure (anterior and posterior). The splitting was scored as 0 for no splitting, 0.5 for partial splitting, and 1 for complete splitting [16]. If PTMV was planned, the previous data were obtained pre-PTMV and within 48 hours post-PTMV. One-year clinical and 2DE examination follow up was completed for 74 patients who underwent PTMV. The following measurements were obtained: 1) MVA, 2) mean transmitral pressure gradient and 3) mitral regurgitation. The end-points were: recurrent symptoms, restenosis, need re-intervention either PTMV or MV surgery.

Table 1: Wilkins' score

	Mobility	Subvalvular thickening	Thickening	Calcification
1	Highly mobile valve with only leaflet tips restricted	Minimal thickening just below the mitral leaflets	Leaflets near normal in thickness (4-5 mm)	A single area of increased echo brightness
2	Leaflet mid and base portions have normal mobility	Thickening of chordal structures extending up to one-third of the chordal length	Midleaflets normal, considerable thickening of margins (5-8 mm).	Scattered areas of brightness confined to leaflet margins
3	Valve continues to move forward in diastole mainly from the base	Thickening extending to the distal third of the chords	Thickening extending through the entire leaflet (5-8 mm).	Brightness extending into the midportion of the leaflets
4	No or minimal forward movement of the leaflets in diastole	Extensive thickening and shortening of all chordal structures extending down to the papillary muscle	Considerable thickening of all leaflet tissue (>8-10 mm)	Extensive brightness throughout much of leaflet tissue

Transesophageal 2DE

Transesophageal 2DE was performed 24 hours pre-PTMV for assessment of MV morphology evidence of left atrial and /or left atrial appendage thrombi and for measurement of interatrial septum thickness.

Transthoracic RT3DE examination

Image acquisition

RT3DE was performed immediately after the 2DE study by the same machine using an X4 matrix transducer capable of providing real-time B-mode and colour-Doppler. Full volume images of three cardiac cycles were collected within 5-7 seconds of breath holding in patients with sinus rhythm. Due to variability of cardiac cycle duration in atrial fibrillation patients, the 3D images of one cardiac cycle were collected. . The 3D data were transferred to an offline analysis system (Tom Tec, Munich, Germany) in the first stage of the study and (Q-lab version 6. Philips) in the second stage. Data were stored digitally and subsequently evaluated by two independent physicians. Data analysis of 3D echo imaging was based on a 2D approach relying on the echo images obtained from the apical 4-chamber and parasternal long axis views in patients with sinus rhythm. Additional two views (apical long axis and parasternal short axis) were needed in atrial fibrillation patients. By using the crop function for images formatting, parallel sections through scanned volume in three perpendicular planes were done. The narrowest slice to enable visualization of MV (leaflets and subvalvular) was selected.

Score Derivation

The new RT3DE morphology score (Table 2) was derived to include both MV leaflets and subvalvular apparatus guided by the well known 2DE Wilkins' score. As seen in Figure 1, each leaflet could be seen clearly by RT3DE divided into three scallops (antero-lateral A1 - P1, middle A2 - P2 and postero-medial A3 - P3) that were scored separately. For the scoring of the subvalvular apparatus, three cut sections of the anterior and posterior chordae were obtained from the full-volume images acquired at parasternal long axis position at three levels: proximal (valve level), middle and distal (papillary muscle level). Each cut section and each chorda were scored separately.

1). Scoring of valve leaflets included thickness, mobility and calcification for each scallop as follow: Normal thickness and mobility was scored as 0 and abnormal thickness or restricted mobility was scored as 1. Absence of calcification was scored as 0, calcification in middle scallop (A2 or P2) was scored as 1, and calcification of commissural scallops of both leaflets (A1, A3 - P1, P3) was scored as 2.

2). Scoring of the subvalvular apparatus included chordal thickness and distance of splitting in-between the chordae as follow: Normal thickness was scored as 0, and abnormal thickness was scored as 1, normal chordal splitting (distance in-between >5 mm)[16] was scored as 0, partial splitting (distance in-between <5 mm) as 1, and absence of splitting as 2.

3). The total points of leaflets and subvalvular apparatus RT3DE score were summed to calculate the total RT3DE score, ranging from 0 to 31 points. The degree of leaflet and subvalvular apparatus involvement were defined as follows:

1. For leaflet thickness and mobility, it was 0 for normal, 1-2 for mild MV involvement, 3-4 for moderate and ≥ 5 for severe
2. For calcification and subvalvular apparatus involvement it was 0 for normal, 1-2 for mild, 3-5 for moderate and ≥ 6 for severe.
3. Total score of mild MV involvement was defined as <8 points, Moderate MV involvement 8 -14, and severe MV involvement ≥ 15 for high

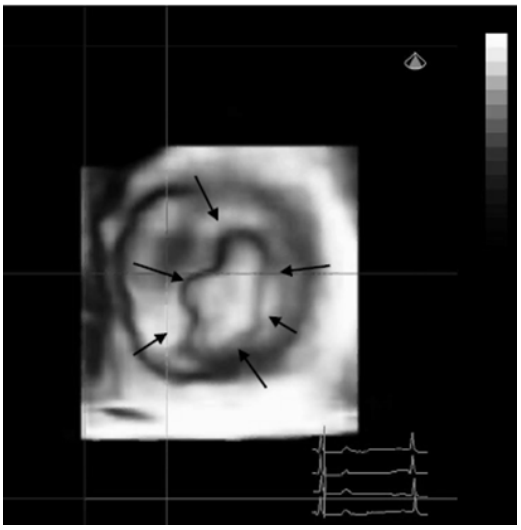

Figure 1: RT3DE en face view of mitral valve as seen from ventricular aspect with the three scallops of each leaflet (A1, A2, A3 – P1, P2, P3).

Table 2: RT3DE score of mitral valve

	Anterior leaflet			**Posterior leaflet**		
	A1	**A2**	**A3**	**P1**	**P2**	**P3**
Thickness (0-6) 0 = normal 1 = thickened	0 – 1	0 - 1	0 – 1	0 – 1	0 - 1	0 – 1
Mobility (0-6) 0 = normal 1 = limited	0 – 1	0 - 1	0 – 1	0 – 1	0 - 1	0 – 1
Calcification (0-10) 0 = no 1,2 = calcified	0 – 2	0 - 1	0 – 2	0 – 2	0 - 1	0 – 2
	Subvalvular Apparatus					
	Proximal 1/3		**Middle 1/3**		**Distal 1/3**	
Thickness (0-3) 0 = normal 1 = thickened	0 – 1		0 – 1		0 – 1	
Splitting (0-6) 0 = normal 1 = partial 2 = no	0, 1, 2		0, 1, 2		0, 1, 2	

Abbreviations: A1- P1: anterolateral parts, A2 - P2: middle parts, A3 – P3: postero-medial

Percutaneous Mitral Valvuloplasty (PTMV):

Seventy four patients of ninety one (mean age 30.4 ± 8.6 years, 70% females) were class I candidate for PTMV according to AHA/ACC guidelines [17]. All of them had <9 MV Wilkins score. PTMV was performed by two experienced operators who were unaware with the RT3DE assessment. After patient consent, one femoral arterial and venous sheaths were introduced after local anaesthesia. A pigtail catheter was advanced just at the aortic valve level. Trans-septal puncture was performed with a Brockenbrough needle. PTMV was performed using the Inoue balloon technique as previously described [18]**.** The definition of optimal success was achievement of 50% increase in MVA as compared to pre PTMV or an achieved MVA ≥1.5 cm^2 which is larger with mitral

regurgitation moderate or less [15]. Suboptimal success was defined as the achieved MVA <1.5 cm^2 with regurgitation moderate or less and severe regurgitation irrespective of the achieved MVA.

STATISTICAL ANALYSES

All statistics were performed using SPSS version 12.0.1 (SPSS inc., Chicago, Illinois). Each component of both scores was assessed separately, and then total score of 2DE and RT3DE were calculated for every patient. Both scores were investigated for correlation using Pearson's correlation analysis to demonstrate the basic differences. Comparisons were considered significant in presence of a p value < 0.05. Interobserver agreement was evaluated with the Kappa index, classified as poor with value 0.01-0.20, slight 0.21- 0.40, fair 0.41- 0.60, good 0.61- 0.80, very good 0.81- 0.92, and excellent 0.93-1.00 [19]. To obtain independent predictors of success and development of significant mitral regurgitation (> grade 2), multiple Cox regression analysis was performed. The 95% confidence interval was derived from the natural algorithm of the coefficient ± 1.96 times the standard error.

RESULTS

First Stage Study Results

Acquisition of RT3DE data was performed successfully in all 17 patients within a reasonable time (3 minutes for acquisition and 10 minutes for data analysis). The MV was clearly visualized in all patients and its morphology could be assessed by both the 2DE and RT3DE scores. Optimal assessment of MV leaflets and commissures by RT3DE was obtained from the parasternal window more than the apical window, while assessment of subvalvular apparatus was optimally assessed from the apical window. The RT3DE score was applied easily by the investigators in all patients. The echocardiographic reports by the investigators were identical for the score points.

Total Results

Data acquisition and analysis were obtained in all patients in the two stages (91 patients). In patients with sinus rhythm (67 patients), the data analysis and score calculation were easily obtained through cropping of a full volume images whitin 10 minutes. In patients with atrial fibrillation (24 patients), the data analysis and score calculation were depend on multiple live 3D images obtained from parasternal and apical views within 13 minutes.

Score Qualification (Table 3)

The study of each part of both MV leaflets by RT3DE helped in more concise description than global evaluation by 2DE. RT3DE assessment of leaflet mobility was clearly and easily obtained. Leaflet calcification was fairly detected by 2DE while RT3DE added more information regarding distribution of calcification on leaflet's parts and its extent (Figure 2 A,B). Annular calcification (site and extent) was clearly defined by RT3DE while not depicted well by 2DE. For subvalvular apparatus, RT3DE helped in detailed quantitative assessment of chordal thickening and separation at three levels while by Wilkins score, chordal separation was not obtained (Figure 2 D). Width of anterior and posterior commissures post-PTMV could be assessed well by RT3DE while by 2DE was inadequate.

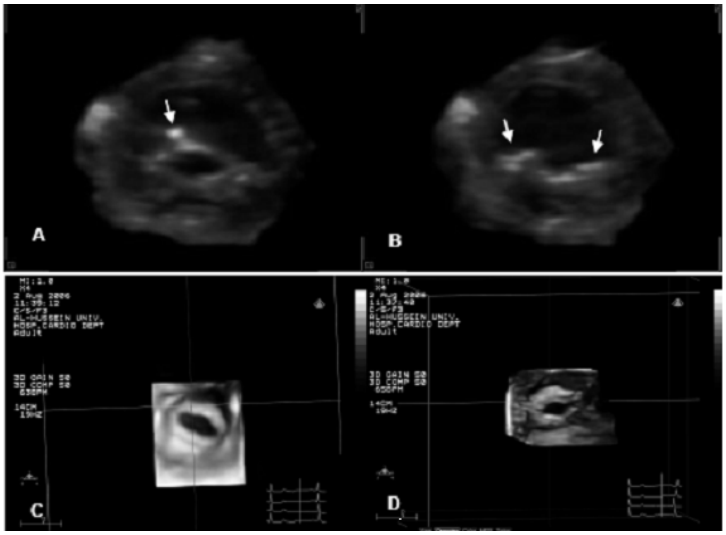

Figure 2: A). Stenotic MV with calcification involved middle part of anterior leaflet (A2), B). Stenotic MV with calcification involved both commissures (arrows) with closed mitral valve, C). Marked thickening of both leaflets of MV, D) thickening of chordae tendinae.

Table 3: Qualitative value of RT3DE compared with 2DE in assessment of MV morphology

	Wilkins score	**RT3DE score**
Site of calcification	+	++
Extent of calcification	+	++
Chordal thickening	+	++
Chordal separation	-	+
Commissures	+	++
Mitral Annulus	+	++

++: clearly defined, +: defined, -: ill-defined

Score Quantification

Thickness score: 2DE detected mild thickening in 40%, moderate in 55%, and severe in 5%, while RT3DE detected 24% as mild, 62% as moderate, and 14% as severe. Both scores correlated well ($r = 0.63$, $p < 0.0001$).

Mobility score: 2DE detected freely mobile leaflets in 3%, mildly restricted leaflet mobility in 48%, moderate in 39% and severe in 10%, while by RT3DE, 16% were defined as normal, 34% as mild, and 51% as moderate. No correlation between both scores was detected.

Calcification score: 2DE score detected no calcification in 40%, mild calcification in 38%, moderate in 19% and severe in 3%, while RT3DE score detected no calcification in 25%, mild calcification in 38%, moderate in 31% and severe in 6%. Both scores were fairly correlated ($r= 0.44$, $p<0.0001$)

Subvalvular apparatus score: 2DE detected mild degree of subvalvular affection in 39%, moderate in 45% and severe in 16%, while RT3DE defined 2% as normal, 25% as mild affection, 55% as moderate and 18% as severe. No correlation between both scores was detected.

Total Scores Quantification

The distribution of all included patients within both scores is shown in Table 4. High score was detected in 10% by 2DE and in 25% by RT3DE. Low score was detected in 35% by 2DE and in 16 % by RT3DE. Both scores were comparable for the definition of intermediate severity ($r = 0.6$, $p = 0.007$), while for low and high were not.

Table 4: Distribution of patients within Wilkins' score and RT3DE score

		Normal	Mild	Moderate	Severe
Thickness	2DE	0 (0%)	36 (40%)	50 (55%)	5 (5%)
	RT3DE	0 (0%)	22 (24%)	56 (62%)	13 (14%)
Mobility	2DE	3 (3%)	44 (48%)	35 (39%)	9 (10%)
	RT3DE	14 (16%)	31 (34%)	46 (51%)	0 (0%)
Calcification	2DE	36 (40%)	35 (38%)	17 (19%)	3 (3%)
	RT3DE	23 (25%)	35 (38%)	28 (31%)	5 (6%)
Subvalvular apparatus	2DE	0 (0%)	35 (39%)	41 (45%)	15 (16%)
	RT3DE	2 (2%)	23 (25%)	50 (55%)	16 (18%)
Total score	2DE	0 (0%)	32 (35%)	50 (55%)	9 (10%)
	RT3DE	0 (0%)	14 (16%)	54 (59%)	23 (25%)

Interobserver variability:

Wilkins score showed fair agreement for the assessment of leaflet thickness and mobility (Kappa index: 0.55 and 0.56 respectively), while it was poor for calcification and subvalvular apparatus (Kappa index: 0.03 and 0.01 respectively). For RT3DE, the agreements were good for the assessment of leaflet thickness and mobility (Kappa

index: 0.66 and 0.63 respectively), and fair for the assessment of calcification (Kappa index: 0.42). Assessment of subvalvular apparatus showed slight agreement (Kappa index: 0.21) for chordal thickening, while for splitting it was excellent (Kappa index: 0.95).

Immediate results of PTMV

Depending upon the previous definition of success, optimal successful dilatation was achieved in 57 patients (77%) and suboptimal success in 17 patients (23%). The immediate echocardiographic and hemodynamic outcome is shown in Table 5. Serious complications including cardiac tamponade, or need for surgical interference were not present.

Table 5: Hemodynamic and echocardiographic results of PTMV

Variable	Pre-PTMV	Post-PTMV	P value
MVA_{2DE} (cm^2)	0.91 ± 0.13	1.9 ± 0.30	<0.0001
MVA_{RT3DE} (cm^2)	0.92 ± 0.14	2.1 ± 0.30	<0.0001
Mean pressure gradient (mmHg)	20.0 ± 5.8	7.0 ± 2.5	<0.0001
LA diameter (cm)	5.1 ± 0.95	4.7 ± 7.7	<0.001
LV fractional shortening (%)	31.7 ± 6.8	35.1 ± 5.2	0.002
Mitral regurgitation			
No	37 (50%)	5 (6.6%)	
Grade 1	32 (43.3%)	37 (50%)	0.001
Grade 2	5 (6.7%)	15 (20%)	
Grade 3-4	0 (0%)	17 (23.3%)	

By 2DE: MVA was increased from 0.91 ± 0.13 to 1.9 ± 0.30 cm^2, $p < 0.0001$. Significant reduction in the mean transmitral PG was reduced from 20.0 ± 5.8 to 7.0 ± 2.5 mmHg; $p< 0.0001$. 17 patients (23 %) developed mitral regurgitation > grade 2 and in the remaining percentage of patients (77%) mitral regurgitation was ≤ grade 2. Complete splitting of anterior commissure was achieved in 48 patients (65%) and partial splitting in 18 patients (25%). Complete splitting of posterior commissure was achieved in 37 patients (50%) and partial splitting in 22 patients (30%). Bilateral complete commissural splitting was obtained in 37 patients (50%).

By RT3DE: MVA was increased from 0.92 ± 0.14 to 2.1 ± 0.30 cm^2, $p < 0.0001$. Splitting of both commissures could be assessed clearly (Figure 3). Complete splitting of anterior commissure was achieved in 46 patients (62%) and partial splitting in 22 patients (30%). Complete splitting of posterior commissure was achieved in 37 patients (50%) and partial splitting in 18 patients (25%).

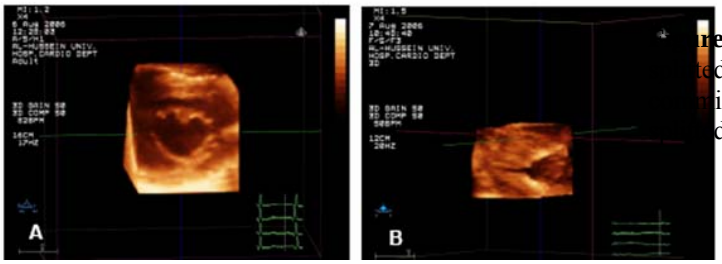

re 3: A) RT3DE en face view of a widely
d antero-lateral and postero-medial
issures post-PTMV, B) side view of partially
d anterior commissure.

PTMV results and Wilkins score

Using multiple stepwise Cox regression analysis for Wilkins score components, calcification and subvalvular apparatus involvement were the only two independent predictors of successful PTMV (p= 0.025 and 0.028 respectively). Thus the lower the score points of calcification and subvalvular apparatus involvement, the larger the achieved MVA. No independent predictors could be identified for the development of >grade 2 mitral regurgitation.

PTMV results and RT3DE score

Analysis of RT3DE score components showed that leaflet mobility and subvalvular thickening were independent predictors of successful PTMV (p= 0.0045 and 0.04 respectively). High mean transmitral gradient was detected in 12 patients (16.6%) despite successful PTMV. In those patients, subvalvular apparatus score was mild according to Wilkins score while by RT3DE score it was moderate in 5 of them and severe in 7 of them. For the development of >grade 2 mitral regurgitation, calcification was the only independent predictor. In 4 out of 17 patients who developed >grade 2 mitral regurgitation, RT3DE calcification score was severe while by Wilkins score it was mild. In the remaining 13 patients, calcification score was moderate by both Wilkins and RT3DE scores. The calcification was detected in the commissural segments of MV leaflets in 10 patients by RT3DE.

One-year follow up

Clinical and 2DE follow up were completed for all patients underwent PTMV. In patients with optimal successful PTMV (57 patients), 7 patients developed recurrence of dyspnea (grade II-III), while the remaining 50 patients were asymptomatic. 2DE of those 7 patients showed insignificant reduction of MVA from 1.7 ± 0.25 cm2 to 1.5 ± 0.21 cm2 but the mean transmitral gradient increased from 10.0 ± 2.1 mmHg to 14.2 ± 1.9 mmHg; p< 0.01. In those patients, the subvalvular apparatus score before PTMV was severe by RT3DE and mild by 2DE. In patients with suboptimal PTMV (17 patients), 5 of them became severely symptomatic. 3 patients were referred for surgery due to increased MR grade (grade 3/4) and 2 patient underwent repeat PTMV due to restenosis (MVA was reduced from 1.4 ± 0.34 to 1.0 ± 0.11 cm2). The 3 patients whom referred to surgery had

severe calcification score by RT3DE before PTMV while in the 2 patients referred to repeat PTMV, the calcification score was moderate. The 2DE calcification score in those 5 patients was mild.

DISCUSSION

For a proper selection of therapeutic strategy in patients with MS, clinical evaluation and assessment of MV anatomy are essential [20-22]. Transthoracic 2DE allows classification of patients into anatomic groups to predict immediate and long-term outcome[23,24]. Although, most cardiologists use the Wilkins' score, several echocardiographic scoring systems have been suggested for evaluation of MV anatomy[4,5,7,15]. None of the available scores has been shown to be superior to any of the others[25].

With RT3DE, the MV can be evaluated en face. Additionally, rotation and orientation of the MV to the desired plane are easy and independent of the orientation of the acoustic window where image acquisition is done[14,26]. Many studies demonstrated the superior value of RT3DE for the qualitative morphological description of MV[27-29]. RT3DE may become the standard echo technique in the future for the assessment of MS patients due to its unique orientation of MV leaflets, commissures and MVA that could be obtained in a high population percentage[11]. RT3DE could be relied on for evaluation of success of valvuloplasty through accurate measurement of the achieved MVA, verification of commissural splitting and differentiation between splitting and stretch [14].Thus the need to construct a new RT3DE score for quantitative MV assessment paving the way for RT3DE to be totally dependable pre and post-PTMV.

The current study described the feasibility of RT3DE for evaluation of patients with MS after PTMV. It helped in the measurement of the achieved MVA and width of commissures. For the first time, the study used a new easily applicable quantitative RT3DE score for assessment of MV morphology pre-PTMV and compared it with Wilkins score as a predictor of the PTMV immediate outcome. The RT3DE score has several potential benefits and include the following:

1) RT3DE could detect the thickness of each leaflet part, so a higher percentage of moderate to severe degree of thickening was found (76% by RT3DE vs. 60% by 2DE).
2) The whole leaflet length could not be evaluated by a single 2DE image especially for the posterior leaflet, which is short and naturally less mobile than the anterior one (Table 6) (Figure 4). By RT3DE, visualization and assessment of the whole length of both leaflets is possible through single image plane especially in sinus rhythm. Leaflet mobility could be well assessed and scored by RT3DE and its score was a good independent predictor for successful PTMV.

Table 6: Observed scallop in each 2D echocardiographic views

View	A1	A2	A3	P1	P2	P3
PLAX	-	+	-	-	+	-
AP 4-CH	-	+	+	+	-	-
AP 2-CH	+	+	-	-	+	-
AP LAX	-	+	-	-	+	-
PSAX	±	+	±	+	+	+

Abbreviations: PLAX: parasternal long axis, AP4-CH: apical 4-chamber, AP2-CH: apical 2-chamber, AP LAX: apical long axis, PSAX: parsternal short axis, + = Visualized, - = Not visualized, ± = May be visualized

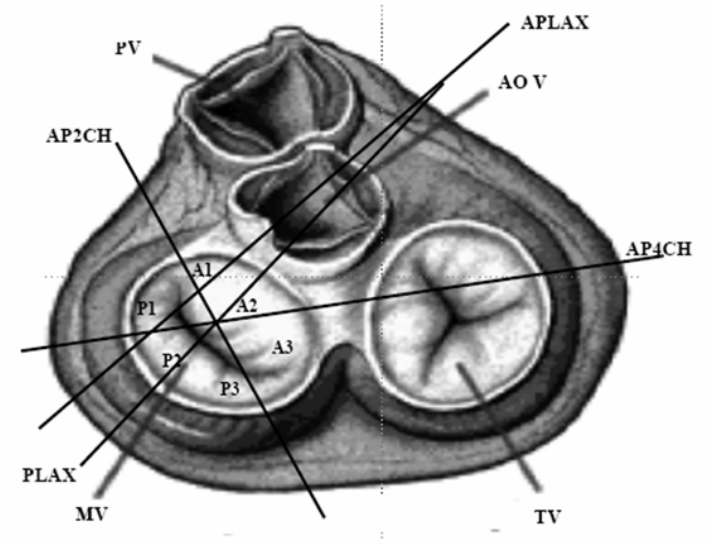

Figure 4: Diagram showing the direction of 2D echocardiographic cut planes with each MV scallop could be visualized through each plane

3) The assessment of leaflet calcification and in particular the distribution of calcification along the leaflet parts plays an important role in the outcome of patients after PTMV as the percentage of success decreases and incidence of complication increase[30-32]. 2DE Wilkins score depends on the bright areas and the extension of calcification along the leaflet length[8,9]. Multiple cut planes are needed for detection of calcification in all scallops of both MV leaflets (Figure 3), while RT3DE could predict the extent and distribution of calcification in each scallop from single short axis cut plain. Calcification of commissures is one of the strong predictors of outcome after PTMV because it affects the degree of commissural splitting[8-10]. That is why in the new RT3DE score, calcification at the commissural parts of leaflet was described by a higher score than the middle leaflets calcification. In our study, calcification by RT3DE score was the only predictor for the development of >grade 2 mitral regurgitation post PTMV not only due to calcification extent but also the calcification site. In 13 out of 17 patients who developed >grade 2 mitral regurgitation, the calcification score was moderate by both Wilkins and RT3DE scores, however it was detected at the commissural segments of MV leaflets in 10 patients by RT3DE. The presence of annular calcification is an important information in patients with atrio-

ventricular conduction defect, cerebral stroke and for surgical decision[32-36]. RT3DE could clearly detect the site and extent of calcification, as the whole annular circumference was clearly defined.

4) Rheumatic involvement of subvalvular apparatus includes fusion, thickening, retraction, shortening and calcification. As a consequence, the free interchordal space diminishes and the opened "leaflet – chordae tendineae tunnel" available for diastolic flow is limited[37]. Currently, assessment of MVA morphology and functional anatomy in relation to other valvular components remains a clinical challenge. Qualitative assessment of subvalvular apparatus by 2DE underestimates severity[38]. Assessment of the subvalvular apparatus by transesophageal 2DE is still controversial. Although, Stewart et al[39] considered transesophageal 2DE the method of choice for evaluation of subvalvular apparatus, Levin et al[40] reported limited ability of it to accurately identify and evaluate specific subvalvular features that influence valvuloplasty outcome. RT3DE score assessed the chordal thickness and separation at three levels by dividing their length into three parts (proximal, middle and distal). For each third, chordal thickness and distance in-between were scored. This detailed information especially for chordal separation was not obtained by Wilkins score which may explain absence of correlation between both scores for assessment of subvalvular apparatus. Chordal calcification was not included in our RT3DE score because in patients with chordal calcification, the MV leaflets are always heavily calcified and thus unfavorable for PTMV. Chordal thickening and fusion is a good independent predictor for successful PTMV. This may explain the residual higher transmitral gradient despite successful PTMV in 12 patients (16.6%). with subvalvular affection that was considered low by Wilkins score, while by RT3DE score, it was moderate to severe. Chordal separation can be used as a marker of successful PTMV[16].

5) Retrospective analysis of MV morphology score before PTMV by both RT3DE and 2DE showed that the severe subvalvular RT3DE score was associated with poor outcome after 1 year (expressed by recurrent symptoms and increased transmitral gradient). Also, moderate and severe calcification RT3DE score was associated with the need for repeat PTMV and MV surgery. In both conditions, 2DE underestimated the severityof calcification and subvalvular scores.

6) The detailed morphological assessment of MV will help in proper selection of therapeutic strategy for significant MS. Prediction of PTMV success and complications could be detected more accurately by RT3DE score than by Wilkins score.

7) The RT3DE score is simple and more helpful particularly for less experienced operators as it provides a simple number for each leaflet scallop and subvalvular apparatus segment separately. This was evident by good interobserver variability for most of the score components.

The new RT3DE score may not superior to the standard Wilkins' score and it will not replace it at the current time but at least the study paved the way to standardize RT3DE in future and to achieve both quantitative and qualitative assessment of the MV. The time spent for analysis of RT3DE images is slightly longer than with 2D images, however the benefits of its application compensate this time

Study Limitation:

The number of RT3DE score points is high due to the detailed information given for each MV leaflet scallop and chordal segment however, its simplicity and clear definition of grades of severity overcame the increased score points. Application of RT3DE is easy in patients with sinus rhythm because its analysis depends on a full volume images. Due to variability of R-R interval in atrial fibrillation, full volume could not be obtained well and application of RT3DE score needs 3D images from multiple views. Although arrhythmias such as atrial fibrillation was considered in the past as a limitation for RT3DE image acquisition, the current ultrasound systems which allow for 7 subvolumes per beat and late experience found that this is not a limitation anymore. The study included patients with good 2DE image quality, however RT3DE assessment of MV could be obtained in 80% of general population irrespective of image quality[11]. With the advance in software and transducers, it is expected that the number of good analyzable studies will increase in the future. The new transesophageal RT3DE was not used because it was not available during the study accomplishment. However, no standard score by the transesophageal 2DE to compare with the transesophageal RT3DE. PTMV procedure was done using Inoue balloon and other devices (double balloon and metallic valvulotome) were not used. However, the comparison between these devices is beyond the study aim

Conclusions

The new proposed RT3DE score for morphological assessment of MV was applied for the assessment of MS patients and compared to 2DE Wilkins score. It shows more valuable information to the morphological assessment of the MV and should be the preferred score for proper selection and outcome prediction of PTMV.

References

1. Rahimtoola SH, Durairaj A, Mehra A, Nuno I. Current evaluation and management of patients with mitral stenosis. *Circulation* 2002;106:1183-8.

2. Robiolio PA, Rigolin VH, Harrison JK, Kisslo KB, Bashore TM. Doppler pressure half-time method of assessing mitral valve area: aortic insufficiency does not adversely affect validity. *Am Heart J* 1998;136:718-23.

3. Vahanian A, Michel PL, Cormier B, Vitoux B, Michel X, Slama M, Sarano LE, Trabelsi S, Ben Ismail M, Acar J. Results of percutaneous mitral commissurotomy in 200 patients. *Am J Cardiol* 1989;63:847-52.

4. Reid CL, Otto CM, Davis KB, Labovitz A, Kisslo KB, mckay CR. Influence of mitral valve morphology on mitral balloon commissurotomy: immediate and six-month results from the NHLBI Balloon Valvuloplasty Registry. *Am Heart J* 1992;124:657-65.

5. Reid CL, Chandraratna PA, Kawanishi DT, Kotlewski A, Rahimtoola SH. Influence of mitral valve morphology on double-balloon catheter balloon valvuloplasty in patients with mitral stenosis. Analysis of factors predicting immediate and 3-month results. *Circulation* 1989;80:515-24.

6. Wilkins GT, Weyman AE, Abascal VM, Block PC, Palacios IF. Percutaneous balloon dilatation of the mitral valve: an analysis of echocardiographic variables related to outcome and the mechanism of dilatation. *Br Heart J* 1988;60:299-308.

7. Padial LR, Freitas N, Sagie A, Newell JB, Weyman AE, Levine RA, Palacios IF. Echocardiography can predict which patients will develop severe mitral regurgitation after percutaneous mitral valvulotomy. *J Am Coll Cardiol* 1996;27:1225-31.

8. Cannan CR, Nishimura RA, Reeder GS, Ilstrup DR, Larson DR, Holmes DR, Tajik AJ. Echocardiographic assessment of commissural calcium: a simple predictor of outcome after percutaneous mitral balloon valvotomy. *J Am Coll Cardiol* 1997;29:175-80.

9. Fatkin D, Roy P, Morgan JJ, Feneley MP. Percutaneous balloon mitral valvotomy with the Inoue single-balloon catheter: commissural morphology as a determinant of outcome. *J Am Coll Cardiol* 1993;21:390-7.

10. Sutaria N, Shaw TR, Prendergast B, Northridge D. Transoesophageal echocardiographic assessment of mitral valve commissural morphology predicts outcome after balloon mitral valvotomy. *Heart* 2006;92:52-7.

11. Sugeng L, Coon P, Weinert L, Jolly N, Lammertin G, Bednarz JE, Thiele K, Lang RM. Use of real-time 3-dimensional transthoracic echocardiography in the evaluation of mitral valve disease. *J Am Soc Echocardiogr* 2006;19:413-21.

12. Sugeng L, Weinert L, Lammertin G, Thomas P, Spencer KT, Decara JM, mor-Avi V, Huo D, Feldman T, Lang RM. Accuracy of mitral valve area measurements using transthoracic rapid freehand 3-dimensional scanning: comparison with non-invasive and invasive methods. *J Am Soc Echocardiogr* 2003;16:1292-1300.

13. Zamorano J, Cordeiro P, Sugeng L, Perez de Isla L, Weinert L, Macaya C, Rodrigo JL, Lang RM. Real-time three-dimensional echocardiography for rheumatic mitral valve stenosis evaluation: an accurate and novel approach. *J Am Coll Cardiol* 2004;43:2091-2096.

14. Zamorano J, Perez de Isla L, Sugeng L, Cordeiro P, Rodrigo JL, Almeria C, Weinert L, Feldman T, Macaya C, Lang RM, Hernandez Antolin R. Non-invasive assessment of mitral valve area during percutaneous balloon mitral valvuloplasty: role of real-time 3D echocardiography. *Eur Heart J* 2004;25:2086-91.

15. Roberts BJ, Grayburn PA. Color flow imaging of the vena contracta in mitral regurgitation: technical considerations. J Am Soc Echocardiogr 2003;16:1002-1006.

16. El-Sayed MA, Anwar MA. Comparative study between various methods of percutaneous transvenous mitral commissurotomy (Metallic Valvotome, Inoue balloon, and Double balloon techniques) VID study. *J Interven Cardiol* 2000;13:357-364.

17. ACC/AHA2006 practice guidelines for the management of patients wih valvular heart disease: Excutive summary. *J Am Coll Cardiol* 2006;48(3):598-675**.**

18. Park SJ, Kim JJ, Park SW, JK Song JK, Doo YC, Lee SJ. Immediate and one-year results of percutaneous mitral balloon valvuloplasty using Inoue and double-balloon techniques. *Am J Cardiol* 1993;71;938-943.

19. Byrt T. How good is that agreement? *Epidemiology* 1996;7:561.

20. Palacios IF, Tuzcu ME, Weyman AE, Newell JB, Block PC. Clinical follow-up of patients undergoing percutaneous mitral balloon valvotomy. *Circulation* 1995;91:671-6.

21. Goswami KC, Bahl VK, Talwar KK, Shrivastava S, Manchanda SC. Percutaneous balloon mitral valvuloplasty using the Inoue balloon: analysis of echocardiographic and other variables related to immediate outcome. *Int J Cardiol* 1999;68:261-8.

22. Post JR, Feldman T, Isner J, Herrmann HC. Inoue balloon mitral valvotomy in patients with severe valvular and subvalvular deformity. *J Am Coll Cardiol* 1995;25:1129-36.

23. Patel JJ, Shama D, Mitha AS, Blyth D, Hassen F, Le Roux BT, Chetty S. Balloon valvuloplasty versus closed commissurotomy for pliable mitral stenosis: a prospective hemodynamic study. *J Am Coll Cardiol* 1991;18:1318-22.

24. Lee TM, Su SF, Chen MF, Liau CS, Lee YT. Changes of left ventricular function after percutaneous balloon mitral valvuloplasty in mitral stenosis with impaired left ventricular performance. *Int J Cardiol* 1996;56:211-5.

25. Vahanian A. Balloon valvuloplasty. *Heart* 2001;85:223-8.

26. Valocik G, Kamp O, Visser CA. Three-dimensional echocardiography in mitral valve disease. *Eur J Echocardiogr* 2005;6:443-54.

27. Mannaerts HF, Kamp O, Visser CA. Should mitral valve area assessment in patients with mitral stenosis be based on anatomical or on functional evaluation? A plea for 3D echocardiography as the new clinical standard. *Eur Heart J* 2004;25:2073-4.

28. Binder TM, Rosenhek R, Porenta G, Maurer G, Baumgartner H. Improved assessment of mitral valve stenosis by volumetric real-time three-dimensional echocardiography. *J Am Coll Cardiol* 2000;36:1355-61.

29. Langerveld J, Valocik G, Plokker HW, Ernst SM, Mannaerts HF, Kelder JC, Kamp O, Jaarsma W. Additional value of three-dimensional transesophageal echocardiography for patients with mitral valve stenosis undergoing balloon valvuloplasty. *J Am Soc Echocardiogr* 2003;16:841-9.

30. Hildick-Smith DJ, Taylor GJ, Shapiro LM. Inoue balloon mitral valvuloplasty: long-term clinical and echocardiographic follow-up of a predominantly unfavourable population. *Eur Heart J* 2000;21:1690-7.

31. Zhang HP, Allen JW, Lau FY, Ruiz CE. Immediate and late outcome of percutaneous balloon mitral valvotomy in patients with significantly calcified valves. *Am Heart J* 1995;129:501-6.

32. Iung B, Cormier B, Ducimetiere P, Porte JM, Nallet O, Michel PL, Acar J, Vahanian A. Immediate results of percutaneous mitral commissurotomy. A predictive model on a series of 1514 patients. Circulation 1996;94:2124-30

33. Fink N, Adler Y, Wiser I, Sagie A. [Association between mitral annulus calcification and atherosclerosis]. *Harefuah* 2001;140:838-43, 894.

34. Kizer JR, Wiebers DO, Whisnant JP, Galloway JM, Welty TK, Lee ET, Best LG, Resnick HE, Roman MJ, Devereux RB. Mitral annular calcification, aortic valve sclerosis, and incident stroke in adults free of clinical cardiovascular disease: the Strong Heart Study. *Stroke* 2005;36:2533-7.

35. Fox CS, Parise H, Vasan RS, Levy D, O'Donnell CJ, D'Agostino RB, Plehn JF, Benjamin EJ. Mitral annular calcification is a predictor for incident atrial fibrillation. *Atherosclerosis* 2004;173:291-4.

36. Fox CS, Vasan RS, Parise H, Levy D, O'Donnell CJ, D'Agostino RB, Benjamin EJ. Mitral annular calcification predicts cardiovascular morbidity and mortality: the Framingham Heart Study. *Circulation* 2003;107:1492-6.

37. Schoen FJ, Sutton MS. Contemporary issues in the pathology of valvular heart disease. *Hum Pathol* 1987;18:568-76.

38. Turgeman Y, Atar S, Rosenfeld T. The subvalvular apparatus in rheumatic mitral stenosis: methods of assessment and therapeutic implications. *Chest* 2003;124:1929-36.

39. Stewart WJ, Griffin B, Thomas JD. Multiplane transesophageal echocardiographic evaluation of mitral valve disease. *Am J Card Imaging* 1995;9:121-8.

40. Levin TN, Feldman T, Bednarz J, Carroll JD, Lang RM. Transesophageal echocardiographic evaluation of mitral valve morphology to predict outcome after balloon mitral valvotomy. *Am J Cardiol* 1994;73:707-10.

CHAPTER 9

Assessment of Pulmonary valve and Right Ventricular outflow Tract with Real-time Three-Dimensional Echocardiography

Ashraf M. Anwar[1,2], Osama I.I. Soliman[1,2], Annemien E.van den Bosch[1], Jackie S. McGhie[1], Marcel L. Geleijnse[1], Folkert J. ten Cate[1], Folkert J. Meijboom[1]

[1]Department of Cardiology, Thoraxcenter, Erasmus University Medical Center, Rotterdam, The Netherlands
[2]Department of Cardiology, Al-Hussein University Hospital, Al-Azhar University, Cairo, Egypt

International Journal of Cardiovascular Imaging 2007;23:167-175

ABSTRACT

Aim: Assessment of pulmonary valve (PV) and right ventricular outflow tract (RVOT) using real-time 3-dimensional echocardiography (RT3DE).

Methods: Two-dimensional echocardiography (2DE) and RT3DE were performed in 50 patients with congenital heart disease (mean age 32 ± 9.5 years, 60% female). Measurements were obtained at parasternal views: short axis (PSAX) at aortic valve level and long axis (PLAX) with superior tilting. RT3DE visualization was evaluated by 4-point score (1: not visualized, 2: inadequate, 3: sufficient, and 4: excellent). Diameters of PV annulus (PVAD), and RVOT (RVOTD) were measured by both 2DE and RT3DE, while areas (PVAA) and (RVOTA) by RT3DE only**.**

Results: By RT3DE, PV was visualized sufficiently in 68% and RVOT excellently in 40%. PVAD and PVAA were measured in 88%. RVOTD and PVAD by 2DE at PLAX were significantly higher than PSAX (P <0.0001) and lower than that by RT3DE (P <0.001).

Conclusion: RT3DE helps in RVOT and PV assessment adding more details supplemental to 2DE.

INTRODUCTION

The right ventricular outflow tract (RVOT) extends from the antero-superior aspect of the right ventricle to the pulmonary artery (PA), and includes the pulmonary valve (PV). It is best imaged by 2-dimensional echocardiography (2DE) from the parasternal long axis view angulated superiorly and the parasternal short axis at the base of the heart. It can also be imaged from the subcostal long and transverse windows and the apical window [1]. Visualization of the PV leaflets by 2DE in long axis is limited especially in adults because 2DE images only one or two leaflets well and a short axis view often is not obtainable [2]. The level of RVOT obstruction can be determined using pulsed Doppler and color flow to identify the anatomic site at which the flow velocity increases and the post-stenotic flow disturbance appears. The obstruction itself may be depicted on 2DE as a muscular subpulmonic ridge, as deformed doming PV valve leaflet or as narrowing in the PA [2]. Transesophageal echocardiography helps in imaging RVOT from a high esophageal position at 0^o rotation with a long axis view of the PA from the valve plane to its bifurcation. The PV also may be visualized in the 90^o long axis plane. The PV is seen in its perpendicular relationship to the aortic valve in the far field of the image, so it remains virtually impossible to assess the precise morphology of valve cusps or its commissures [3]. Magnetic resonance imaging may add to the assessment of the obstruction level, PA size and may detect other associated lesions such as PA stenosis and coexisting pulmonary regurgitation [4]. Until now, it has not been possible to visualize all three leaflets of the PV simultaneously by non-invasive diagnostic tools except in rare cases in which the valve pushed interiorly [5]. The introduction of 3-dimensional echocardiography (3DE) helps in displaying the intracardiac anatomy in views that are similar to the ones encountered during operation [6]. With more advances in the techniques, probe and software, it is now possible to assess intracardiac structure and function accurately within a reasonable time with the real-time 3DE (RT3DE). We hypothesize that RT3DE will clarify the knowledge of PV anatomy and RVOT by direct visualization from all aspects. The study aimed to use RT3DE in assessment of the morphology of pulmonary valve (PV) and right ventricular outflow tract (RVOT) and comparing its measurements with that obtained by 2DE.

SUBJECTS and METHODS

Fifty patients (mean age 32 ± 9.5 years, 60% female) (Table 1) referred for echocardiography lab for evaluation of adult congenital heart disease. All patients were in sinus rhythm. In all 2DE was done

with the patient in the left lateral decubitus position using both apical and parasternal views with a commercially available ultrasound system (Philips Sonos 7500 with 3.5 MHz probe, Best, The Netherlands). RVOT and PV were examined at parasternal short axis (PSAX) view at aortic valve level and parasternal long axis (PLAX) with moving transducer towards the base angulating superiorly. The subtotal short axis view at aortic valve level was used instead of parasternal one in 10 cases. Zooming was used to clarify images and minimize artefacts. The following variables were measured in each patient [7]: (1) RVOT diameter (RVOTD) measured just proximal to the PV at both views at its maximal width (end-diastole), (2) PV annulus diameter (PVAD) at same frame, (3) proximal PA diameters (PPAD), and (4) distal PA diameters (DPAD) just before its bifurcation. Measurements were obtained only from good image quality without echo dropout.

Table 1: Distribution of congenital heart defects in studied patients

Type of congenital defect	Number of patients (%)
Atrio-ventricular septal defect (AVSD)	13 (26%)
Valvular Pulmonary stenosis (PS)	7 (14%)
Post defect closure	7 (14%)
Atrial septal defect (ASD)	5 (10%)
Atrial septal defect + Ventricular septal defect	4 (8%)
Transposed great arteries (TGA)	4 (8%)
Ventricular septal defect (VSD)	3 (6%)
Ebstein's anomaly	2 (4%)
Coronary AV fistula	2 (4%)
Normal	2 (4%)
Fallot's tetralogy	1 (2%)

Transthoracic RT3DE

RT3DE was done by the same ultrasound system attached to a X4 matrix array transducer, capable of providing real-time B-mode images. 3D images were collected approximately within 5-7 seconds of breath holding in full volume mode. The 3D data set was transferred to an offline analysis software package (TomTec, Munich, Germany). Data were stored digitally and subsequently evaluated by two blinded observers (AMA, JMcG). Data analysis of 3D echo imaging had been based on a 2D approach relying on the echo images obtained from both views (PSAX and PLAX). By using the crop function for image formatting, multiple sections through the scanned volume were done. We selected the narrowest slice to enable visualization of RVOT and PV from both aspects (proximal ventricular and distal pulmonic). RT3DE gain and brightness were adjusted to improve delineation of anatomic structures. The relevant features of RVOT, PV, PPA and DPA were checked and classified according to a subjective 4-point scale for image quality (1= not visualized, 2 = inadequate, 3 = sufficient and 4 =

excellent). By manual tracing of the inner border of RVOT and the PVA, the surface area was automatically delineated and could be visualized from different points of view. The following measures were obtained: (1) RVOTD included maximum RVOTD (max RVOTD) defined as the widest diameter of the RVOT, and minimum RVOTD (min RVOTD) defined as the shortest diameter of the RVOT, (2) RVOT area (RVOTA): measured at its maximal width (end-diastole), (3) PVAD: included two diameters: included maximum PVAD (max PVAD) defined as the widest diameter of the PVA, and minimum PVAD (min PVAD) defined as the shortest diameter of the PVA, (4) PVA area (PVAA): measured at its maximal width (end-diastole), and (5) PPAD, DPAD.

STATISTICAL ANALYSES

All data obtained by 2D TTE and RT3DE were presented as mean ± SD to determine whether the difference in values between both techniques was statistically significant or not. A paired sample *t*-test was performed for comparing between means of variables. The level of significance was set to $P < 0.05$. Interobsever agreement for visualization score was estimated using kappa values for each morphologic feature and classified as excellent with value of 0.93-1.0, very good 0.81-0.92, good 0.41-0.60 [8]. For 2DE measurements, a random sample consisted of 20 patients was selected and *t*-test was applied for interobserver variability. Interobserver variability for RT3DE measurements in all patients was estimated according to the Bland and Altman method [9].

RESULTS

RVOT and PV by 2DE

Higher percentage of clear visualization and measurements of RVOT and PVA could be obtained from the PLAX view than from the PSAX view. RVOTD could be measured from the PLAX view in 28 patients (56%) and in 26 patients (52%) from the PSAX view. PVAD was measured in 48 patients (96%) from the PLAX view and in 46 patients (92%) from the PSAX view. PPAD and DPAD were recorded from both views in equal percentage (78% for PPA and 42% for DPA). Measurements of RVOTD and PVAD from both views correlated well (Figure $2_{A,D}$). However, RVOTD and PVAD were significantly higher as measured from the PLAX view than from the PSAX ($P < 0.0001$).

RVOT and PV by RT3DE

Acquisition and analysis of RT3DE data were performed successfully within 5-7 minutes per patient. RVOT was visualized excellently in 20 patients (40%) and not visualized in 24 patients (48%). Its shape appeared as an oval shape and not completely circular (Figure 1_A). Calculated RVOTA, max RVOTD and min RVOTD were obtained in 26 patients (52%). The mean RVOTA was 41.5 ± 33.4 mm. PVA was visualized excellently in 44 patients (88%) and was not visualized in two patients (4%). The mean PVAA was 33.5 ± 30.1 mm. PV was visualized sufficiently in 34 patients (68%) and excellently in 12 patients (24%). The number, thickness and mobility of cusps could be studied in 35 patients (70%). Bicuspid pulmonary valve was seen in 3 patients. The diagnosis of the three patients was transposed great arteries, Fallot's tetralogy, and pulmonary stenosis. Pulmonary valve commissures and lines of closure were seen in 35 patients (70%) (Figure $1_{C,D}$). Pulmonary valve area could not be obtained well in a considerable number of patients with high interobserver variability.

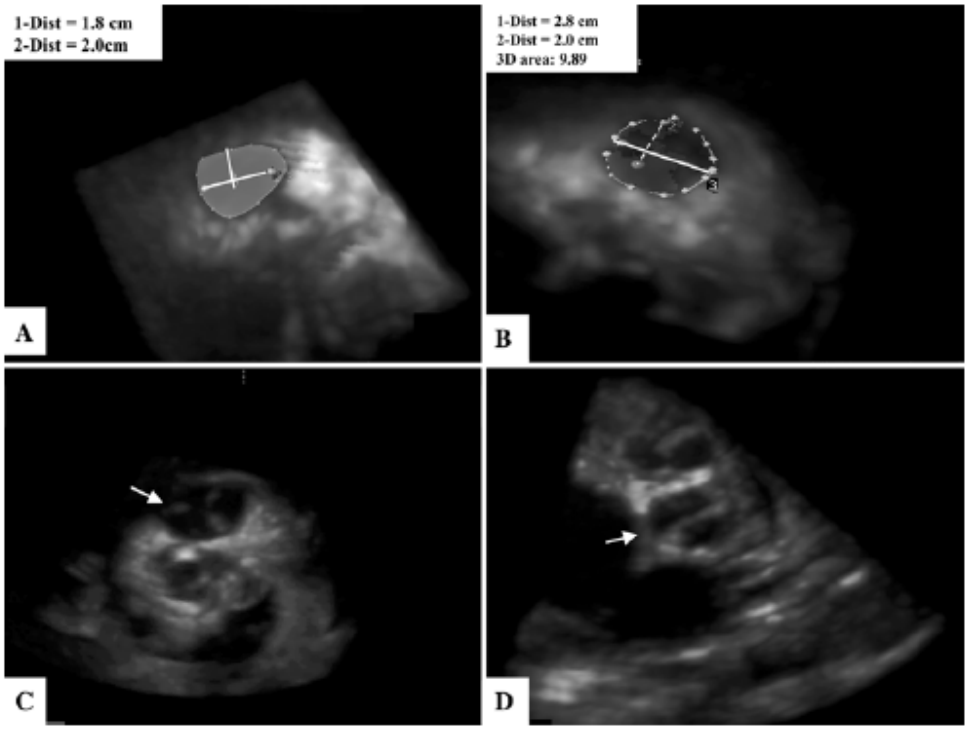

Fig. 1 (A) RT3DE showed the morphology of the traced oval shaped RVOT. The vertical line (1) appears inside it is the RVOTD measured by 2DE at PSAX, and the horizontal line (2) is RVOTD at PLAX. Both lines are away from the true RVOTD, (B) Traced PVA visualized by RT3DE. The horizontal line (1) is PVAD measured by RT3DE and vertical dashed line is PVAD by 2DE in PLAX, (C) RT3DE image of closed tricuspid pulmonary valve with its closure lines and (D) Bicuspid pulmonary valve with central closure line

Comparison of 2DE and RT3DE

The RT3DE quadscreen showed that RVOTD obtained by 2DE from PSAX view was perpendicular on the max RVOTD and parallel to the min RVOTD, while RVOTD obtained from PLAX was parallel to the max RVOTD but was not extended to the annular ends. The same findings were found for PVAD (Figure $1_{A,B}$). Measurements of RVOTD with 2DE and RT3DE were significantly correlated with each other (Figure $2_{B,C}$), and also for PVAD (Figure $2_{E,F}$). The max RVOTD was significantly larger than RVOTD measured by 2DE from both views (P <0.0001), while the min RVOTD was comparable to RVOT measured from PSAX view (P = 0.8). PVAD measurement by RT3DE was significantly larger than that measured by 2DE from both views (P <0.0001). The value for RT3DE application in comparison with 2DE is shown in Table 4.

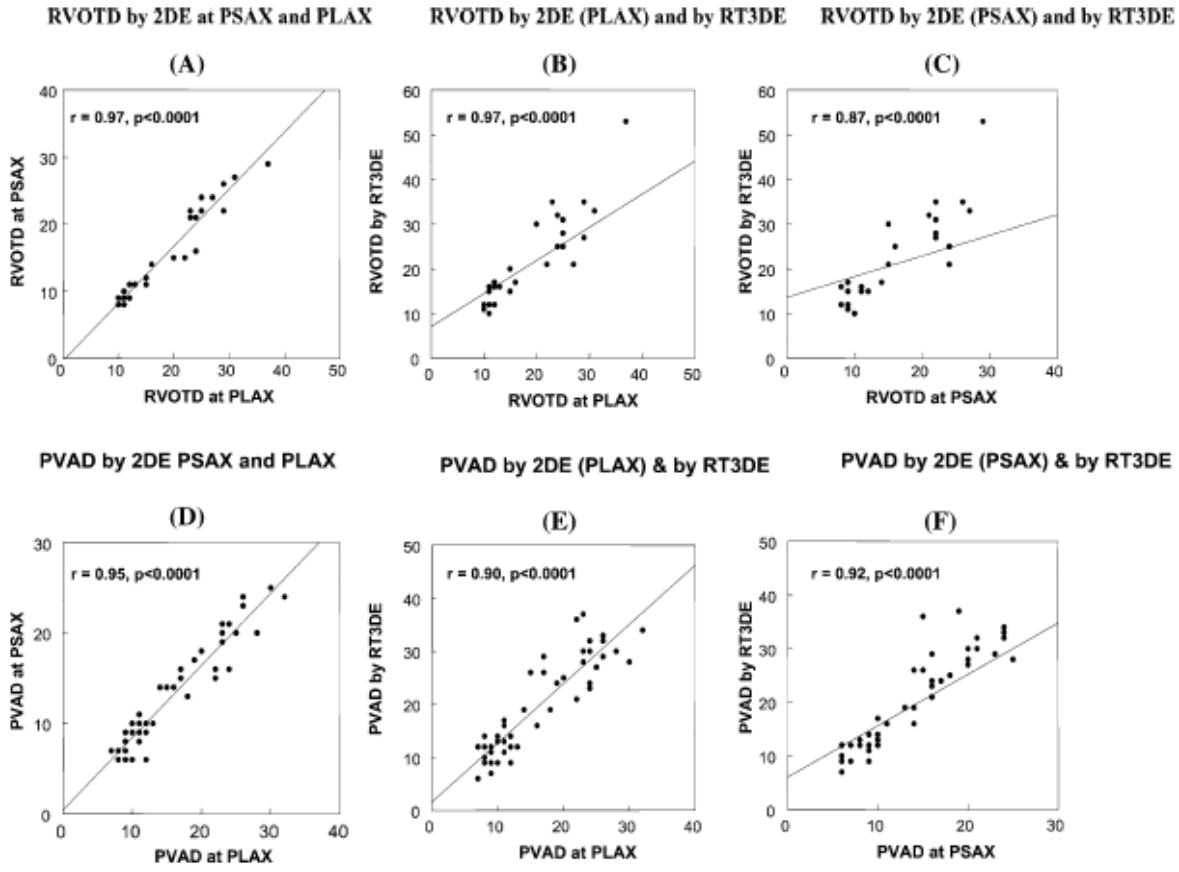

Fig. 2 (A) Correlation between RVOTD measured by 2DE in PLAX and PSAX, (B) Correlation between RVOTD measured by 2DE in PLAX and max RVOTD measured by RT3DE, (C) Correlation between RVOTD measured by 2DE in PSAX and max RVOTD measured by RT3DE, (D) Correlation between PVAD measured by 2DE in PLAX and PSAX, (E) Correlation between PVAD measured by 2DE in PLAX and that measured by RT3DE, and (F) Correlation between PVAD measured by 2DE in PSAX and that measured by RT3DE

PPA and DPA by 2DE and RT3DE

Measurements of PPAD and DPAD were equal in both 2DE views (PSAX and PLAX). By RT3DE, PPA was excellently visualized in 29 patients (58%) and sufficiently in 10 patients (20%). DPA was excellently visualized in 15 patients (30%) and not visualized in 27 patients (54%) (see Table 3). Measurements of PPAD and DPAD by 2DE and RT3DE were comparable (see Table 2).

Table 2: Measurements of 2DE and RT3DE

	2DE (PLAX)	2DE (PSAX)	RT3DE	P value *	P value **
RVOTD (mm)	19.7 ± 7.7	16.4 ± 6.8	22.2 ± 10.0 (max) 15.7 ± 6.2 (min)	0.0001	0.001
PVAD (mm)	16.4 ± 7.3	13.5 ± 6.1	19.4 ± 9.1	0.0001	0.0001
PPAD (mm)	18.3 ± 7.1	18.1 ± 7.1	17.4 ± 5.3	NS	NS
DPAD (mm)	19.3 ± 9.1	19.1 ± 8.0	18.6 ± 6.4	NS	NS

2DE: 2 dimensional echocardiography, PLAX: parasternal long axis, PSAX: parasternal short axis, RT3DE: real-time 3-dimensional echocardiography, DPAD: distal pulmonary artery diameters, PPAD: proximal pulmonary artery diameter, PVAD: pulmonary valve annulus diameter, and right ventricular outflow tract (RVOT).
* *P* value between 2DE measurements at both views (PLAX and PSAX)
** *P* value between measurements of RT3DE and 2DE at PLAX

Table 3: Scores for RT3DE visualization of RVOT, PVA, PV, PPA and DPA

Score	RVOT	PVA	PV	PPA	DPA
Excellent (4)	20 (40%)	44 (88%)	12 (24%)	29 (58%)	15 (30%)
Sufficient (3)	6 (12%)	4 (8%)	34 (68%)	10 (20%)	8 (16%)
Inadequate (2)	0 (0%)	0 (0%)	4 (8%)	0 (0%)	0 (0%)
Missed (1)	24 (48%)	2 (4%)	0 (0%)	11 (22%)	27 (54%)
Median score	2.4	3.8	3.1	3.1	2.2
Mean score	2.4 ± 1.4	3.8 ± 0.6	3.2 ± 0.6	3.2 ±0.5	2.2 ± 1.4

Abbreviations: DPAD: Distal pulmonary artery, PPAD: proximal pulmonary artery, PV: Pulmonary valve, PVA: pulmonary valve annulus and RVOT: right ventricular outflow tract.

Interobsever correlation and agreement

The agreement for visualization score by RT3DE was fair for the assessment of PV (Kappa value: 0.59), good for RVOT (Kappa value: 0.71) and very good for PVA, PPA and DPA (Kappa value: 0.91). Excellent interobserver correlation was found for RT3DE measurements (r = 0.94, *P* <0.0001) for RVOTD, and PVAD. Excellent interobserver correlation also was found for 2DE (r = 0.98, *P* <0.0001) for RVOTD and PVAD. According to the Bland - Altman analysis of agreement, the mean differences were (mean difference: - 0.15 ± 1.4, agreement: 2.65 - 2.95; p = 0.7) (mean difference: - 0.57 ± 1.90, agreement: 3.33 - 4.37; p = 0.09) (mean difference: 0.08 ± 1.5, agreement: 3.08 - 2.92; *P*

= 0.7) (mean difference: - 0.40 ± 1.90, agreement: 3.40 - 4.20; *P* = 0.1) for RVOT by 2DE, PVAD by 2DE, RVOT by RT3DE, and PVAD by RT3DE, respectively (Figure 3, 4).

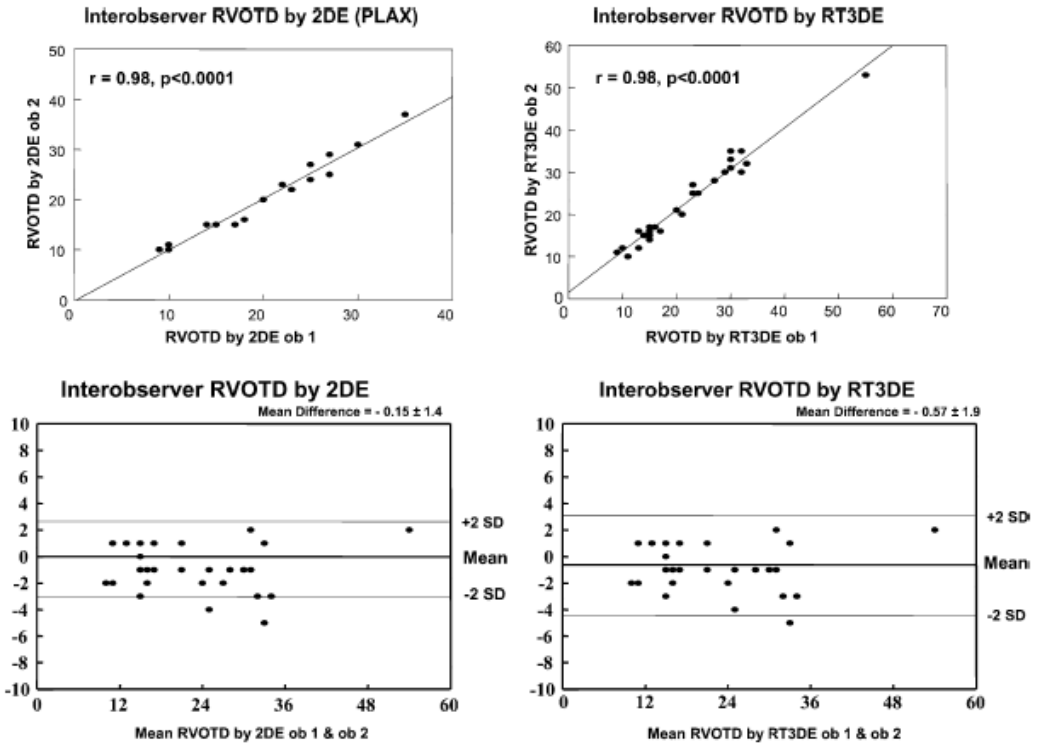

Fig. 3 Interobserver correlation and agreement according to Bland and Altman principle for measuring RVOTD by 2DE and RT3DE

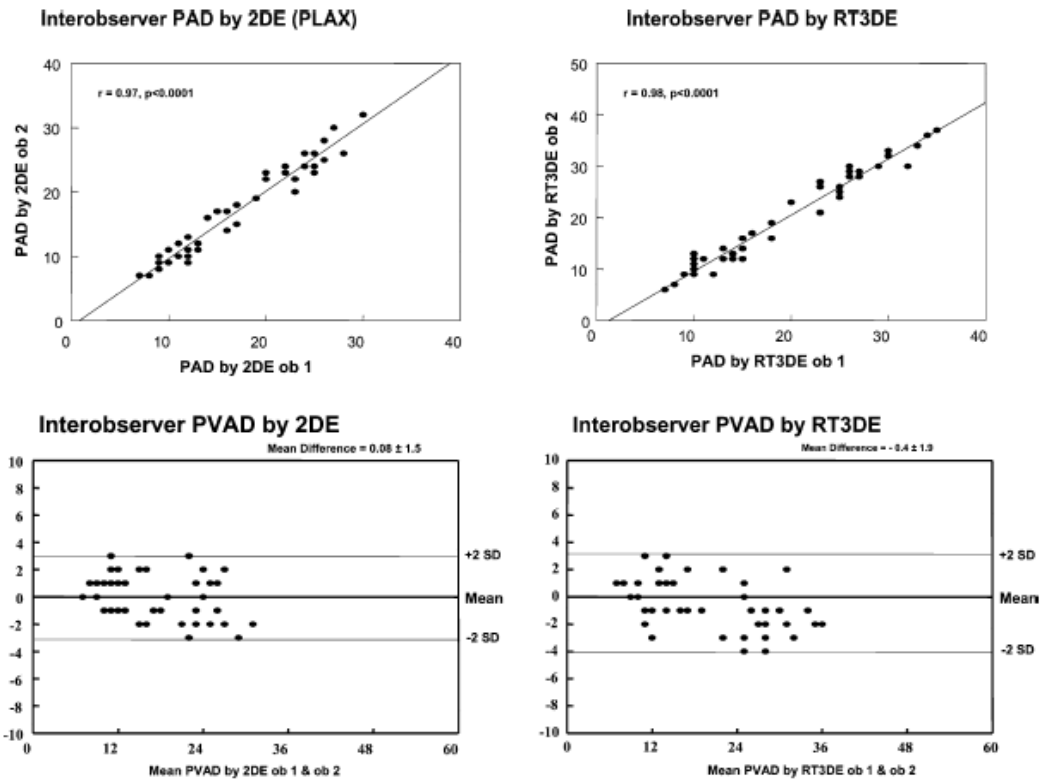

Fig. 4 Interobserver correlation and agreement according to Bland and Altman principle for measuring PVAD by 2DE and RT3DE

DISCUSSION

The study applied RT3DE for the assessment of PV and RVOT morphology and compared its measurements to those obtained with 2DE. This assessment could be obtained excellently or at least sufficiently in a higher percentage of patients. The main findings of our study are (1) RVOT shape was not circular but oval, (2) RVOTA and PVAA could be measured by RT3DE, and (3) RT3DE measurements of RVOTD and PVAD were higher than 2DE measurements. Assessment of PV and RVOT is of clinical importance because the understanding of normal morphology and function helps in detection of anomalies and selection of therapeutic strategies. For example, in pulmonary stenosis, therapeutic strategy is totally dependent on RVOT and PV morphology and function. The incidence of anomalies included within the term of pulmonary stenosis varies between 10.7% and 30% of all congenital heart defects [10,11]. Despite this incidence, the pulmonary valve is the least studied valve. Its assessment is totally dependent on 2DE, but images often less satisfactory in adolescents and adults [7]. The use of pulsed and continuous wave Doppler helps in accurate estimation of subvalvular and transvalvular pressure gradients for detection of pulmonary stenosis and selection for balloon valvuloplasty [12]. Several methods have attempted to accurately characterize PV morphology and detailed anatomy [13]. Kinelitze et al used bright blood cine magnetic resonance to visualize leaflets of the valve in 14 patients following Ross operation and he achieved good visualization with signal to noise ratio 7.5 ± 2.2 in patient group versus 9.8 ± 3.0 in normal control group [14]. Berdajs et al constructed a geometric model of the pulmonary root in 20 normals. By morphometric measurements of the distances between commissures and between intervalvular triangles, they described the asymmetrical structure of pulmonary root [15]. The current study shows that measurement of PVAD and RVOTD by 2DE according to the standard echocardiographic views leads to significant underestimation in comparison with RT3DE measurements. This could be explained by the fact that 2DE measures the distance from the basal attachment of one leaflet to the basal attachment of adjacent leaflet and these lines do not necessarily span the full diameter of RVOT but provide a tangential profile of the outlet [16]. Lines of RVOTD and PVAD measurements from PSAX view are perpendicular on the max RVOTD and PVAD by RT3DE. Thus, if 2DE is the only available method for PV and RVOT assessment, PLAX view should be used due to better visualization, and more alignment with RT3DE measurements of RVOTD and PVAD than PSAX. The study showed that RT3DE achieved excellent visualization of PVAA and calculation of its diameters in 88% of patients. In contrast, RVOT

visualization and diameter measurement was not optimal and this may be due to tissue dropout and gain adjustment during acquisition. The PV visualization was sufficiently achieved in 92% of patients. The number, thickness and mobility of leaflets could be clearly visualized in 70% of patients. Commissures and direction of closure lines also could be visualized. Since calculation of PV area was not obtained well in considerable number of studied group and had wide interobserver variability, it was excluded from further analysis. This may be due to multiple levels at which area could be calculated as well as time points; no standardized method is available. Providing these data potentially constitute future application of RT3DE in a wider clinical routine and may enhance understanding valve morphology by providing accurate measurements necessary for selection of proper management (balloon valvuloplasty, surgical valvotomy, stented pulmonary valve or valve replacement). Another advantage of RT3DE application was visualization of PPA in 78% of patients and DPA in 46% of patients, which may help in visualization of supravalvular stenosis (by measuring luminal reduction and level(s) of stenosis), post-stenotic dilatation (by measuring % of luminal dilatation) or evaluation prior to surgery (shunts or correction).

Limitation of study

The study was conducted in a small number of patients characterized by heterogeneous congenital heart defects. The age of patients 32 ± 9.5 years affected the image quality of 2DE and RT3DE leading to significant difficulties in visualization of the RVOT. The data of the studied patients were not correlated with direct surgical visualization because a considerable number of patients were studied after corrective surgery or surgery was not the selected therapeutic strategy.

Perspective

The clinical value of RT3DE has to be validated in future studies by including selected group of patients with pulmonary stenosis with reference to intraoperative findings or MRI. For example a comparison of PV area by RT3DE at various levels to surgical findings could be helpful to develop a standardized approach to PV assessment.

CONCLUSION

RT3DE could help in clarification of detailed anatomy of RVOT and PV beyond the scope of established 2DE. A detailed assessment may provide a basis for proper selection of therapeutic strategy.

REFERENCES

1. Lang RM, Bierig M, Devereux RB, Flachskampf FA, Foster E, Pellikka PA, Picard MH, Roman MJ, Seward J, Shanewise JS, Solomon SD, Spencer KT, Sutton MS, Stewart WJ. Recommendations for chamber quantification: a report from the American Society of Echocardiography's Guidelines and Standards Committee and the Chamber Quantification Writing Group, developed in conjunction with the European Association of Echocardiography, a branch of the European Society of Cardiology. *J Am Soc Echocardiogr* 2005;18:1440-63.
2. King MEE. Echocardiographic evaluation of the adult with unoperated congenital heart disease. *In Otto, The practice of clinical echocardiography* 2002;Otto c (ed0; WB Saunders:868-899.
3. Stumper O, Witsenburg M, Sutherland GR, Cromme-Dijkhuis A, Godman MJ, Hess J. Transesophageal echocardiographic monitoring of interventional cardiac catheterization in children. *J Am Coll Cardiol* 1991;18:1506-14.
4. Vick GW, 3rd, Rokey R, Huhta JC, Mulvagh SL, Johnston DL. Nuclear magnetic resonance imaging of the pulmonary arteries, subpulmonary region, and aorticopulmonary shunts: a comparative study with two-dimensional echocardiography and angiography. *Am Heart J* 1990;119:1103-10.
5. McAleer E, Kort S, Rosenzweig BP, Katz ES, Tunick PA, Phoon CK, Kronzon I. Unusual echocardiographic views of bicuspid and tricuspid pulmonic valves. *J Am Soc Echocardiogr* 2001;14:1036-8.
6. Vogel M, Ho SY, Lincoln C, Yacoub MH, Anderson RH. Three-dimensional echocardiography can simulate intraoperative visualization of congenitally malformed hearts. *Ann Thorac Surg* 1995;60:1282-8.
7. Foale R, Nihoyannopoulos P, McKenna W, Kleinebenne A, Nadazdin A, Rowland E, Smith G. Echocardiographic measurement of the normal adult right ventricle. *Br Heart J* 1986;56:33-44.
8. Byrt T. How good is that agreement? *Epidemiology* 1996;7:561.
9. Bland JM, Altman DG. Statistical methods for assessing agreement between two methods of clinical measurement. *Lancet* 1986;1:307-10.
10. Hoffman JI. Incidence of congenital heart disease: I. Postnatal incidence. *Pediatr Cardiol* 1995;16:103-13.
11. Rocchini AP E. Pulmonary stenosis. In: Emmanouilides GC RT, Allen HD, Gutgesell HP, ed. Moss and Adams' Heart disease in infants, children, and adolescents. Baltimore: William & Wilkins, 1995: 930-962.
12. Mulhern KM, Skorton DJ. Echocardiographic evaluation of isolated pulmonary valve disease in adolescents and adults. *Echocardiography* 1993;10:533-43.
13. Nascimento R, Campelo M, Maciel J, Lourenco A, Carneiro M, Cunha D, Van-Zeller P. [Echocardiographic evaluation of pulmonary valve stenosis for valvuloplasty in children and adults]. *Rev Port Cardiol* 1993;12:141-50.
14. Kivelitz DE, Dohmen PM, Lembcke A, Kroencke TJ, Klingebiel R, Hamm B, Konertz W, Taupitz M. Visualization of the pulmonary valve using cine MR imaging. *Acta Radiol* 2003;44:172-6.
15. Berdajs D, Lajos P, Zund G, Turina M. Geometrical model of the pulmonary root. *J Heart Valve Dis* 2005;14:257-60.
16. Martinez RM, Anderson RH. Echocardiographic features of the morphologically right ventriculo-arterial junction. *Cardiol Young* 2005;15 Suppl 1:17-26.

CHAPTER 10

Assessment of Left Atrial Volume and Function by Real-Time Three-Dimensional Echocardiography

Ashraf M. Anwar[1,2], Osama I.I. Soliman[1,2], Marcel L. Geleijnse[1], Attila Nemes[1,3], Wim B. Vletter[1], and Folkert J. ten Cate[1]

[1]Department of Cardiology, Thoraxcenter, Erasmus University Medical Center, Rotterdam, The Netherlands
[2]Department of Cardiology, Al-Hussein University Hospital, Al-Azhar University, Cairo, Egypt
[3]Second Department of Medicine and Cardiology Center, University of Szeged, Szeged, Hungary

International Journal of Cardiology 2008;123(2): 155-61

ABSTRACT

Background: Determination of left atrial (LA) size and function is important in clinical decision-making. Calculation of LA volume (LAV) is the most accurate index of LA size.

Aim: To compare real-time 3-dimensional echocardiography (RT3DE) and 2-dimensional echocardiography (2DE) for calculation of LAV and function.

Methods: Fifty patients were studied using 2DE and RT3DE for calculating LAV including: Maximum (Vmax), minimum (Vmin) and pre atrial contraction (VpreA) volumes. For 2DE, the formula: LAV = 8 (A_1) $(A_2)/3\ \pi$ (L) was used, while for RT3DE, offline analysis was performed using commercially available software. LA function indices including total atrial stroke volume (TASV), active ASV (AASV), total atrial emptying fraction (TAEF), active AEF (AAEF), passive AEF (PAEF), and atrial expansion index (AEI) were calculated.

Results: Patients were classified into 2 equal groups: group I with normal Vmax (<50ml) and group II with Vmax (≥50ml). Good correlation was obtained between RT3DE and 2DE for LAV (r = 0.64, P = 0.001) in group I and (r = 0.83, P <0.0001) in group II. In group I, LAV and functions showed no significant difference by both techniques, while in group II, the Vmin and VpreA were significantly lower by RT3DE than 2DE (P = 0.009, 0.006). TAEF, AEI, and PAEF indices were significantly higher by RT3DE than 2DE in group II.

Conclusion: RT3DE provides a reproducible assessment of active and passive LA function by volumetric cyclic changes. It is comparable and may be superior to 2DE due to its higher sensitivity to volume changes.

INTRODUCTION

The left atrium (LA) serves as a reservoir, a conduit and a booster pump for blood returning from the lungs to the heart. Changes in LA size and function are associated with cardiovascular disease and are risk factors for atrial fibrillation, stroke and death [1-3]. Echocardiography is the most commonly used non-invasive imaging technique for estimation of LA size. The M-mode measurement of the LA antero-posterior dimension as indicator for size has several limitations due to geometric assumption made about LA shape and due to slightly diverging position and orientation of imaging planes [4]. It has been suggested that LA volume (LAV) may be a superior index for LA size [5]. Two-dimensional echocardiographic (2DE) derived LAV has been shown to provide a more accurate assessment of LA size than M-mode but the problem of geometric assumption still remains [6,7]. Three-dimensional echocardiography (3DE) has demonstrated superior accuracy for measuring left ventricular volume comparable to conventional 2DE and the 3DE reconstruction has been validated for LAV quantification [8-10]. Real-time 3DE (RT3DE) allows fast acquisition from a single acoustic window of dynamic pyramidal data structure that encompasses the entire heart [11]. The purpose of the present study was to compare between 2DE and RT3DE for calculation of LAV and assessment of LA function in normal-sized and dilated LA.

METHODS

The study retrospectively comprised randomly selected fifty patients in sinus rhythm with good 2DE image quality. A standard 2DE and RT3DE examinations were performed for all patients.

Transthoracic 2DE

2DE was undertaken with the patient lying in the left lateral decubitus with quite respiration using both apical and parasternal views. 2DE studies were performed using a 3.5 MHZ probe and a commercially available ultrasound system (Philips Sonos 7500, Best, The Netherlands). The following measures were taken: LA area at apical 4-chamber view (A1) by manual tracing of LA endocardial border. The superior border of atrial outline was a straight line connecting both sides of the mitral leaflet base attachment points. Both the atrial appendage and the pulmonary veins were excluded when visualized, LA area at apical 2-chamber (A2) with same tracing, and LA long axis (L): defined as the distance of the perpendicular line measured from the middle of the plane of mitral annulus to the superior aspect of LA in both 4 and 2-chamber views and the shortest of both lines was used (Figure 1).

LAV was calculated according to the formula(12): Volume = $8(A_1)\ (A_2) / 3\pi$ (L) at 3 phases of ventricular cardiac cycle: 1) maximum volume (V max): at end-systole, the time at which atrial volume was largest just before mitral valve opening, 2) minimum volume (V min): at end-diastole, the time at which atrial volume at its nadir before mitral valve closure, and 3) volume before atrial contraction (V pre A): the last frame before mitral valve reopening or at time of P wave on ECG. From the three volumes, the following measurements were selected as indices of LA function and calculated according to previous studies [13, 14]:

1) Total Atrial Stroke Volume (TASV): V max – V min.
2) Total Atrial Emptying Fraction (TAEF): TA SV/ V max x 100
3) Active Atrial Stroke Volume (AASV): V pre A – V min.
4) Active Atrial Emptying Fraction (AAEF): AA SV/ V pre A x 100
5) Atrial Expansion Index (AEI): TASV / V min x 100.
6) Passive Atrial Emptying Fraction (PAEF): (V max – V pre A) / V max x 100

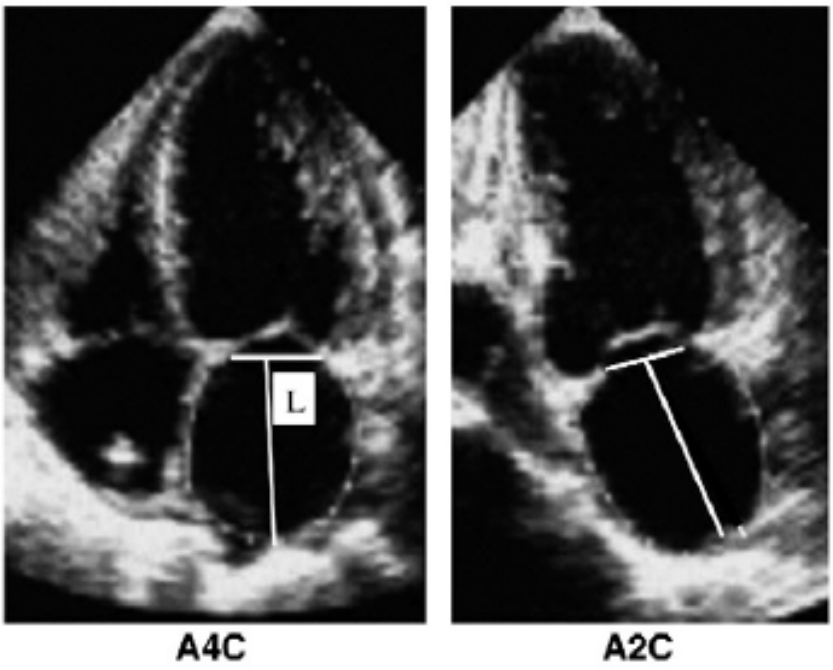

Fig 1: Calculation of LAV using 2DE by manual tracing of LA endocardial border at apical 4 chambers (A1) and apical 2 chamber views (A2), L is the long axis, then apply the formula.

Transthoracic RT3DE

RT3DE was performed also with the patient lying in the left lateral decubitus using 4 MHZ transducer capable of providing real-time B-mode and colour-Doppler using same ultrasound system. The system scans a 60 ^{o} x 30 ^{o} 3D pyramid of data. 3D images were collected in full volume mode

approximately within 5-7 seconds of seconds of breath holding in expiration. The 3D data were transferred to an offline Q-lab system for analysis. Data were stored digitally and subsequently analysed. Analysis of 3D echo imaging had been based on a 2D approach relying on the echo images obtained from the apical views and on a semi automated tracing of endocardial border. This is performed by mark 5 points in the atrial surfaces of mitral annulus: at anterior, inferior, lateral and septal annuli and the 5^{th} point at apex of LA. Once this is completed, the endocardial surface was automatically delineated and a mathematical model of the LA could be visualized from different points of views and the LAV calculation was obtained (Figure 2). Manual modification was made to correct the automatic tracings if needed. LAV was measured at the same phases as measured by 2DE and the same measurements calculated. All the recorded images were analysed at different times by two independent echocardiographers. The same images were also analyzed on a different day by one of these same observers.

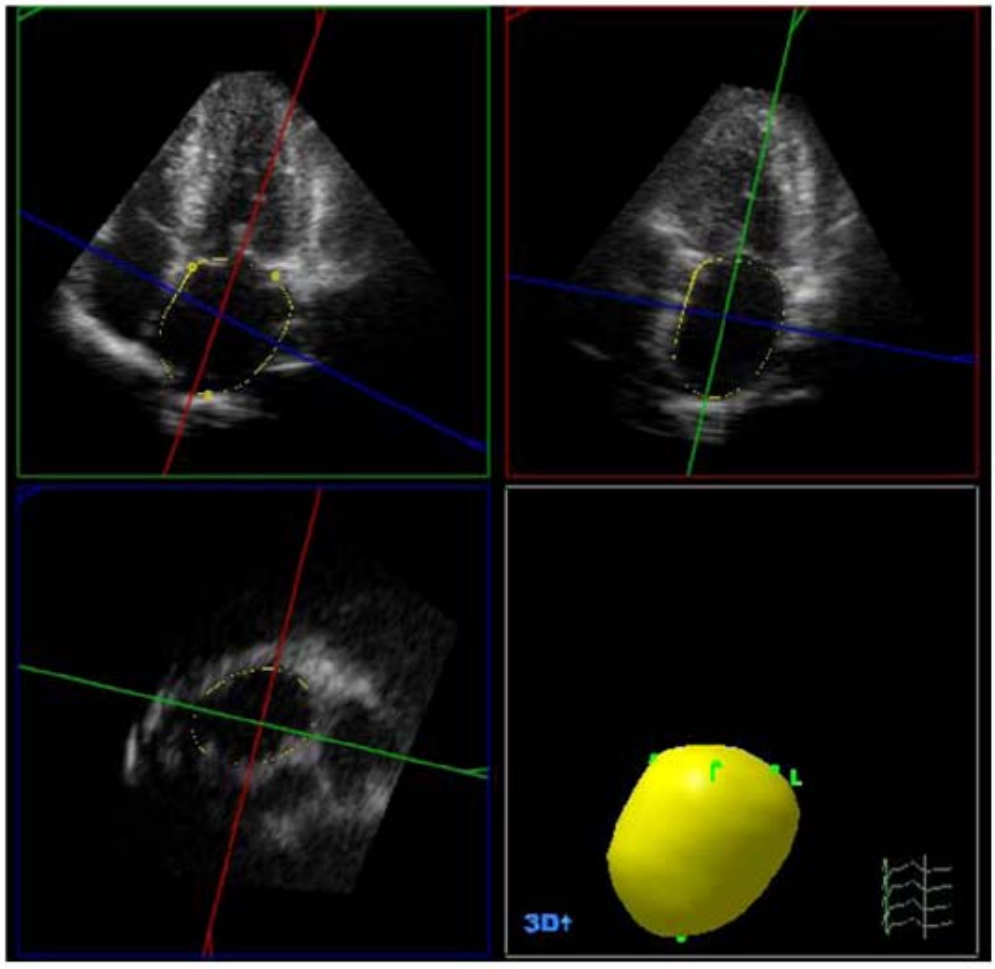

Fig 2: Calculation of LAV using RT3DE by automatic tracing using Q lab software. Upper 2 images is apical 4 chamber and 2 chamber views, by marking 5 points, the whole LA cast was obtained.

STATISTICAL ANALYSES

All values of LAV and its functions were expressed as mean ± SD. Paired sample t-test was performed to determine whether the difference in the values between 2 methods was significant or not. The level of significance was set to $p<0.05$. Regression analysis for detection of correlation between both techniques for all values, the correlation considered being significant <0.05 level. The statistical package used was SPSS version 12.1. Pearson's coefficient was used for inter and intraobserver correlation between all LAV by both techniques. Interobserver agreement was studied according to Bland and Altman method [15].

RESULTS

A total of 50 patients with mean age 43.6 ± 9.3 years and male percentage 66% were included in this study. The baseline criteria of all patients are listed in (Table 1). Calculation of LAV was obtained by 2DE in all patients within 10 minutes as mean time for every patient. According to V max, patients were classified into 2 equal groups: group I included patients with V max <50 ml, and group II included patients with V max ≥50 ml. There were no significant differences between both groups in age and sex distribution. Mild mitral regurgitation was present in 11 patients: 3 patients (12%) in Group I, 8 patients (32%) in Group II. Cardiac abnormalities (hypertension, coronary artery disease, or cardiomyopathy) were detected in 20 patients (80%) in Group II, whereas in Group I only 5 patients (20%) had cardiac abnormalities.

Table 1: Baseline criteria for all patients in both groups

	Total patients n= 50	**Group I (V max < 50 ml) n= 25**	**Group II (V max ≥ 50 ml) n= 25**
Age (year)	43.6 ± 9.3	42.2 ± 7.5	44.8 ± 8.5
Male Gender (%)	33 (66%)	17 (68%)	16 (66%)
Clinical Diagnosis			
Normal	25 (50%)	20 (80%)	5 (20%)
Hypertension	13 (26%)	3 (12%)	10 (40%)
Coronary disease	7 (14%)	2 (8%)	5 (20%)
Cardiomyopathy	5 (10%)	0 (0%)	5 (20%)
Mitral regurgitation			
None	39 (78%)	22 (88%)	17 (68%)
Mild (grade 1)	11 (22%)	3 (12%)	8 (32%)
Medications			
None	25 (50%)	20 (80%)	5 (20%)
B-Blockers	2 (4%)	0 (0%)	2 (8%)
ACE/I	9 (18%)	2 (8%)	7 (28%)
Ca channel blocker	9 (18%)	3 (12%)	6 (24%)
Nitrates	5 (10%)	0 (0%)	5 (20%)

Both groups were compared to each other with respect to cyclic changes of LAV during the cardiac cycle and indices of functions were calculated (see Table 2). The three LAV were increased in group II, and thus TASV was nearly twice as large in group II than group I. All indices of active LA functions including TAEF, AAEF, and AEI were lower for group II indicating an impaired LA function.

Table 2: Values of LAV and parameters of LA function in both groups using RT3DE and 2DE

	Group I (V max< 50 ml) n= 25		**Group II (V max≥ 50 ml) n= 25**		**P value**	**P value**
	RT3DE	**2DE**	**RT3DE**	**2DE**	*****	******
V max	37.1 ± 11.5	38.2 ± 10.7	79.1 ± 26.4	84.2 ± 33.6	NS	NS
V min	15.6 ± 6.1	17.7 ± 8.1	39.7 ± 17.8	46.8 ± 21.4	0.05	0.009
V pre A	23.5 ± 8.1	25.0 ± 7.6	52.0 ± 17.3	61.0 ± 23.5	NS	0.006
TSV	21.5 ± 10.2	20.4 ± 7.0	39.3 ± 15.7	38.4 ± 18.1	NS	NS
TA EF	56.3 ± 15.6	55 ± 14%	50.5 ± 13.4	46.1 ± 13.2	NS	0.04
AA SV	8.0 ± 6.	7.3 ± 4	12.2 ± 6.1	15.0 ± 7.3	NS	NS
AA EF	30.2 ± 28.1	31.4 ± 17.8	25.7 ± 14.0	26.4 ± 12	NS	NS
AEI	17.0 ± 12	14.2 ± 7.4	11.5 ± 5.4	9.4 ± 4.0	NS	0.04
AP EF	34.1 ± 10.1	34.0 ± 10.1	33.6 ± 10.3	26.8 ± 12.1	NS	0.01

***RT3DE acquisition*:**

All RT3DE examination was carried out successfully and automatic tracing was possible. The acquisition time for RT3DE dataset was 15 seconds. Calculation of LAV was obtained within 5-7 minutes per patient depending on image quality. LAV in group II was twice as large as group I. Indices of active LA function including (AAEF, AEI) were significantly less than group I.

Comparison of 2DE and RT3DE

There was a good correlation between both techniques for the three LAV measurements (r = 0.64, P = 0.001) in group I and (r = 0.83, P < 0.0001) in group II. The results of linear regression analysis for both techniques are shown in Figure 3. By comparing the absolute figures of LAV and indices of function by both techniques, the values of RT3DE were not significantly different from that measured by 2DE either for LAV or function in group I. In group II, however the V min and V pre A were significantly lower by RT3DE than by 2DE and this was reflected on TAEF, AEI and PAEF indices which became higher by RT3DE than by 2DE (see Table 2).

Observer agreement

There was excellent concordance for the three LAV analysed between two independent observers (r = 0.97, P <0.0001) for RT3DE and (r = 0.98, P < 0.0001) for 2DE (Figure 3). According

to the Bland and Altman principle, 2DE showed good agreement with V min (mean difference: - 0.26 ± 3.17, agreement = - 6.6, 6.08) but with V max and V Pre A, the agreement was less (mean difference: 6.03 ± 9.43, agreement = - 12.83, 24.89) and (mean difference: 1.71 ± 4.31, agreement = - 6.91, 10.33) respectively. Interobserver agreement for RT3DE was good in the three LAV. For V max, mean difference: 1.34 ± 4.34, agreement = - 7.34, 10.02, for V pre A, mean difference: - 0.26 ± 3.36, agreement = - 6.98, 6.56, and for V min, mean difference: 0.19 ± 3.29, agreement = - 3.10, 3.48) (Figure 4,5,6). Intraobserver correlation was ($r = 0.90$, $p<0.0001$) and ($r = 0.88$, $p < 0.0001$) for RT3DE and 2DE respectively for the three LAV.

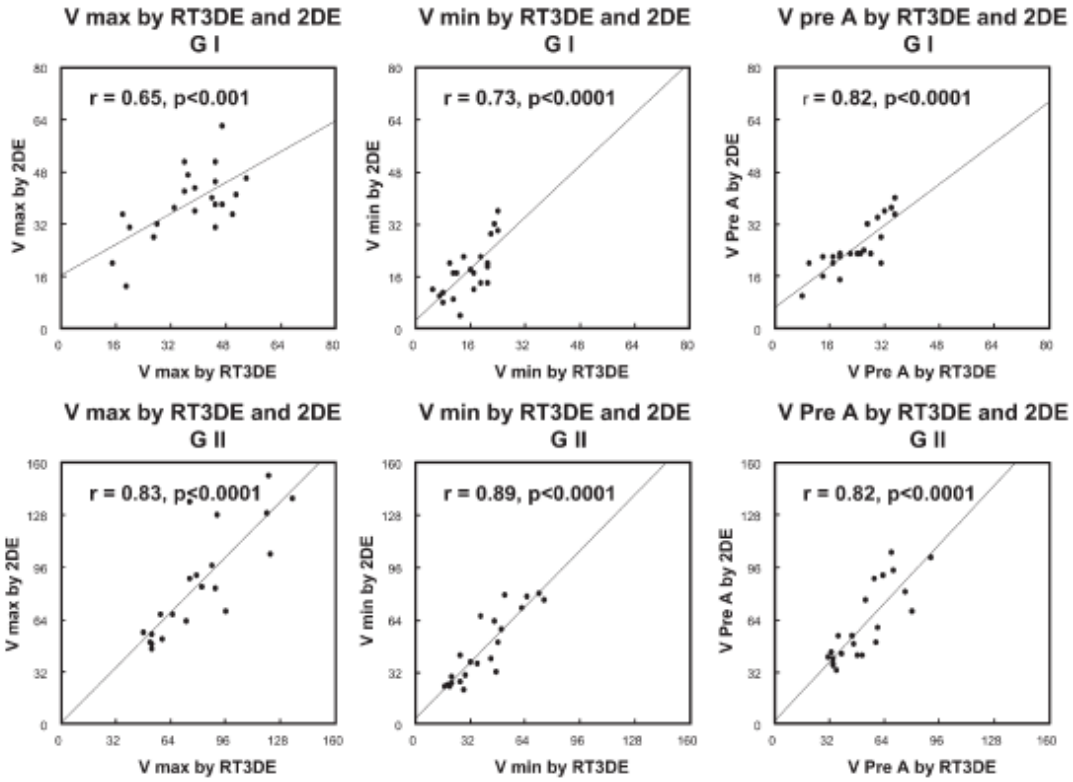

Fig 3: Correlation between RT3DE and 2DE in calculation of the three LAV: V max, V min and V pre A in both groups

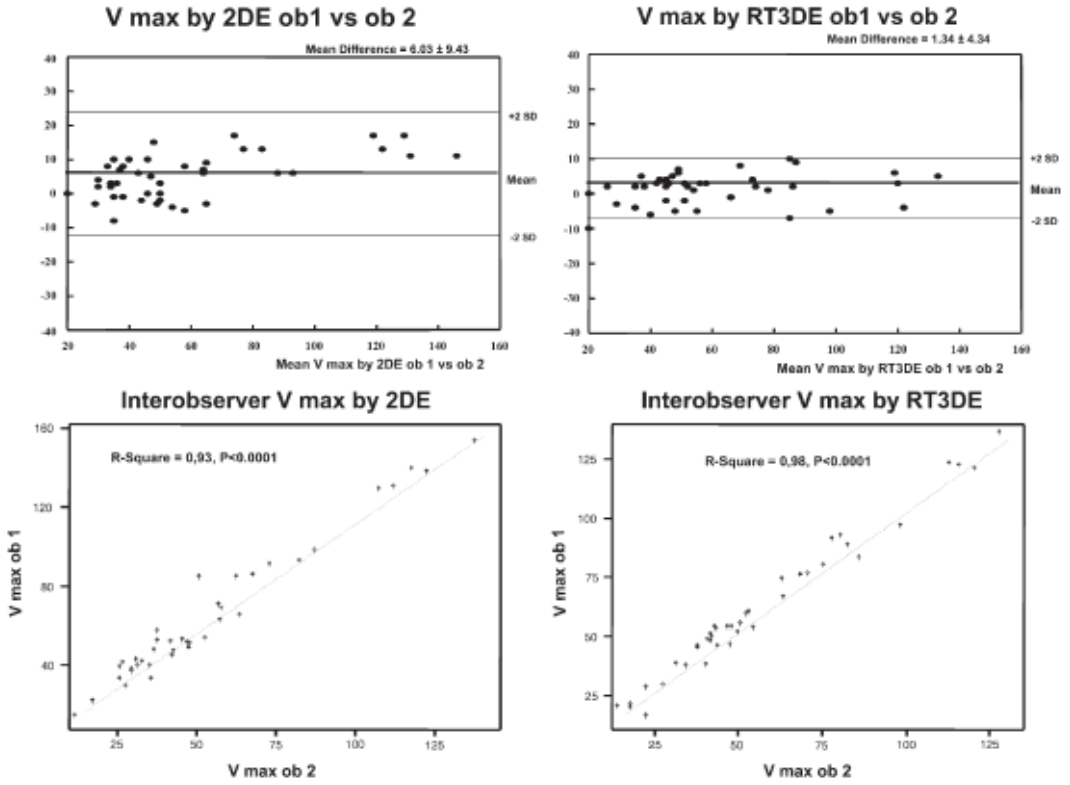

Fig 4: Interobserver agreement and correlation for measuring V max by 2DE and RT3DE

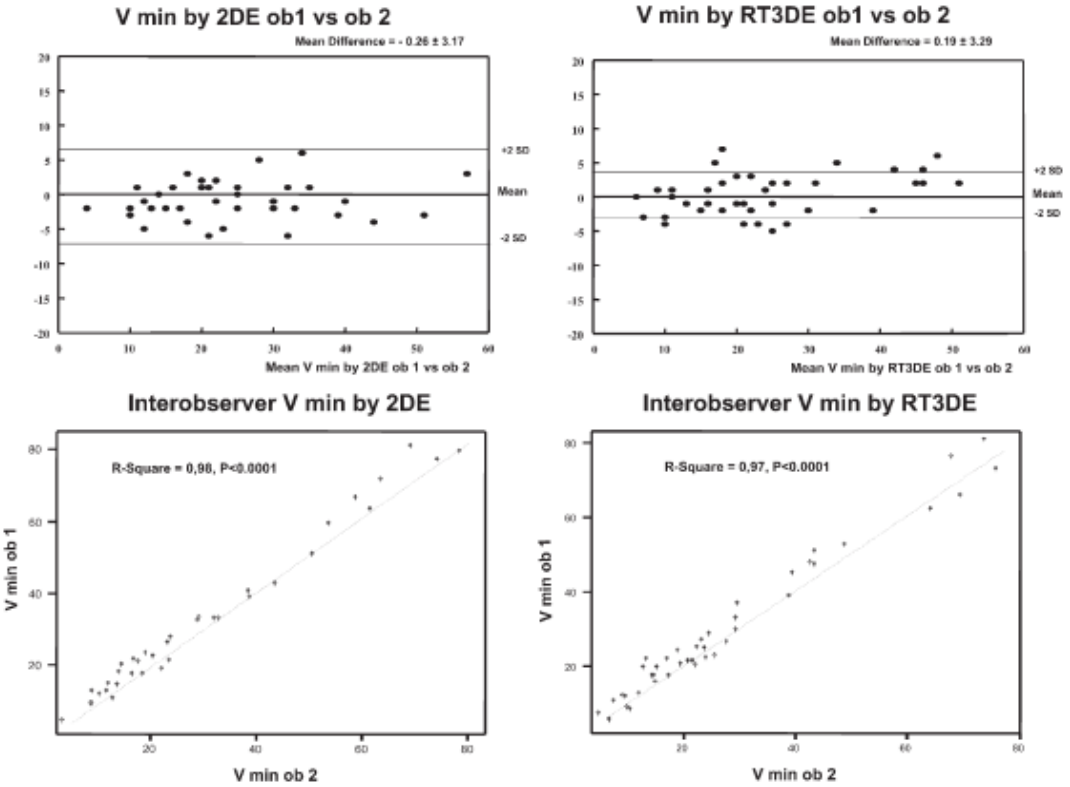

Fig 5: Interobserver agreement and correlation for measuring V min by 2DE and RT3DE.

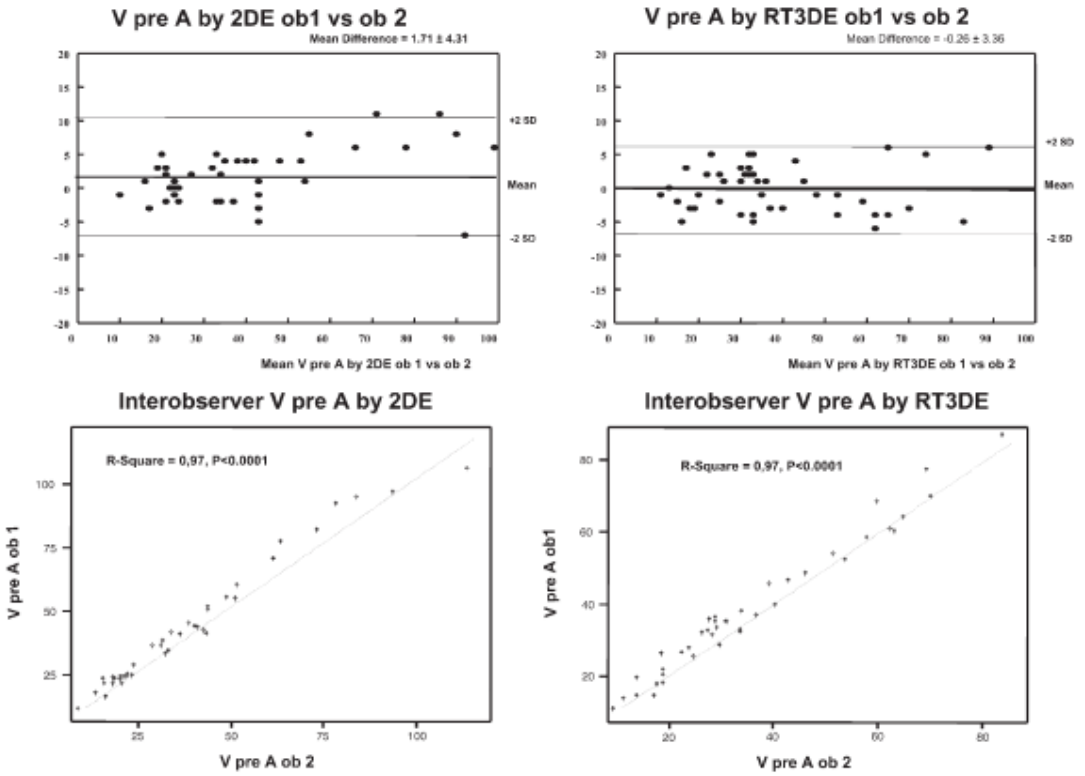

Fig 6: Interobserver agreement and correlation for measuring V pre A by 2DE and RT3DE.

DISCUSSION

This study showed feasibility and reproducibility of RT3DE in detection of cyclic changes in LAV and calculation of its function either in normal or dilated LA. Good correlation was found between RT3DE and 2DE. Studying LAV by RT3DE seems more logical because LA is a slightly tapered pillow shaped 3D structure without a natural long or short axis. Its shape can be distorted by its dilatation or dilatation of neighbouring structures. Hence, LAV measurement may be a better indicator of true LA size [(5)]. The M-mode echocardiography for estimation of LA size is commonly used and widely accepted because of its simplicity and historical assumption that LA is spherical in shape but studies showed that it seriously underestimates the LA size [(9,10)]. Use of 2D view to calculate LAV by single plane planimetry has limited reproducibility with a mean interobserver variability of 21% [(16)]. 2D calculation of LAV by biplane method has a close correlation with LAV measured by cinecomputed tomography [(17)] and magnetic resonance imaging (MRI) [(10)]. Reports about use of 3D reconstruction for calculation of LAV recommended its clinical application due to time saving and low interobserver variability [(9)] and its values are comparable to MRI [(10)]. In the present study, the patients were classified

into normal and dilated LAV groups depending on large population study included 2041 normals and 1274 abnormals where normal LAV was (47.35 ± 17.38ml) and abnormal LAV was (50.8 ± 19.3ml) [18]. LAV was estimated by 2DE using biplane apical images and compared to values that obtained by RT3DE. In accordance with previous studies [4,10,19], it was found that there is a linear correlation between both techniques in calculation of LAV and function in normal or dilated LA. However, 2DE measurement of V min and V pre A was overestimated in the dilated LA group. Due to this overestimation, lower values of AA EF, AEI and AP EF were calculated. This in discordance with the previous study by Khankirawantana et al [9] which concluded that 2D calculation of LAV has a close correlation with 3D with underestimation of LAV especially if the volume was greater than 35 ml. The discrepancy between both studies is that they included LA appendage as a part of LA chamber, which was excluded by our measures. The overestimation of 2DE to cyclic changes in LAV may be due to the gain dependent nature of boundary echoes, which leads to inclusion of pulmonary veins or portion of appendage despite efforts to exclude them. With V min, both techniques showed higher interobserver agreement but with the larger volumes (V max and V Pre A), RT3DE showed better agreement than 2DE. This also could be explained by difficulty in total exclusion of LA appendage and pulmonary veins by 2DE especially when LA dilates. This explanation was confirmed by previous studies that reported less clear visualization of LA appendage by 2DE than by 3D [20,21].

Study Limitations

We did not include LA appendage for calculation of LAV and function. Its variability in shape, its difficulty to measure and the lack for standard figures for its normal volume seems reasonable to exclude it. Also, the previous studies do not discuss the role of it [22,23]. Another limitation with using RT3DE is total dependency on 2DE image quality and image artefacts could be created by motion or ectopics.

CONCLUSION

RT3DE provides an accurate measurement of LAV and function and could be considered as feasible and reproducible method for its clinical application. The visualization of LA in 3D shape independent of geometric assumption favours its use.

REFERENCES

1. Benjamin EJ, D'Agostino RB, Belanger AJ, Wolf PA, Levy D. Left atrial size and the risk of stroke and death. The Framingham Heart Study. Circulation 1995;92(4):835-41.
2. Sanfilippo AJ, Abascal VM, Sheehan M, Oertel LB, Harrigan P, Hughes RA, et al. Atrial enlargement as a consequence of atrial fibrillation. A prospective echocardiographic study. Circulation 1990;82(3):792-7.
3. Vaziri SM, Larson MG, Benjamin EJ, Levy D. Echocardiographic predictors of nonrheumatic atrial fibrillation. The Framingham Heart Study. Circulation 1994;89(2):724-30.
4. Kawai J, Tanabe K, Wang CL, Tani T, Yagi T, Shiotani H, et al. Comparison of left atrial size by freehand scanning three-dimensional echocardiography and two-dimensional echocardiography. Eur J Echocardiogr 2004;5(1):18-24.
5. Lester SJ, Ryan EW, Schiller NB, Foster E. Best method in clinical practice and in research studies to determine left atrial size. Am J Cardiol 1999;84(7):829-32.
6. Khankirawatana B, Khankirawatana S, Porter T. How should left atrial size be reported? Comparative assessment with use of multiple echocardiographic methods. Am Heart J 2004;147(2):369-74.
7. Gottdiener JS. Left atrial size: renewed interest in an old echocardiographic measurement. Am Heart J 2004;147(2):195-6.
8. Tanabe K, Belohlavek M, Jakrapanichakul D, Bae RY, Greenleaf JF, Seward JB. Three-Dimensional Echocardiography: Precision and Accuracy of Left Ventricular Volume Measurement Using Rotational Geometry with Variable Numbers of Slice Resolution. Echocardiography 1998;15(6):575-580.
9. Khankirawatana B, Khankirawatana S, Lof J, Porter TR. Left atrial volume determination by three-dimensional echocardiography reconstruction: validation and application of a simplified technique. J Am Soc Echocardiogr 2002;15(10 Pt 1):1051-6.
10. Keller AM, Gopal AS, King DL. Left and right atrial volume by freehand three-dimensional echocardiography: in vivo validation using magnetic resonance imaging. Eur J Echocardiogr 2000;1(1):55-65.
11. Corsi C, Lang RM, Veronesi F, Weinert L, Caiani EG, MacEneaney P, et al. Volumetric quantification of global and regional left ventricular function from real-time three-dimensional echocardiographic images. Circulation 2005;112(8):1161-70.
12. Lang RM, Bierig M, Devereux RB, Flachskampf FA, Foster E, Pellikka PA, et al. Recommendations for Chamber Quantification: A Report from the American Society of Echocardiography's Guidelines and Standards Committee and the Chamber Quantification Writing Group, Developed in Conjunction with the European Association of Echocardiography, a Branch of the European Society of Cardiology. J Am Soc Echocardiogr 2005;18:1440-1463.
13. Poutanen T, Jokinen E, Sairanen H, Tikanoja T. Left atrial and left ventricular function in healthy children and young adults assessed by three dimensional echocardiography. Heart 2003;89(5):544-9.
14. Blondheim DS, Osipov A, Meisel SR, Frimerman A, Shochat M, Shotan A. Relation of left atrial size to function as determined by transesophageal echocardiography. Am J Cardiol 2005;96(3):457-63.
15. Bland JM, Altman DG. Statistical methods for assessing agreement between two methods of clinical measurement. Lancet 1986;1(8476):307-10.
16. Himelman RB, Cassidy MM, Landzberg JS, Schiller NB. Reproducibility of quantitative two-dimensional echocardiography. Am Heart J 1988;115(2):425-31.
17. Kircher B, Abbott JA, Pau S, Gould RG, Himelman RB, Higgins CB, et al. Left atrial volume determination by biplane two-dimensional echocardiography: validation by cine computed tomography. Am Heart J 1991;121(3 Pt 1):864-71.
18. Pritchett AM, Jacobsen SJ, Mahoney DW, Rodeheffer RJ, Bailey KR, Redfield MM. Left atrial volume as an index of left atrial size: a population-based study. J Am Coll Cardiol 2003;41(6):1036-43.
19. Jenkins C, Bricknell K, Marwick TH. Use of real-time three-dimensional echocardiography to measure left atrial volume: comparison with other echocardiographic techniques. J Am Soc Echocardiogr 2005;18(9):991-7.
20. Valocik G, Kamp O, Michciokur M, Mannaerts HF, Li Y, Ripa S, visser CA. Assessment of the left atrial appendage mechanical function by three-dimensional echocardiography**.** Eur J Echocardiogr 2002;3(3): 207-13.

21. Agoston I, Xie T, Tiller FL, Rahman AM, Ahmed M. Assessment of left atrial appendage by live three-dimensional echocardiography: early experience and comparison with transesophageal echocardiography. Echocardiogr 2006;23(2):127-32
22. Spencer KT, Mor-Avi V, Gorcsan J, 3rd, DeMaria AN, Kimball TR, Monaghan MJ, et al. Effects of aging on left atrial reservoir, conduit, and booster pump function: a multi-institution acoustic quantification study. Heart 2001;85(3):272-7.
23. Boudoulas H, Triposkiadis F, Barrington W, Wooley CF. Left atrial volumes and function in patients with mitral stenosis in sinus rhythm. Acta Cardiol 1991;46(1):147-52.

CHAPTER 11

Left Atrial Frank-Starling Law Assessed by Real-Time Three-Dimensional Echocardiographic Left Atrial Volume Changes

Ashraf M. Anwar[1,2], Marcel L. Geleijnse[1], Osama I.I. Soliman[1,2], Attila Nemes[1,3], and Folkert J. ten Cate[1]

[1]Department of Cardiology, Thoraxcenter, Erasmus University Medical Center, Rotterdam, The Netherlands
[2]Department of Cardiology, Al-Hussein University Hospital, Al-Azhar University, Cairo, Egypt
[3]Second Department of Medicine and Cardiology Center, University of Szeged, Szeged, Hungary

Heart 2007;39:1393-1397

ABSTRACT

Background: The Frank-Starling law describes the relation between left ventricular volume and function. However, only a few studies described the relation between left atrial volume (LAV) and function.

Objective: To describe a LA Frank-Starling law by studying changes in LAV measured by real-time three-dimensional echocardiography (RT3DE).

Methods: LAV was calculated by RT3DE in 70 patients at end-systole (LAV_{max}), end-diastole (LAV_{min}) and pre-atrial contraction (LAV_{pre-A}). According to LAV_{max}, patients were classified into three groups: LAV_{max} <50 ml (group I), LAV_{max} 50 to 70 ml (group II), and LAV_{max} >70 ml (group III). Calculated indices of LA pump function were active atrial stroke volume (SV) defined as LAV_{pre-A} – LAV_{min} and active atrial emptying fraction (EF), defined as active atrial SV / LAV_{pre-A} x 100%

Results: Active atrial SV was significantly higher in group II than in group I (mean (SD) 19.0 (9.2) vs. 8.2 (4.9) ml, P <0.0001), in group III it was non-significantly lower compared to group II (16.7 (12.5) vs. 19.0 (9.2) ml). Active atrial SV correlated well with LAV_{pre-A} (r = 0.56, P <0.0001), but decreased with larger LAV_{pre-A}. Active atrial EF tended to be higher in group II than in group I (43.1 (18.2) vs. 33.2 (17.5), P < 0.10), in group III it was significantly lower than in group II (26.2 (18.5) vs. 43.1 (18.2), P <0.01).

Conclusion: A Frank-Starling mechanism in the LA could be described by RT3DE, shown by an increase in LA contractility in response to an increase in LA preload up to a point, beyond which LA contractility decreased.

INTRODUCTION

The Frank-Starling law, describing the relationship between increased length of myocardial fibres and its mechanical performance, is important for cardiac function [1]. The relation between myocardial preload and mechanical performance is described by a curve in which an upward position on the curve means increased performance, while a downward position means decreased myocardial performance [2]. Assessment of left atrial (LA) function has important therapeutic and prognostic value [3]. The instantaneous LA pressure-volume relation provides an accurate index of LA contractility [4]. However, measurement of this index is invasive and technically difficult and therefore not suitable for routine clinical application [3]. Non-invasive assessment of LA contractility has been studied by two-dimensional echocardiography, Doppler parameters, cine computed tomography, radionuclide methods, and magnetic resonance imaging [5-9]. In previous studies it was suggested that a Frank-Starling mechanism also existed in the human LA [10-12]. The LA serves as a reservoir, conduit and booster pump for blood returning from the lungs to the heart. LA volume (LAV) is a superior index of LA size [13] and owing to complex LA anatomy it may echocardiographically be best assessed by three-dimensional echocardiography [14,15]. This study aimed at describing LA Frank-Starling law by studying changes in LAV measured by real-time three-dimensional echocardiography (RT3DE).

METHODS

The study comprised 70 clinically stable patients (mean age 45.6 ± 9.3 years, 66% males) in sinus rhythm without atrio-ventricular or intra-ventricular conduction abnormalities on a resting 12-lead electrocardiogram. Nineteen patients (27%) were not known with cardiovascular disease, 20 patients (29%) had essential hypertension, 16 patients (23%) had coronary heart disease, and 15 patients (21%) had non-compaction cardiomyopathy. None of these patients had mitral stenosis or significant (more than grade 1) mitral regurgitation. The patients were selected on good two-dimensional image quality.

Transthoracic RT3DE

RT3DE was performed with a Sonos 7500 ultrasound system (Philips Sonos 7500, Best, The Netherlands) attached to an X4 matrix array transducer capable of providing real-time B-mode images. Full volume three-dimensionsl images were collected within about 5-7 seconds of breath holding. Zoom function and gain adjustment were used to clarify the endocardial border. The probe position was modified to include the whole left atrium in the centre of the RT3DE image sector. The three-

dimensional dataset was transferred to a Q-LAB system for offline analysis. Analysis of three-dimensional images was based on a two-dimensional approach relying on the images obtained from an apical four-chamber view and on semi-automated tracing of the LA endocardial border for calculation of LAV. Tracing was performed by marking five atrial points: the anterior, inferior, lateral and septal mitral annuli and the LA apex. Once this was completed, the endocardial surface was automatically delineated and the LA model could be visualized from different points of views and LAV was obtained (Figure 1). Manual modifications were made to correct automatic tracings in the majority of patients, and in particular in patients with dilated LA to exclude the LA appendage and the pulmonary veins entrance from LAV. Borders that manifested as lines were traced in the middle of the line. In addition, careful attention was given to neighbouring well-visualized pixels as guidance for the true LA wall.

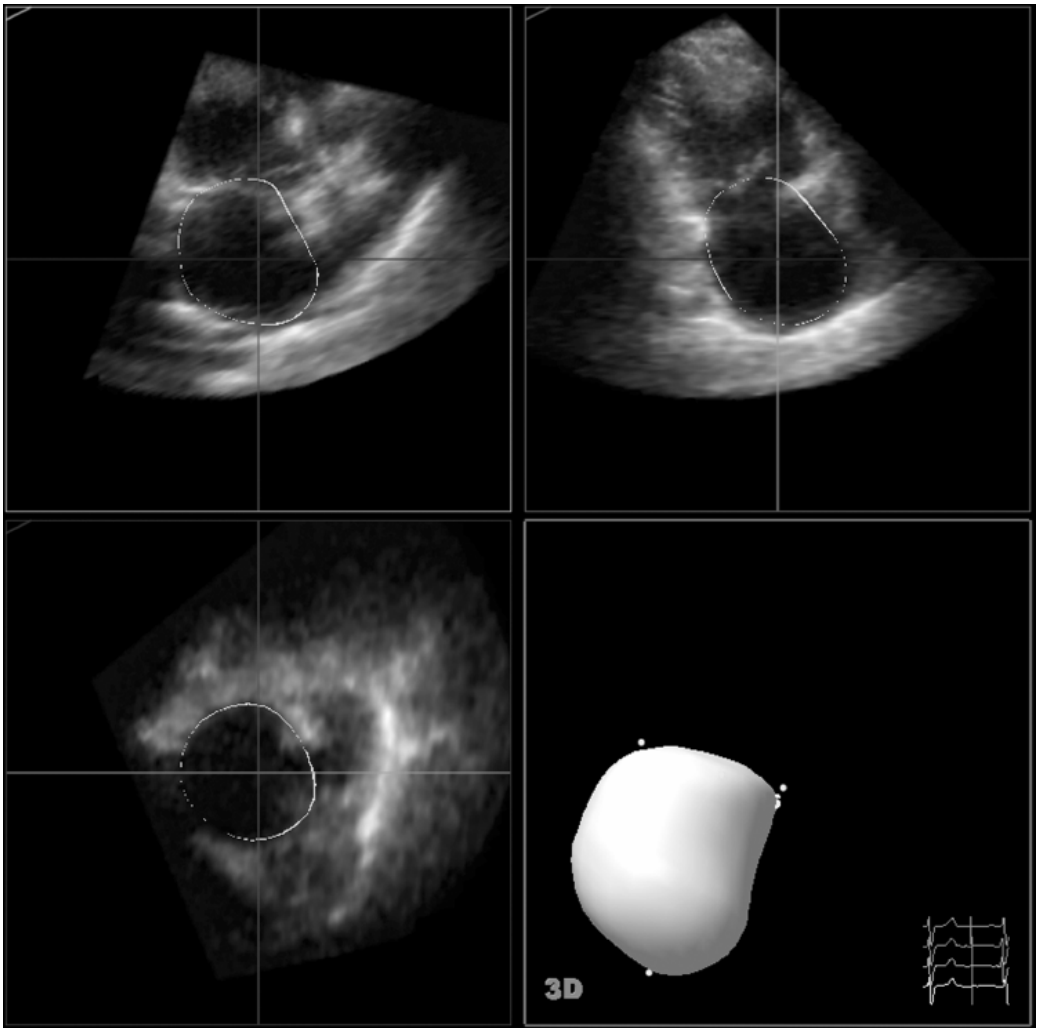

Figure 1. Quad screen display of the Q-LAB analysis software showing methodology for left atrial volume calculation by marking the five left atrial points.

LAV Calculation

LAV was measured at three phases of the cardiac cycle: (*a*) maximum volume (LAV_{max}) obtained from an end-systolic frame just before mitral valve opening, (*b*) minimum volume (LAV_{min}) obtained from an end-diastolic frame just before mitral valve closure, and (*c*) volume before atrial contraction (LAV_{pre-A}) obtained from the last frame just before mitral valve reopening.

In accordance to previous studies [12,16], the following indices of LA function were assessed: (*a*) total atrial stroke volume (SV), defined as LAV_{max} - LAV_{min}, (*b*) total atrial emptying fraction (EF), defined as total atrial SV / LAV_{max} x 100%, (*c*) active atrial SV, defined as LAV_{pre-A} – LAV_{min}, (*d*) active atrial EF, defined as active atrial SV / LAV_{pre-A} x 100%, (*e*) passive atrial SV, defined as LAV_{max} - LAV_{pre-A}, (*f*) passive atrial EF as an index for LA conduit function, defined as passive atrial SV / LAV_{max} x 100%, and (*g*) atrial expansion index as an index for LA reservoir function, defined as (LAV_{max} - LAV_{min}) / LAV_{min} x 100%. To characterize the three phases of LA activity, passive atrial SV and EF were defined as indices for LA conduit function, active atrial SV and EF for LA pump function, and atrial expansion index for LA reservoir function.

Depending on LAV_{max} values, the patients were arbitrary classified into three groups: group I included 29 patients with LAV_{max} <50 ml, group II included 15 patients with LAV_{max} 50 to 70 ml, and group III included 26 patients with LAV_{max} >70 ml.

STATISTICAL ANALYSES

The statistical package used was SPSS version 12.1. All LAV values and its functions were expressed as mean (SD). An independent sample t-test was performed to determine whether the difference in the values was significant with a level of significance set to $P < 0.05$. Interobserver agreements for LAVs, were expressed according to Bland and Altman method[17].

RESULTS

Table 1 lists the baseline criteria of the different LAV groups. There were no significant differences in age and sex distribution between the groups. Mild mitral regurgitation was present in 19 patients: 4 patients (14%) in group I, 5 patients (33%) in group II, and 10 patients (38%) in group III. All patients

in group II and III had cardiac abnormalities (hypertension, coronary artery disease, or cardiomyopathy), whereas in group I only 10 patients (34%) had cardiac abnormalities.

Table 1: Baseline criteria of the studied left atrial volume groups.

	G I: V_{max} <50 ml (n = 29)	**G II: V_{max} 50 -70 ml (n = 15)**	**G III: V_{max} >70 ml (n = 26)**
Age	40.2 ± 7.5	44.8 ± 8.5	46.2 ± 9.5
Male gender (%)	17 (59%)	10 (67%)	19 (73%)
Clinical Diagnosis			
Normal	19 (66%)	0 (0%)	0 (0%)
Hypertension	7 (24%)	10 (67%)	3 (12%)
Coronary disease	3 (10%)	5 (33%)	8 (31%)
Non-compaction CM	0 (0%)	0 (0%)	15 (57%)
Mitral regurgitation			
None	25 (86%)	10 (67%)	16 (62%)
Mild (grade 1)	4 (14%)	5 (33%)	10 (38%)

Calculation of LAV was obtained within 5-7 minutes for each patient. Absolute interobserver agreement for RT3DE was (mean difference 1.3 (4.3) ml, agreement - 7.3, 10.0 ml) for LAV_{max}, (mean difference - 0.3 (3.4) ml, agreement - 7.0, 6.6 ml) for $LAV_{pre\text{-}A}$, and (mean difference 0.2 (3.3) ml, agreement - 3.1, 3.5 ml) for LAV_{min} (Figure 2).

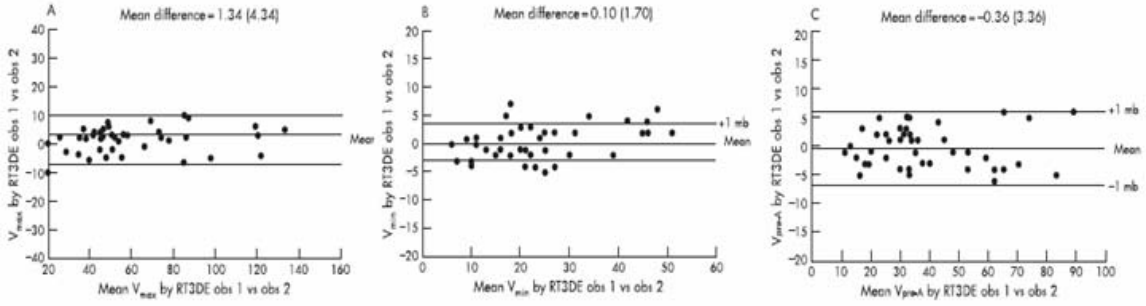

Figure 2. Interobserver agreement for RT3DE measurement of the different left atrial volumes (LAV): maximum, minimum, and pre-atrial contraction according to the Bland and Altman principle.

LA volumes in the different patient groups

Figure 3 shows significant differences (higher values for patients with larger LAV) were noted for LAV_{max} in group I compared with II (36.3 (10.7) vs. 55.2 (5.7) ml, P <0.0001) and in group II compared with III (55.2 (5.7) vs. 92.0 (19.9) ml, P <0.0001), for LAV_{min} in group I compared with II (15.4 (5.5) vs. 23.1 (7.0) ml, P <0.0001) and in group II compared with III (23.1 (7.0) vs. 45.7 (15.9)

ml, P <0.0001), and for LAV_{pre-A} in group I compared with II (23.6 (7.7) vs. 42.1 (9.6) ml, P <0.0001) and in group II compared with III (42.1 (9.6) vs. 62.4 (16.5) ml, P <0.0001).

LA pump function

Active atrial SV was significantly higher in group II than in group I (19.0 (9.2) vs. 8.2 (4.9) ml, P <0.0001), in group III it was non-significantly lower than in group II (16.7 (12.5) vs.19.0 (9.2) ml). Figure 4A shows that active atrial SV correlated well with LAV_{pre-A} (r = 0.56, P <0.0001), but decreased with larger LAV_{pre-A}. Active atrial EF tended to be higher in group II than in group I (43.1 (18.2) vs. 33.2 (17.5), P < 0.10), in group III it was significantly lower than in group II (26.2 (18.5) vs. 43.1 (18.2), P <0.01).

LA conduit function

Passive atrial SV was comparable in group I and group II (12.8 (7.4) vs. 13.2 (8.5) ml), but more than two-fold greater in group III than in group II (29.6 (24.4) vs.13.2 (8.5) ml, P <0.005). Passive atrial EF tended to be lower in group II than in group I (23.8 (16.1) vs. 34.0 (14.7) %, P < 0.10), but tended to be higher in group III than in group II (30.0 (19.3) vs. 23.8 (16.1) %, P <0.10).

LA reservoir function

The atrial expansion index was nearly identical in group I and II (156.1 (97.7) % and 158.8 (78.7)%, respectively), and non-significantly lower in group III (128.2 (107.3)%).

Total LA function

Total atrial SV was significantly larger in group II than in group I patients (32.2 (5.5) vs. 20.9 (8.9) ml, P <0.0001), and the largest total atrial SV was in group III (46.5 (25.5) ml, P <0.001). Figure 3B shows that total atrial SV correlated well with LAV_{max} (r = 0.82, P <0.0001). Total atrial EF was comparable in group I, II and III (56.4 (13.3) %, 58.5 (10.5) %, and 49.9 (15.6) %, respectively).

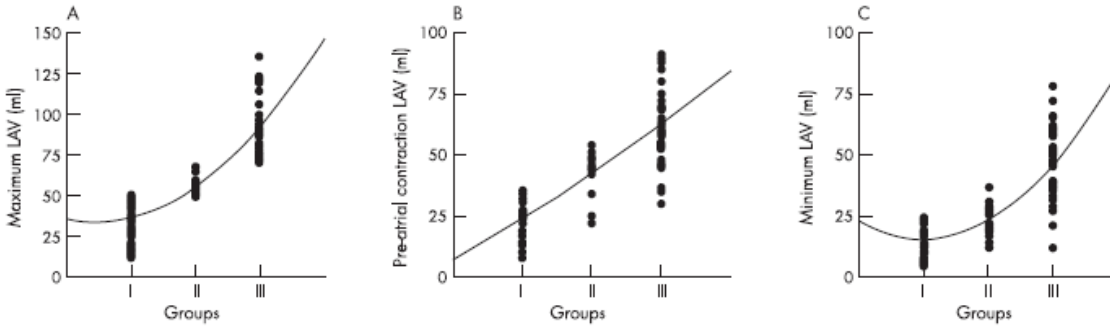

Figure 3. Left atrial volume (LAV) at three phases: (A) Maximum, (B) pre-atrial contraction, and (C) minimum in the different study groups.

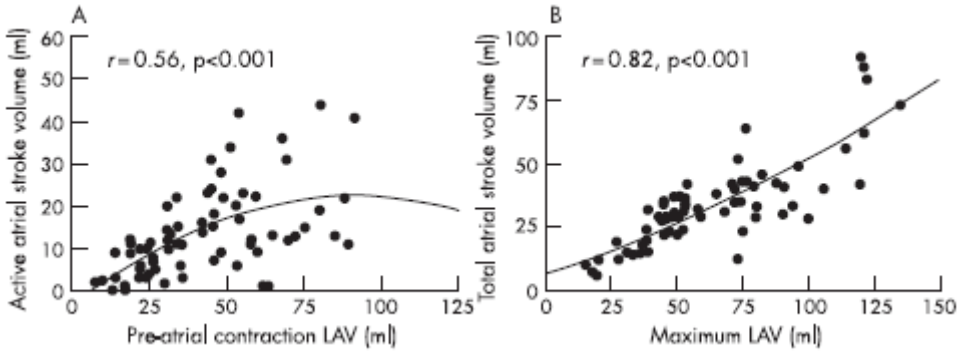

Figure 4. (A) Relation between pre-atrial contraction left atrial volumes (LAV) and active atrial stroke volume; (B) maximum left atrial volumes and total atrial stroke volume *(left).*

DISCUSSION

LA function significantly contributes to the maintenance of cardiac output and impairment of its function contributes to circulatory failure, mitral regurgitation, atrial fibrillation and stroke [18,19]. Previous studies assessed LA function by invasive pressure-volume loop determination [4], or by LAV changes assessed by nuclear scintigraphy, computed tomography, or magnetic resonance imaging [7,9]. RT3DE is an interestingly alternative for LAV assessment because of availability, rapid acquisition and analysis, low cost, no need for contrast or radiation, and relatively high temporal resolution. In this study LAV was assessed in the three atrial phases by RT3DE.

To the best of our knowledge, this is the first RT3DE study to describe the existence of a Frank-Starling mechanism in the LA. The Frank-Starling mechanism was shown by an increase in LA contractility in response to an increase in LA preload up to a point, beyond which LA contractility decreased (Figure 4A).

Despite the correlation between an increase in LAVpre-A and active atrial SV in patients with normal to moderately enlarged LAV, active atrial SV reached a plateau and even decreased in patients with the largest LAV. These findings are in accordance with previous non-invasive and invasive studies [3,5,20]. Active atrial SV increase in response to an increase in LAVpre-A may be related not only to a pressure increase but also to an enhanced inherent inotropic state of LA myocardium. This may explain the improvement of atrial pump function after digoxin administration in patients with heart failure [6]. The clinical implication of the described Frank-Starling law in the LA is its role in heart failure. In early stages of heart failure, the LA compensates well by mechanical adaptation to the increased hemodynamic load which may prevent or delay appearance of symptoms of heart failure [11]. Thus, evaluation of LA function in heart failure patients will have therapeutic and prognostic value.

Another clinical implication is that LA functional assessment may help as a predictor for development of atrial fibrillation and maintenance of sinus rhythm after cardioversion [21].

LA conduit function is mainly determined by the rate of left ventricular relaxation [22]. This may explain the tendency for a reduction in passive atrial EF in group II patients, in whom LV diastolic function is impaired due to a high incidence of hypertension and ischemic heart disease. The increased LA conduit function in group III patients appears as a compensatory mechanism to counterbalance decreased LA pump function [19,23]. These changes in LA conduit function due to impaired left ventricular relaxation are reflected in changes in mitral inflow E/A ratio. This may explain the improvement in LA function in patients with restrictive physiology after angiotensin converting enzyme inhibitor therapy [24].

LA reservoir function is determined by LA myocardial contraction and relaxation, and mitral annulus displacement during left ventricular contraction [25,26]. In this study there was only a non-significant decrease in LA reservoir function in patients with the largest LAV. This may be due to the multi-factorial mechanisms responsible for LA reservoir dysfunction.

Study limitations

LA tracing can be problematic owing to (*a*) decreased resolution of three-dimensional imaging compared with two-dimensional imaging, (*b*) the LA is in the far-field, and (*c*) some LA walls suffering from lateral resolution by which pixels will become lines in the image display. Because the objective of our study was to prove a physiological concept rather than to demonstrate the feasibility of three-dimensional assessment for LA volumes we only included patients with good image quality in our study (representing about one third of routinely referred patients). Because of this selection, we cannot make recommendations on the routine clinical value for routine LAV measurements and assessment of LAV changes. For such recommendations intra- and interobserver variabilities and the accuracy of such measurements (compared to a “gold standard”) should be assessed in the whole spectrum of image qualities.

CONCLUSION

In this RT3DE study, the presence of a Frank-Starling mechanism was shown by an increase in LA contractility in response to an increase in LA preload up to a point, beyond which LA contractility decreased. RT3DE assessment of LAV may help in understanding LA physiology and clinical assessment.

REFERENCES

1. Fuchs F, Smith SH. Calcium, cross-bridges, and the Frank-Starling relationship. *News Physiol Sci* 2001;16:5-10.
2. Aurigemma GP, Zile MR, Gaasch WH. Contractile behavior of the left ventricle in diastolic heart failure: with emphasis on regional systolic function. *Circulation* 2006;113:296-304.
3. Nakatani S, Garcia MJ, Firstenberg MS, Rodriguez L, Grimm RA, Greenberg NL, McCarthy PM, Vandervoort PM, Thomas JD. Noninvasive assessment of left atrial maximum dP/dt by a combination of transmitral and pulmonary venous flow. *J Am Coll Cardiol* 1999;34:795-801.
4. Hoit BD, Shao Y, Gabel M, Walsh RA. In vivo assessment of left atrial contractile performance in normal and pathological conditions using a time-varying elastance model. *Circulation* 1994;89:1829-38.
5. Stefanadis C, Dernellis J, Stratos C, Tsiamis E, Tsioufis C, Toutouzas K, Vlachopoulos C, Pitsavos C, Toutouzas P. Assessment of left atrial pressure-area relation in humans by means of retrograde left atrial catheterization and echocardiographic automatic boundary detection: effects of dobutamine. *J Am Coll Cardiol* 1998;31:426-36.
6. Dernellis JM, Panaretou MP. Effects of digoxin on left atrial function in heart failure. *Heart* 2003;89:1308-15.
7. Kircher B, Abbott JA, Pau S, Gould RG, Himelman RB, Higgins CB, Lipton MJ, Schiller NB. Left atrial volume determination by biplane two-dimensional echocardiography: validation by cine computed tomography. *Am Heart J* 1991;121:864-71.
8. Marmor A, Frankel A, Blondeheim DS, Satinger A, Front D. Scintigraphic assessment of atrial function in patients with longstanding hypertension. *Radiology* 1984;151:483-6.
9. Jarvinen V, Kupari M, Hekali P, Poutanen VP. Assessment of left atrial volumes and phasic function using cine magnetic resonance imaging in normal subjects. *Am J Cardiol* 1994;73:1135-8.
10. Matsuzaki M, Tamitani M, Toma Y, Ogawa H, Katayama K, Matsuda Y, Kusukawa R. Mechanism of augmented left atrial pump function in myocardial infarction and essential hypertension evaluated by left atrial pressure-dimension relation. *Am J Cardiol* 1991;67:1121-6.
11. Dernellis JM, Stefanadis CI, Zacharoulis AA, Toutouzas PK. Left atrial mechanical adaptation to long-standing hemodynamic loads based on pressure-volume relations. *Am J Cardiol* 1998;81:1138-43.
12. Blondheim DS, Osipov A, Meisel SR, Frimerman A, Shochat M, Shotan A. Relation of left atrial size to function as determined by transesophageal echocardiography. *Am J Cardiol* 2005;96:457-63.
13. Lester SJ, Ryan EW, Schiller NB, Foster E. Best method in clinical practice and in research studies to determine left atrial size. *Am J Cardiol* 1999;84:829-32.
14. Keller AM, Gopal AS, King DL. Left and right atrial volume by freehand three-dimensional echocardiography: in vivo validation using magnetic resonance imaging. *Eur J Echocardiogr* 2000;1:55-65.
15. Poutanen T, Ikonen A, Vainio P, Jokinen E, Tikanoja T. Left atrial volume assessed by transthoracic three dimensional echocardiography and magnetic resonance imaging: dynamic changes during the heart cycle in children. *Heart* 2000;83:537-42.
16. Poutanen T, Jokinen E, Sairanen H, Tikanoja T. Left atrial and left ventricular function in healthy children and young adults assessed by three dimensional echocardiography. *Heart* 2003;89:544-9.
17. Bland JM, Altman DG. Statistical methods for assessing agreement between two methods of clinical measurement. *Lancet* 1986;1:307-10.
18. Dittrich HC, Pearce LA, Asinger RW, McBride R, Webel R, Zabalgoitia M, Pennock GD, Safford RE, Rothbart RM, Halperin JL, Hart RG. Left atrial diameter in nonvalvular atrial fibrillation: An echocardiographic study. Stroke Prevention in Atrial Fibrillation Investigators. *Am Heart J* 1999;137:494-9.
19. Quinones MA, Greenberg BH, Kopelen HA, Koilpillai C, Limacher MC, Shindler DM, Shelton BJ, Weiner DH. Echocardiographic predictors of clinical outcome in patients with left ventricular dysfunction enrolled in the SOLVD registry and trials: significance of left ventricular hypertrophy. Studies of Left Ventricular Dysfunction. *J Am Coll Cardiol* 2000;35:1237-44.
20. Spencer KT, Mor-Avi V, Gorcsan J, 3rd, DeMaria AN, Kimball TR, Monaghan MJ, Perez JE, Weinert L, Bednarz J, Edelman K, Kwan OL, Glascock B, Hancock J, Baumann C, Lang RM. Effects of aging on left atrial reservoir, conduit, and booster pump function: a multi-institution acoustic quantification study. *Heart* 2001;85:272-7.
21. Manning WJ, Silverman DI, Katz SE, Riley MF, Come PC, Doherty RM, Munson JT, Douglas PS. Impaired left atrial mechanical function after cardioversion: relation to the duration of atrial fibrillation. *J Am Coll Cardiol* 1994;23:1535-40.

22. Nikitin NP, Witte KK, Thackray SD, Goodge LJ, Clark AL, Cleland JG. Effect of age and sex on left atrial morphology and function. *Eur J Echocardiogr* 2003;4:36-42.
23. Stefanadis C, Dernellis J, Tsiamis E, Toutouzas P. Effects of pacing-induced and balloon coronary occlusion ischemia on left atrial function in patients with coronary artery disease. *J Am Coll Cardiol* 1999;33:687-96.
24. Henein MY, Amadi A, O'Sullivan C, Coats A, Gibson DG. ACE inhibitors unmask incoordinate diastolic wall motion in restrictive left ventricular disease. *Heart* 1996;76:326-31.
25. Barbier P, Solomon SB, Schiller NB, Glantz SA. Left atrial relaxation and left ventricular systolic function determine left atrial reservoir function. *Circulation* 1999;100:427-36.
26. Tabata T, Oki T, Yamada H, Iuchi A, Ito S, Hori T, Kitagawa T, Kato I, Kitahata H, Oshita S. Role of left atrial appendage in left atrial reservoir function as evaluated by left atrial appendage clamping during cardiac surgery. *Am J Cardiol* 1998;81:327-32.

CHAPTER 12

Assessment of Left Atrial Ejection Force in Hypertrophic Cardiomyopathy Using Real-Time Three-Dimensional Echocardiography

Ashraf M. Anwar[1,2], Osama I.I. Soliman[1,2], Marcel L. Geleijnse[1], Michelle Michels[1], Wim B. Vletter[1], Attila Nemes[1,3] and Folkert J. ten Cate[1]

[1]Department of Cardiology, Thoraxcenter, Erasmus University Medical Center, Rotterdam, The Netherlands
[2]Department of Cardiology, Al-Hussein University Hospital, Al-Azhar University, Cairo, Egypt
[3]Second Department of Medicine and Cardiology Center, University of Szeged, Szeged, Hungary

Journal of American Society of Echocardiography 2007; 20:744-748.

ABSTRACT

The study included 30 patients with hypertrophic cardiomyopathy (HCM) (obstructive and non-obstructive) and 15 control subjects. End-diastolic mitral annulus area (MAA_{3D}) and mitral valve area (MVA_{3D}) were measured by real-time 3-dimensional (3D) echocardiography . MVA_{2D} and peak mitral inflow A wave velocity (V) were measured by 2-dimensional (2D) echocardiography. Left atrial ejection force (LA-EF) was calculated by 2D echocardiography and real-time 3D echocardiography using formula: 0.5 x 1.06 x (MAA or MVA) x V^2, where (1.06) is blood viscosity. $LA\text{-}EF_{2D\text{-}MVA}$, $LA\text{-}EF_{3D\text{-}MVA}$, $LA\text{-}EF_{3D\text{-}MAA}$, and V were significantly higher in patients with HCM than control subjects ($p<0.001$). $LA\text{-}EF_{2D\text{-}MVA}$ and $LA\text{-}EF_{3D\text{-}MVA}$ were lower than $LA\text{-}EF_{3D\text{-}MAA}$ in HCM only ($p<0.001$). In obstructive HCM, $LA\text{-}EF_{2D\text{-}MVA}$, $LA\text{-}EF_{3D\text{-}MVA}$, $LA\text{-}EF_{3D\text{-}MAA}$ and V were significantly higher than in non-obstructive HCM ($p<0.05$). LV outflow tract gradient contributed independently to high LA-EF in obstructive HCM. We concluded that HCM is associated with higher LA-EF than normal, and higher in obstructive HCM than non-obstructive indicating a higher atrial workload that is reflected by $LA\text{-}EF_{3D\text{-}MAA}$.

INTRODUCTION

Hypertrophic cardiomyopathy (HCM) is a relatively common form of genetic heart disease affecting approximately 1 in 500 people in the general population [1,2]. The disease is characterized by asymmetric hypertrophy involving primarily the ventricular septum [3-5]. The pathophysiologic appearance of HCM is complex and includes dynamic left ventricular (LV) outflow tract (LVOT) obstruction, mitral regurgitation, diastolic dysfunction, myocardial ischemia and cardiac arrhythmia [6]. Diastolic dysfunction is more common than systolic dysfunction in HCM. Marked LV hypertrophy, interstitial fibrosis and myocardial ischemia all contribute to reduced ventricular compliance and impaired relaxation. These factors contribute to elevated left atrial (LA) and pulmonary vascular pressures [5]. Decreased compliance also affects LA reservoir function and may affect cardiac output [7]. The thin-walled LA is sensitive to volume and pressure changes [8]. Assessment of diastolic function through measurement of the components of ventricular filling usually does not include LA contractile function [9]. LA ejection force (LA-EF) defined as the force exerted by the LA to accelerate blood into the LV during atrial systole provides a physiological assessment of LA systolic function [10]. Based on the second law of Newton that stated force = mass X acceleration, LA-EF was calculated by the equation: 0.5 x 1.06 x (MAA or MVA) x V^2, and 0.5 is a coefficient factor. We believe that LA function should be included in the clinical assessment of HCM. This study aimed to assess LA-EF non-invasively in patients with HCM using real-time (RT) 3-dimensional (3D) echocardiography (3DE).

METHODS

The study included thirty patients (80% males, mean age 38 ± 15 years) with an established diagnosis of HCM[11] and good 2-diensional (2D) echocardiography (2DE) image quality. According to the type of HCM, patients were classified into two groups. The non-obstructive group included 20 patients with LVOT gradient < 50 mmHg, and the obstructive group included 10 patients with LVOT gradient 50 mmHg or greater. A group of 15 healthy age-matched adults (mean age 35 ± 16 years) without evidence of cardiovascular disease served as control subjects. All patients and control subjects were examined by 2DE and RT3DE. Because of 2DE and RT3DE are performed routinely in our lab, only informed consent was obtained from our patients

Transthoracic 2DE

2DE was undertaken with the patient lying in the left lateral decubitus using both apical and parasternal views. The 2DE studies were performed using a 3.5 MHZ transducer and a commercially available ultrasound system (Sonos 7500, Philips, Best, The Netherlands). The following measures were obtained: (1) site and maximal thickness of asymmetric LV hypertrophy from the 2DE images (septal, antero-lateral, apical, or concentric), (2) mitral valve area ($2D_{MVA}$) measured by planimetry from a parasternal short axis view and defined as the narrowest area at maximum valve opening, (3) LV end-diastolic (LV-EDD) and LV end-systolic dimensions (LV-ESD) by M-mode, (4) LV fractional shortening (LV-FS) calculated as (LV-EDD – LV-ESD) / LV-EDD x 100%, (5) V and peak velocity of transmitral E wave with pulsed Doppler, (6) E/A ratio calculation, (7) LVOT gradient with continuous wave Doppler using Bernoulli equation, (8) $LA\text{-}EF_{2D\text{-}MVA}$ calculated as 0.5 x 1.06 x MVA x V^2, where (V) is the peak velocity of A wave, (1.06) is blood viscosity and (0.5) is a coefficient factor[12], and 9) mitral regurgitation graded as mild (jet area <4 cm^2), moderate (jet area 4-8 cm^2), and severe (jet area >8 cm^2) according to maximum jet area by color Doppler [13].

Transthoracic RT3DE

RT3DE was performed using the same ultrasound system, and performed with a X-4 matrix transducer capable of providing RT B-mode and color Doppler. The 3D images were collected within 5 to 7 seconds of breath holding in full volume mode. The 3D data were transferred to an offline analysis system (Tom Tec, Munich, Germany). Data were stored digitally and subsequently evaluated by two echocardiographers. Data analysis of 3D echo imaging was based on a 2D approach relying on the echocardiographic images obtained from the apical views and on manual tracing of inner border of the mitral annulus (MA). Once this was completed the surface area was automatically delineated and could be visualized from different points of views. Manual modification was done to correct any image if necessary. The following measures were obtained: (1) $3D_{MVA}$ measured by planimetry as described in the 2DE section, (2) MA area ($3D_{MAA}$) measured at end-diastole (just before mitral valve closure), (3) $LA\text{-}EF_{3D\text{-}MVA}$ calculated by the same formula used in 2DE, and (4) $LA\text{-}EF_{3D\text{-}MAA}$ calculated by formula[10] as 0.5 x 1.06 x MAA x V^2.

Statistical Analysis

All data obtained by 2DE or RT3DE were presented as mean ± SD. Data analysis was performed using statistical software (SPSS, version 12.1, SPSS Inc, Chicago). Independent sample t-test was performed to compare between means of variables of groups to determine the statistical significance of difference. The level of significance was set to *P* less than 0.05. Interobserver agreement for MAA measurements by RT3DE was expressed according to Bland and Altman method[14].

RESULTS

All patients were in sinus rhythm (mean heart rate 73 ± 14 beats per minute) and had normal LV systolic function and type I diastolic dysfunction (E/A ratio <0.75)[15]. The clinical and echocardiographic data of all HCM patients are displayed in Table 1. Mitral regurgitation was present in 22 patients (73%), 15 patients (50%) had mild regurgitation, and 7 patients (23%) had moderate to severe regurgitation. There were no significant differences in clinical variables (age, sex) between the two patient groups. Obstructive cases had significantly lower LV-ESD (2.3 ± 0.7 vs. 3.1 ± 0.7 cm, *P* <0.01) and significantly higher LV fractional shortening (48.0 ± 6.0 vs. 34.3 ± 8.0 %, *P* <0.001) than non-obstructive cases, whereas LV-EDD was comparable in both patient groups. Mean thickness of LV hypertrophy, its distribution, and the prevalence and severity of mitral regurgitation were comparable in both patients groups. Obstructive cases had a higher mean transmitral V (74.2 ± 19.7 vs. 50.1 ± 13.8 cm/sec, *P* <0.01) and LA-$EF_{2D\text{-}MVA}$ (12.2 ± 6.4 vs. 6.7 ± 4.7 kdynes, *P* <0.001) compared to non-obstructive patients.

Table 1: Clinical and echocardiographic data

	HCM patients (n = 30)	**Non-obstructive (n = 20)**	**Obstructive (n = 10)**
Age (yr)	38 ± 15	37 ± 15	39 ± 14
Male gender	24 (80%)	16 (80%)	8 (80%)
LV-EDD (cm)	4.7 ± 0.8	4.8 ± 0.6	4.4 ± 1.0
LV-ESD (cm)	2.9 ± 0.8	3.1 ± 0.7	2.3 ± 0.7*
LV-FS (%)	38.9 ± 9.8	34.3 ± 8.0	48.0 ± 6.0$
LVOT gradient (mmHg)	24.9 ± 25.5	8.1 ± 8.5	58.9 ± 8.6$
LV hypertrophy (cm)	2.2 ± 0.7	2.2 ± 0.7	2.2 ± 0.4
Site of LV hypertrophy			
Septal	22 (73%)	13 (65%)	9 (90%)
Septal + Anterolateral	4 (13%)	3 (15%)	1 (10%)
Apical	2 (7%)	2 (10%)	0 (0%)
Symmetrical	2 (7%)	2 (10%)	0 (0%)

$2D_{MVA}$ (cm^2)	4.3 ± 1.4	4.4 ± 1.5	4.0 ± 1.3
$3D_{MVA}$ (cm^2)	4.2 ± 1.3	4.3 ± 1.3	4.0 ± 1.4
$3D_{MAA}$ ($cm^{2)}$	10.1 ± 4.7	10.2 ± 4.7	9.8 ± 5.1
Peak A velocity (cm/s)	61.5 ± 20.3	50.1 ± 13.8	74.2 ± 19.7*
LA-EF_{2D-MVA} (kdynes)	9.2 ± 6.1	6.7 ± 4.7	12.2 ± 6.4$
LA-EF_{3D-MVA} (kdynes)	9.1 ± 5.6	6.8 ± 5.1	11.4 ± 7.1$
LA-EF_{3D-MAA} (kdynes)	21.5 ± 16.3	14.7 ± 12.0	29.5 ± 17.6*
Mitral regurgitation			
No	8 (27%)	5 (25%)	3 (30%)
Mild	15 (50%)	10 (50%)	5 (50%)
Moderate-severe	7 (23%)	5 (25%)	2 (20%)

HCM: Hypertrophic cardiomyopathy; *LA-EF:* left atrial ejection force; *LV:* left ventricular; *LV-EDD:* LV end-diastolic dimension, *LV-ESD:* LV end-systolic dimension, *LV-FS:* LV fractional shortening, *LVOT:* LV outflow tract, *MAA:* mitral annulus area; *MVA:* mitral valve area, *2D:* 2-diensional; *3D:*3-diensional, *P* value <0.05*and <0.001$

Acquisition and post-processing of RT3DE data were performed successfully with clear delineation of the MA in all patients (Figure 1). $3D_{MAA}$ showed good agreement between two independent observers (mean difference = 0.01 ± 0.17 cm^2, agreement = - 0.33, 0.35 cm^2). No significant differences between the obstructive and non-obstructive patient groups were found for $3D_{MAA}$ and $3D_{MVA}$. In the overall HCM group, LA-EF_{2D-MVA} was well correlated to LA-EF_{3D-MVA} (r = 0.96, *P* <0.0001) and LA-EF_{3D-MAA} (r = 0.67, *P* <0.001). No significant difference was found between LA-EF_{2D-MVA} and LA-EF_{3D-MVA}. Both LA-EF_{3D-MVA} (11.4 ± 7.1 vs. 6.8 ± 5.1 kdynes, *P* <0.05) and LA-EF_{3D-MAA} (29.5 ± 17.6 vs. 14.7 ± 12.0 kdynes, *P* <0.05) were significantly higher in obstructive group than in non-obstructive group. In all patients with HCM, LA-EF_{3D-MAA} was significantly higher than LA-EF_{2D-MVA} (21.5 ± 16.3 vs. 9.2 ± 6.1 kdynes, *P* <0.001) and LA-EF_{3D-MVA} (21.5 ± 16.3 vs. 9.1 ± 5.6 kdynes, *P* <0.001). V was well correlated to LA-EF_{3D-MVA} (r = 0.75, *P* <0.0001), LA-EF_{3D-MAA} (r = 0.85, *P* <0.0001), and LA-EF_{2D-MVA} (r = 0.85, *P* <0.0001). To detect the contributing factors associated with higher LA-EF in the obstructive group, multivariate regression analysis was done. Among the echocardiographic factors that differed in both studied groups (LV-ESD, LV fractional shortening, LVOT gradient), the LVOT gradient was the only contributing factor associated with higher LA-EF by 2DE and RT3DE in the obstructive group.

Compared with control subjects, $3D_{MAA}$ was significantly larger in both HCM groups than in control group (*P* <0.01). V was higher in both HCM groups than control group (*P* <0.05). Contrary to patients with HCM, no significant difference was detected between LA-$EF_{3D-MAA,}$ LA-EF_{2D-MVA}, and LA-EF_{3D-MVA} in control subjects. LA-$EF_{3D-MAA,}$ LA-EF_{2D-MVA}, and LA-EF_{3D-MVA} were significantly

lower than both obstructive and non-obstructive HCM groups (*P* <0.001). In obstructive HCM group, significantly higher values for and LA-EF by 2DE and RT3DE were found (Table 2).

Table 2: Comparison between patients with hypertrophic cardiomyopathy and normal subjects

	Normal subjects (n = 15)	**Non-obstructive HCM (n = 20)**	**Obstructive HCM (n = 10)**
MVA_{2D} (cm^2)	4.8 ± 0.9	4.4 ± 1.5	4.0 ± 1.3
MVA_{3D} (cm^2)	4.9 ± 0.7	4.3 ± 1.3	4.0 ± 1.4
MAA_{3D} ($cm^{2)}$	6.1 ± 1.7$^{\$}$	10.2 ± 4.7	9.8 ± 5.1
Peak A velocity (cm/s)	39.7 ± 9.9$^{\$}$	50.1 ± 13.8	74.2 ± 19.7*
$LA\text{-}EF_{2D\text{-}MVA}$ (kdynes)	4.2 ± 2.9$^{\$}$	6.7 ± 4.7	12.2 ± 6.4*
$LA\text{-}EF_{3D\text{-}MVA}$ (kdynes)	4.3 ± 2.3$^{\$}$	6.8 ± 5.1	11.4 ± 7.1*
$LA\text{-}EF_{3D\text{-}MAA}$ (kdynes)	5.0 ± 2.1$^{\$}$	14.7 ± 12.0	29.5 ± 17.6*

HCM: Hypertrophic cardiomyopathy; *LA-EF:* left atrial ejection force; *MAA:* mitral annulus area; *MVA:* mitral valve area, *2D:* 2-dimensional; *3D:*3-dimensional, * *P* value< 0.05 between obstructive group and non-obstructive, $ *P* value <0.05 between control group and both HCM groups.

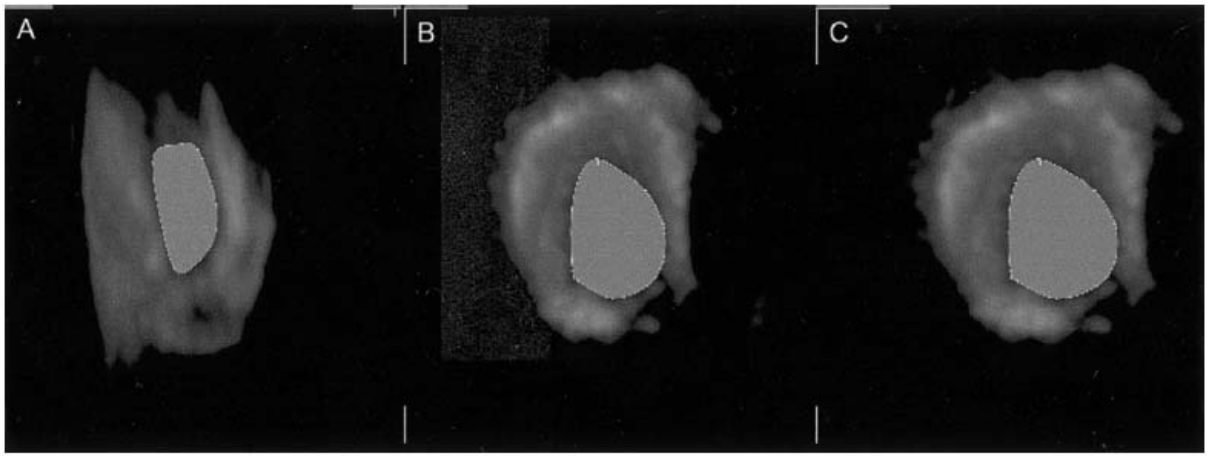

Figure 1 Real-time 3-dimensional (*3D*) echocardiography images of mitral annulus shape as normal (**A**), and in nonobstructive (**B**) and obstructive (**C**) hypertrophic cardiomyopathy.

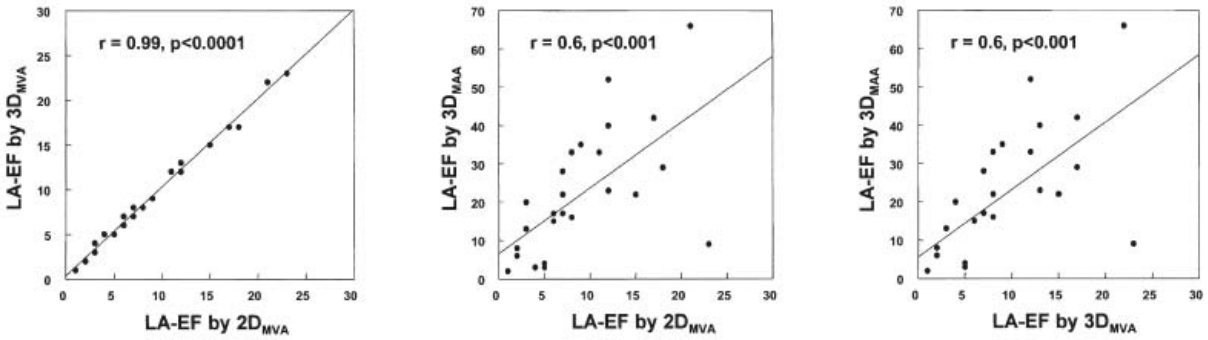

Figure 2 Correlations between left atrial ejection force (LA-EF) by real-time 3-dimensional (3D) imaging using: mitral valve area (MVA) ($LA\text{-}EF_{3D\text{-}MVA}$) and 2-dimensional (2D) echocardiography ($LA\text{-}EF_{2D\text{-}MVA}$) (**A**); mitral annulus area (MAA) ($LA\text{-}EF_{3D\text{-}MAA}$) and $LA\text{-}EF_{2D\text{-}MVA}$ (**B**); and MAA ($LA\text{-}EF_{3D\text{-}MAA}$) and $LA\text{-}EF_{3D\text{-}MVA}$ (**C**).

DISCUSSION

In this study, LA-EF was used as a marker for LA contractile function in HCM. LA-EF by 2DE and RT3DE was higher in patients with HCM compared with control subjects, with the highest value found in obstructive HCM. $LA\text{-}EF_{3D\text{-}MAA}$ calculated by the MAA_{3D}-derived formula in HCM patients was higher than by the MVA-derived formula either by 2DE or RT3DE. This difference was not present in control subjects. As seen in Figure 3, high LA-EF in HCM was correlated with the V, and thus the severity of LV diastolic dysfunction. In our opinion, the clinical implication of this study is the concept that LA-EF is a sensitive indicator for LA work that reflects the severity of LV diastolic dysfunction.

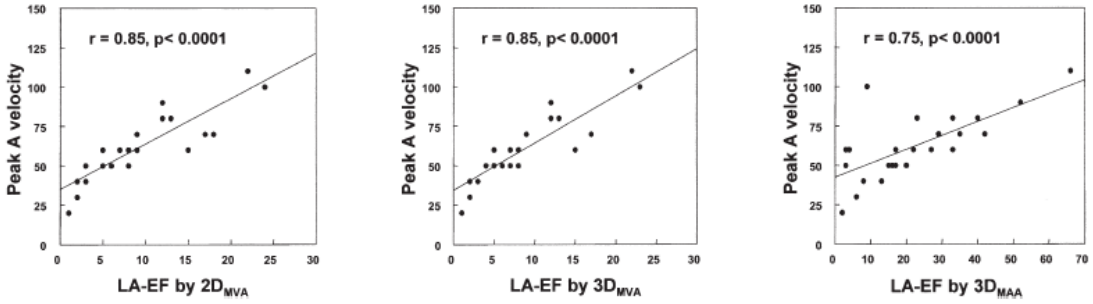

Figure 3 Correlations between left atrial ejection force $(LA\text{-}EF)_{2D\text{-}MVA}$ (**A**), $LA\text{-}EF_{3D\text{-}MVA}$ (**B**), or $LA\text{-}EF_{3D\text{-}MAA}$ (**C**) and peak A velocity.

In this study, RT3DE helped in good visualization of MA in all patients. Tracing of $3D_{MAA}$ was successfully performed with good interobserver agreement. Previous studies describing LA-EF by 2DE used MVA for calculation[12,16,17], whereas in the current study, LA-EF was assessed by RT3DE using $3D_{MVA}$ and $3D_{MAA}$. The values of LA-EF by both techniques regardless of the formula used were well correlated. However, a higher $LA\text{-}EF_{3D\text{-}MAA}$ compared to $LA\text{-}EF_{3D\text{-}MVA}$ and $LA\text{-}EF_{2D\text{-}MVA}$ was found in HCM patients but not in control subjects. This could be explained by overstretching and dilatation of MAA in patients with HCM, [18] which increased the difference between MAA and MVA compared to control subjects. The high $LA\text{-}EF_{3D\text{-}MAA}$ value in patients with HCM is concordant with the concept that LA work increases significantly with higher LA preload [12,17,19]. Our findings are in accordance with Nagueh et al [20] who reported high $LA\text{-}EF_{2D\text{-}MAA}$ in patients with obstructive HCM. The higher value of LA-EF in patients with obstructive HCM compared with non-obstructive HCM may be explained by augmentation of LA contractility because of higher LV resistance. Therefore, successful therapeutic attempts to decrease LVOT gradients such as septal ablation reduced LA-EF indicating reduction of LA workload [20].

CONCLUSION

HCM is associated with high LA-EF indicating a high LA workload especially in obstructive type. For RT3DE, LA-EF should be determined in patients with HCM by MAA-derived formula instead of MVA-derived formula because of MA dilatation. Thus, $LA\text{-}EF_{3D\text{-}MAA}$ is recommended as a better indicator for LA work in HCM and this may help in the clinical assessment and follow up.

REFERENCES

1. Maron BJ, Gardin JM, Flack JM, Gidding SS, Kurosaki TT, Bild DE. Prevalence of hypertrophic cardiomyopathy in a general population of young adults. Echocardiographic analysis of 4111 subjects in the CARDIA Study. Coronary Artery Risk Development in (Young) Adults. *Circulation* 1995;92:785-9.
2. Maron BJ, Gardin JM, Flack JM, Gidding SS, Bild DE. HCM in the general population. *Circulation* 1996;94:588-9.
3. Klues HG, Schiffers A, Maron BJ. Phenotypic spectrum and patterns of left ventricular hypertrophy in hypertrophic cardiomyopathy: morphologic observations and significance as assessed by two-dimensional echocardiography in 600 patients. *J Am Coll Cardiol* 1995;26:1699-708.
4. Obeid AI, Maron BJ. Apical hypertrophic cardiomyopathy developing at a relatively advanced age. *Circulation* 2001;103:1605.
5. Braunwald E, Seidman CE, Sigwart U. Contemporary evaluation and management of hypertrophic cardiomyopathy. *Circulation* 2002;106:1312-6.
6. Spirito P, Seidman CE, McKenna WJ, Maron BJ. The management of hypertrophic cardiomyopathy. *N Engl J Med* 1997;336:775-85.
7. Sanada H, Shimizu M, Kita Y, Sugihara N, Shimizu K, Murakami T, Takeda R, Mifune J. [Left atrial booster pump function in patients with hypertrophic cardiomyopathy and essential hypertension: evaluations based on left atrial pressure-volume relationship]. *J Cardiol* 1992;22:99-106.
8. Michalak E, Michalak JM, Chojnowska L, Ruzyllo W, Hoffman P. [Echocardiographic assessment of left atrial volume and emptying in hypertrophic cardiomyopathy]. *Przegl Lek* 2004;61:729-32.
9. Stefanadis C, Dernellis J, Toutouzas P. A clinical appraisal of left atrial function. *Eur Heart J* 2001;22:22-36.
10. Manning WJ, Silverman DI, Katz SE, Douglas PS. Atrial ejection force: a noninvasive assessment of atrial systolic function. *J Am Coll Cardiol* 1993;22:221-5.
11. Rakowski H, Sasson Z, Wigle ED. Echocardiographic and Doppler assessment of hypertrophic cardiomyopathy. *J Am Soc Echocardiogr* 1988;1:31-47.
12. Hesse B, Schuele SU, Thamilasaran M, Thomas J, Rodriguez L. A rapid method to quantify left atrial contractile function: Doppler tissue imaging of the mitral annulus during atrial systole. *Eur J Echocardiogr* 2004;5:86-92.
13. Spain MG, Smith MD, Grayburn PA, Harlamert EA, DeMaria AN. Quantitative assessment of mitral regurgitation by Doppler color flow imaging: angiographic and hemodynamic correlations. *J Am Coll Cardiol* 1989;13:585-90.
14. Bland JM, Altman DG. Statistical methods for assessing agreement between two methods of clinical measurement. *Lancet* 1986;1:307-10.
15. Khouri SJ, Maly GT, Suh DD, Walsh TE. A practical approach to the echocardiographic evaluation of diastolic function. *J Am Soc Echocardiogr* 2004;17:290-7.
16. Qirko S, Tase M, Lushnjari V, Sinjari T. [Left atrial contractility function in hypertension]. *Arch Mal Coeur Vaiss* 1996;89:1003-7.
17. Qirko S, Goda T, Rroku LI. [Relationship between the force of left atrial ejection to left ventricular function in arterial hypertension]. *Arch Mal Coeur Vaiss* 1999;92:971-4.
18. Flachskampf FA, Chandra S, Gaddipatti A, Levine RA, Weyman AE, Ameling W, Hanrath P, Thomas JD. Analysis of shape and motion of the mitral annulus in subjects with and without cardiomyopathy by echocardiographic 3-dimensional reconstruction. *J Am Soc Echocardiogr* 2000;13:277-87.
19. Stefanadis C, Dernellis J, Lambrou S, Toutouzas P. Left atrial energy in normal subjects, in patients with symptomatic mitral stenosis, and in patients with advanced heart failure. *Am J Cardiol* 1998;82:1220-3.
20. Nagueh SF, Lakkis NM, Middleton KJ, Killip D, Zoghbi WA, Quinones MA, Spencer WH, 3rd. Changes in left ventricular filling and left atrial function six months after nonsurgical septal reduction therapy for hypertrophic obstructive cardiomyopathy. *J Am Coll Cardiol* 1999;34:1123-8.

CHAPTER 13

SUMMARY, CONCLUSION AND FUTURE PERSPECTIVES

Ashraf M. Anwar; MD, MSC

Department of Cardiology, Thoraxcenter,
Erasmus University Medical Center, Rotterdam, The Netherlands
Department of Cardiology, Al-Hussein University Hospital, Al-Azhar University, Cairo, Egypt

Summary

Over the last few years, the introduction of matrix array transducer and advances in computer software analysis technology led to enhancement of real-time three-dimensional echocardiography (RT3DE) to be applied for clinical utility. By this transducer, the entire heart image could be obtained by a pyramidal full-volume acquisition of four cardiac cycles. The development in software made the data off-line analysis faster and easier. Application of RT3DE for diagnosis of many cardiovascular abnormalities has been proven and well validated. RT3DE assessment of LV volumes, function, mass, and testing dyssynchrony is more accurate and reproducible than 2DE and comparable to MRI. RT3DE assessment of valves (especially mitral valve), and congenital septal defects has a good advantage for direct visualization in a surgical view. Time now, RT3DE achieved rapid transition from academic research field limited to selected patient series to the daily routine clinical practice. RT3DE In the course of time RT3DE will be more integrated with 2DE for full and accurate echocardiographic examination. The aim of this thesis was to investigate the feasibility and clinical applicability of RT3DE anatomical and functional assessment of other important cardiac structures little or not studied before.

RT3DE assessment of tricuspid annulus: ***(Chapter 2, 3)***

In both chapters, an actual description of the tricuspid valve annulus morphology was obtained by RT3DE. Its shape was evident as an oval and not completely circular. RT3DE measurement of tricuspid annulus area and diameter is superior to 2DE measurements and comparable to MRI. The ability to study the cyclic changes of the annulus area and diameter during systole and diastole helps in calculation of the annular function. RT3DE functional assessment of the annulus has an important surgical implication and can be used as a marker of right ventricular function.

RT3DE assessment of tricuspid valve: ***(Chapter 4, 5)***

RT3DE was applied for quantitative and qualitative assessment of the normal tricuspid valve. The qualitative assessment included morphologic description of the three leaflets shape, position and their relation to each other and to the surrounding structures. By RT3DE description, the identification of the each leaflet seen by variable 2DE views could be clearly defined. The quantative assessment included measurements of tricuspid valve area, commissural width, tricuspid annular area and diameter. Chapter 4 described the value of RT3DE assessment in rheumatic tricuspid valve stenosis. Through RT3DE enface view, a detailed morphological assessment of mobility, thickness and calcification of all tricuspid valve leaflets was achieved. RT3DE was helpful for assessment of stenosis severity through measurement of valve orifice area, and the three commissural widths. All these information had an impact on the selection of therapeutic strategy.

RT3DE assessment of mitral annulus: ***(Chapter 6, 7)***

Chapter 6 explained the feasibility and reliability of RT3DE for assessment of the true mitral annulus area and diameter. Its shape was seen as D-shaped and not completely circular. MRI measurements of mitral annulus were used as a gold standard to compare between 2DE and RT3DE measurements. It showed underestimation of 2DE while RT3DE was superior to it and comparable to MRI. The accuracy of RT3DE measurements was obtained with good interobserver and intraobserver agreements. Chapter 7 assessed the morphological and functional changes of mitral annulus in both dilated and hypertrophic cardiomyopathy. The annulus increased in size and

became flat due to over stretching in both types. Assessment of mitral annulus function by RT3DE calculation of fractional area changes and fractional shortening showed augmented function in hypertrophic cardiomyopathy and impaired in dilated cardiomyopathy. RT3DE measurements in both types were comparable with MRI measurements with good interobserver agreement.

RT3DE assessment of mitral stenosis: ***(Chapter 8)***

Chapter 8 applied a new proposed RT3DE score for evaluation of mitral valve stenosis before percutaneous mitral valvuloplasty. Through RT3DE enface view, the score assessed each part of the two leaflets separately including mobility, thickness, and calcification. In addition, chordal thickness, mobility and separation are included in the score. The definition of mild, moderate and severe valve affection was settled. Compared to the standard 2DE Wilkins' score, the score has many advantages including simple, less subjective and less interobserver variability. Its application added more valuable information needed before valvuloplasty and could predict the results and complications.

RT3DE assessment of right ventricular outflow tract and pulmonary valve: ***(Chapter 9)***

Chapter 9 applied RT3DE for morphologic description of right ventricular outflow tract and pulmonary valve. Qualitative assessment of outflow tract, pulmonary valve annulus, pulmonary valve, and proximal pulmonary artery was achieved in a considerable number of patients. RT3DE measurements of the outflow tract and pulmonary valve annulus diameter were higher than that obtained by 2DE.

RT3DE assessment of left atrial volume and function: ***(Chapter 10, 11, 12)***

Chapter 10 described the feasibility and reliability of RT3DE for assessment of left atrial volume at three phases of cardiac cycle (maximum volume, minimum volume, and pre-atrial contraction volume). The advantage of RT3DE over 2DE in calculation of left atrial volume is the absence of geometric assumption and thus accuracy in both normal and dilated left atrium. Both active and passive left atrial function could be assessed through the volumetric changes during the cardiac cycle. The logic understanding of left atrial physiology accepts the existence of left atrial Frank-Starling mechanism that evidenced by an increase in left atrial contractility in response to an increase in preload up to a certain point, beyond which the left atrial contractility decreased (Chapter 11). Chapter 12 described the calculation of left atrial ejection force in normals and in patients with hypertrophic cardiomyopathy which provides a physiologic assessment of left atrial systolic function. The RT3DE calculation of ejection force by the annulus area-derived formula showed that hypertrophic cardiomyopathy is associated with higher ejection force than normal, and higher in obstructive type than non-obstructive indicating a higher atrial workload which is logic. The study concluded that ejection force should be determined by the annulus area-derived formula especially in hypertrophic cardiomyopathy instead of valve area-derived formula due to annular dilatation.

Conclusion

1. RT3DE is reliable and feasible technique achieved an accurate assessment (shape, size and function) of both mitral and tricuspid annulus irrespective to the annulus size (normal or dilated) comparable to MRI.
2. RT3DE is helpful in morphologic and functional assessment of the tricuspid valve both normal and stenotic through the measurement of valve area and commissural width.
3. The newly proposed RT3DE score for assessment of mitral valve before percutaneous valvuloplasty is simple, reliable and clinician can depend on it for better prediction of the procedure outcome.
4. RT3DE provided detailed qualitative and quantitative information on the right ventricular outflow tract and pulmonary valve.
5. RT3DE became a standard for volume quantification of both ventricles. With the same principle, left atrial volume quantification was easily obtained by RT3DE.
6. RT3DE study of the left atrial volume through cardiac cycle helped in assessment of active and passive atrial function and described the existence of Frank-Starling mechanism.
7. Calculation of left atrial ejection force by RT3DE annulus area-derived formula is superior than valve area-derived formula especially in condition of increased atrial load e.g. hypertrophic cardiomyopathy.

Future Perspectives

Development and advances in probe technology and software analysis are ongoing. This will improve image quality and analysis that will be impacted on the diagnostic performance and clinical application. One of the major advance is the introduction of broadband monocrystal transducer that will allow high-resolution harmonic imaging with improved cavity delineation due to its better penetration and increased signal to noise ratio. Transesophageal monocrystal matrix transducer will carry good imaging performance. Real-time tissue tagging and tracking for mechanical quantification of the myocardium will help in assessment of myocardial strain in all directions (radial, longitudinal, and circumferential). Development of one transducer capable to do 2DE, RT3DE, color and tissue Doppler examination will help in full assessment within short time. Advances in software analysis can incorporate the 3D data set into digital system.

SAMENVATTING, CONCLUSIE EN TOEKOMSTPERSPECTIEVEN

Folkert J. ten Cate MD, PhD, FESC, FACC[1]
Ashraf M. Anwar; MD, MSC, FESC [1,2]

[1] Afdeling Cardiologie, Thoraxcentrum,
Erasmus Medisch Centrum, Rotterdam, Netherlands
[2] Department of Cardiology, Al-Hussein University Hospital, Al-Azhar University, Cairo, Egypt

Samenvatting

Gedurende de laatste paar jaar heeft de introductie van de matrix transducer en vooruitgang in computer programmatuur geleid tot verbetering van de real-time drie dimensionale echo (RT3DE) voor klinisch gebruik. Met behulp van deze transducer kan het hele hart in beeld worden gebracht door acquisitie van piramidaal volumes van vier hart cycli. De nieuwe ontwikkelingen in programmatuur hebben de analyse sneller en gemakkelijker gemaakt. Toepassingen van RT3DE voor diagnose van vele cardiovasculaire afwijkingen is aangetoond en gevalideerd. RT3DE bepaling van linker kamer volume functie massa en beoordeling van dyssynchrony is meer precies en reproduceerbaar geworden dan 2DE en vergelijkbaar met MRI. RT3DE bepaling van klepafwijkingen (speciaal de mitraalklep) en congenitale afwijkingen kunnen worden getoond in chirurgische doorsneden. Het is dus nu tijd voor RT3DE om een transitie te maken van academische research naar dagelijkse routine praktijk. RT3DE moeten worden geïntegreerd met 2DE voor een volledige echocardiografische onderzoek.

Het doel van dit proefschrift is om de mogelijkheden en klinische toepassingen van RT3DE in zijn anatomische en functionele bepaling van andere belangrijke cardiale structuren zichtbaar te maken.

RT3DE bepaling van de annulus tricuspidalis (Hoofdstuk 2, 3)

In beide hoofdstukken wordt een beschrijving gegeven van de morfologie van tricuspidalis klep annulus welke bepaald werd met RT3DE. De vorm was ovaal en niet geheel circulair. RT3DE bepaling van tricuspidalis annulus oppervlakte en diameter is beter dan de 2DE bepalingen en vergelijkbaar met MRI. De mogelijkheid om de cyclische verandering van de oppervlakke van de annulus en de diameter tijdens de systole en diastole te bepalen helpt in de bepaling van de annulaire functie. RT3DE functionele bepaling van de annulus heeft belangrijke chirurgische implicaties en kan gebruikt worden als onderdeel van rechter kamer functie.

RT3DE bepaling van tricuspidalis klep (Hoofdstuk 4,5)

RT3DE werd gebruikt voor de kwantitatieve en kwalitatieve bepalingen van de normale tricuspidalis klep. De kwalitatieve bepaling hield in een morfologische beschrijving van de drie onderdelen van de klep voor wat betreft zijn vorm, positie en de relatie tot elkaar. Met behulp van RT3DE kan elk klepblad goed gedefinieerd worden. De kwantitatieve bepaling hielp o.a. in bepaling van de tricuspidalis klep oppervlakte, de wijdte van de commissure, de tricuspidalis annulus oppervlakte en diameter. Hoofdstuk 4 beschrijft de waarde van RT3DE in de reumatische tricuspidalis klep stenose door een enface bepaling van de klep.

RT3DE kan een gedetailleerde morfologische bepaling van de beweeglijkheid, dikte en calcificatie van alle klepdeeltjes geven. RT3DE was behulpzaam voor de bepaling van de ernst van de tricuspidalis stenose d.m.v de bepaling van het klep oppervlakte en de drie wijdtes van de commissure. Al deze informatie zou een impact kunnen hebben voor de selectie van een strategie voor een eventuele therapie.

RT3DE bepaling van de mitraalklep annulus (Hoofdstuk 6,7)

In hoofdstuk 6 wordt de mogelijkheid en de betrouwbaarheid van RT3DE bepaling van de echte annulus oppervlakte van de mitralis en zijn diameter getoond. De vorm van de annulus wordt gezien als een zogenaamde D-vorm en is niet compleet circulair. De metingen van de mitraal annulus werden getest met een gouden standaard zoals MRI en er werd vergeleken tussen de 2DE en de 3DE bepalingen. 2DE toont een onderschatting van de meting terwijl 3DE superieur was aan 2DE en vergelijkbaar met MRI. De nauwkeurigheid van RT3DE bepalingen werd bepaald met goede interobserver en intraobserver overeenkomsten. Hoofdstuk 7 bepaalde de morfologische en functionele veranderingen van de mitraal annulus in zowel hypertrofische als gedilateerde cardiomyopathie. De annulus was toegenomen in grootte en werd overrekt in beide types cardiomyopathie. De bepaling van de mitraal klep annulus functie door 3DE voor wat betreft de meting van de veranderingen in oppervlakte en verkorting toonde een toegenomen functie in hypertrofische cardiomyopathie en een afgenomen functie in gedilateerde cardiomyopathie. De bepaling met RT3DE in beide types waren vergelijkbaar met MRI met goede interobserver vergelijking.

RT3DE bepaling mitraal stenose (Hoofdstuk 8)

In hoofdstuk 8 wordt een nieuwe RT3DE score voor de evaluatie van de mitraal klep stenose voor een percutane mitraal klep valvuloplastiek voorgesteld door en enface RT3DE view. De score wordt bepaald door elk van de twee klepdelen te meten en te bepalen voor wat betreft mobiliteit, dikte en calcificatie. Verder werd de dikte van het chorda beweeglijkheid en stand tussen twee chorda in de score geïncludeerd. De definitie van milde, matige en ernstige klepafwijking werd vastgesteld en vergeleken met de standaard 2DE Wilkin's score. De beschreven score had vele voordelen omdat het eenvoudig is, minder subjectief en minder interobserver variabiliteit heeft. De toepassing geeft inzicht in een keuze voor een valvuloplastiek en kan eventueel de resultaten en complicaties voorspellen.

RT3DE bepaling van de rechter ventrikel uitstroombaan en pulmonaal klep (Hoofdstuk 9)

In hoofdstuk 9 wordt de morfologische beschrijving van de rechter ventrikel uitstroombaan en pulmonaal klep met RT3DE beschreven. Er is een een kwalitatieve bepaling van de uitstroombaan, pulmonaal klep annulus, pulmonaal klep zelf en de proximale pulmonale arterie te verkrijgen in een aantal patiënten. De bepalingen van RT3DE van de uitstroombaan en pulmonale klep annulus diameter waren hoger dan in het verleden bepaald met 2DE.

RT3DE bepaling van linker atrium volume en functie (hoofdstuk 10, 11, 12)

In hoofdstuk 10 beschrijven wij de mogelijkheid en betrouwbaarheid van RT3DE voor een bepaling van linker atrium volume in drie fasen van de cardiale cyclus (op het maximale volume, op het kleinste volume en vlak voor de atrium contractie). Het voordeel van RT3DE boven 2DE in bepaling van linker atrium volume is dat wij voor RT3DE echo geen geometrische aannames moeten hebben en dus een grotere betrouwbaarheid van de meting als gedilateerd linker atrium. Zowel de actieve en passieve linker atrium functie kon worden vastgesteld door volumetrische verandering te bepalen gedurende de hartcyclus. Met behulp van deze metingen kan linker atrium fysiologie bepaald worden door gebruik te maken van het Frank-Straling mechanisme voor linker atrium waarbij een vergroot linker atrium contractiliteit wordt gezien in response naar een toename in preload (hoofdstuk 11). In hoofdstuk 12 wordt de bepaling van het linker atrium ejectie

kracht bepaald in normale patiënten en patiënten met hypertrofische cardiomyopathie zodat een fysiologische bepaling van linker atrium systolische functie kan worden verkregen. De RT3DE bepaling van ejectie kracht door de formule afgeleid van de annulus oppervlakte liet zien dat hypertrofische cardiomyopathie is geassocieerd met hogere ejectie kracht dan normaal en hoger in obstructieve dan non-obstructieve patiënten die dus een hogere atriale workload laten zien. Uit de studie wordt geconcludeerd dat ejectie kracht moet worden bepaald door een formule afgeleid van de annulus oppervlakte in hypertrofische cardiomyopathie en niet door een formule afgeleid van klepoppervlakte

Conclusie

1. RT3DE is betrouwbaar en het is goed mogelijk om een accurate bepaling te krijgen van vorm, grootte en functie van zowel mitralis en tricuspidalis annulus onafhankelijk van de vraag of de annulus vergroot of normaal is. Deze gegevens zijn vergelijkbaar met MRI.

2. RT3DE is behulpzaam in de morfologische en functionele bepaling van tricuspidalis klep stenose en normale tricuspidalis klep door de bepaling van klepoppervlakte en de wijdte van de commisuren.
3. De hierbij voorgestelde RT3DE score voor de bepaling van mitraalklep voor een percutane valvuloplastiek is relatief eenvoudig, betrouwbaar en de clinicus kan hierop vertrouwen voor een waarschijnlijk betere voorspelling van de uitkomst van de procedure.
4. RT3DE geeft een gedetailleerde kwalitatieve en kwantitatieve informatie van de rechter ventrikel uitstroombaan en pulmonale klep.
5. RT3DE is standaard geworden voor bepaling van volumes van beide kamers. Met hetzelfde principe kan linker atrium volume gekwantificeerd worden.
6. RT3DE van linker atrium volume door de cardiale cyclus is behulpzaam in de bepaling van actieve en passieve linker atrium functie d.m.v. een Frank-Starling mechanisme.
7. Meting van linker atrium kracht door RT3DE afgeleid van een formule waarbij de annulus oppervlakte wordt gebruikt, is beter dan een formule waarbij de klepoppervlakte wordt gebruikt, met name in hypertrofische cardiomyopathie.

Toekomstperspectieven

De ontwikkeling en voordelen van transducer technologie en programmatuur is nog steeds aan de gang. Daarom wordt verwacht dat beeldkwaliteit en analyse nog sterker wordt verbeterd welke een invloed kan hebben op de diagnostische betrouwbaarheid en klinische applicatie. Op dit ogenblijk wordt gewerkt aan de introductie van een breedband monokristal transducer die hoog resolutie harmonic beeldvorming mogelijk maakt d.m.v. betere penetratie en toename van een signaal ruis verhouding.

Transoesophagale monokristal matrix transducer zullen een goede beeldvorming laten zien. Myocardiale strain in alle richtingen (radiaal, longitudinaal en circumferentieel) kan waarschijnlijk in de toekomst bepaald worden met RT3DE tissue tracking. De RT3DE transducer kan gebruikt worden voor zowel 2DE, RT3DE, kleur en tissue doppler en geeft dus een compleet beeld van hartfunctie in een korte tijd. Deze ontwikkelingen worden nog gesteund door betere software die in alle digitale systemen kan worden verwerkt.

Acknowledgment

I would like to express my thanks and appreciation to my promotor ***Prof. Dr. Maarten L. Simons***, the head of cardiology department for allowing me to get a chance of fellowship and to start the process to defend a PhD thesis

I am particularly indebted to my co-promotor ***Dr. Folkert J. ten Cate***, the chief of echocardiography lab for his encouragement and support that continued throughout my fellowship period at Thoraxcenter and 3 years after. Thanks for his kind scientific and social care

My gratitude to ***Dr. Marcel L. Geleijnse*** for his valuable scientific criticism during reviewing many of my manuscripts that made it more powerful and therefore be published

I would like to convey my deepest appreciation to ***Dr. Osama I Soliman*** for his kind friendship and care to follow many issues after I left the Thoraxcenter. Without his help, many of these issues couldn't be accomplished

Deep thanks to ***Dr. Annemien E. van den Bosch, Mrs. Jackie McGhie and Mr.Wim Vletter*** for their help during the first days of dealing with RT3DE software. I get a lot of experience in data acquisition and analysis by their help.

I would like to thank ***Dr. Youssef F.M. Nosir*** for his brotherhood throughout his guidance, kind care and follow up during and after my stay in Rotterdam. He did a lot to get the chance of fellowship in Thoraxcenter.

Thanks to all staff (doctors, technicians& secretaries) in echocardiography lab that I enjoyed with them a family life during my stay in Thoraxcenter.

My special gratitude to ***Mrs. Kitty Oosterman-van Helmond*** for her kind helps to finalize the paper work and follow the progress of measures in the university.

Great thanks to my colleagues and all staff in the cardiology department, Al-Azhar University especially for ***Prof Dr. Safwat El-Hawarry*** the head of cardiology department and ***Prof Dr. Ali M El-Amin,*** the chief of echocardiography lab.

Finally, I would like to thank my wife Asmaa and children Maryam and Abdullah for their help. I spent a lot of time away from them to finalize my work.

Curriculum Vitae and Publication List

Personal Data:

Name : Ashraf Mohammed Anwar Ali
Date of Birth : o8.08.1969
Religion : Islam
Marital Status : Married
Residence : 25 th Saqr Qurish El-Kanady, Maadi, Cairo, Egypt.
Mailing address : Al-Husein University Hospital, Cardiology Dep.,
Darrasa, Cairo, Egypt.
King Fahd Armed Force Hospital, Cardiology Department
Altahlia Square. Po Box 9862; 21159 Jeddah- KSA
E Mail : ashrafanwar2000@hotmail.com, ashrafanwar42@yahoo.com
Telephone :002-105262774 (Egypt), 00996- 566
Language : Arabic (Excellent)
English (Very Good).

Academic Qualifications

- **1993-** Graduated from Faculty of Medicine, AI-Azhar University with a degree of Very Good with honor.
- **1998-** Granted M.SC Degree in Cardiology from Faculty of Medicine, Al-Azhar University with a degree of Very Good.
- **2002-** Granted MD Degree in Cardiology from Faculty of Medicine, Al-Azhar University
- **2005**- Registered as Consultant Cardiologist in the Egyptain Medical Syndicate

Position Held

- **1994**: House Officer (Rotations in different clinical department) at Al-Azhar University Hospitals.
- **1995**: Resident in Cardiology department at Al-Azhar University Hospitals.
- **1998**: Associated Lecturer in Cardiology Department, Faculty of Medicine, Al-Azhar University.
- **2002**: Lecturer in Cardiology Department, Faculty of Medicine, Al-Azhar University.
- **2003**: Consultant Cardiology in Naser Heart Institute- Ministry of Health and Population for echocardiographic assessment pre-, intra and post-operative cardiac surgery.
- **2003** Consultant Echocardiographer in Health Insurance Clinics- Ministry of Health and Population
- **2004**: Consultant Cardiology in non-invasive Cardiac check up unit (resting and stress ECG and echocardiography, Holter Monitoring and Ambulatory blood pressure Recording) at Al-Giza International Hospital.
- **2004**: Consultant Cardiology in Assalam International Hospital- Maadi- Cairo for outpatient clinic, echocardiographic assessment, and in-patient follow up.

Current Position

- 2002 till now: Lecturer in Cardiology Department, Faculty of Medicine, Al-Azhar University.
- 2006 till now: Senior registrar Cardiology in King Fahd Armed Force hospital – Jeddah. Saudi Arabia
- 2008. Associate Professor in Cardiology Department, Faculty of Medicine, Al-Azhar University.

Scientific Activity

1. Active participant in local cardiology conferences:
    - Annual international meetings of Egyptian Society of Cardiology since 1996 and every year after.
    - Annual meetings of Cardiac Intervention Working Group at 2000, 2001, 2002.
    - Annual meetings of Egyptian Society of Atherosclerosis at 1999 and 2000.

- Annual meetings of Echocardiography working group since 2000 and every year.

2. Attendant in the 18th annual scientific session of the Saudi Heart association held on 2007 at Jeddah (30 CME hours).
3. Attendant in the 15th annual cardiovascular conference held on 2007 at Taif, KSA (18 CME hours).
4. Attendant in the 16th annual cardiovascular conference held on 2008 at Taif, KSA (23 CME hours).
5. Attendant in the 17th annual cardiovascular conference held on 2009 at Taif, KSA (25 CME hours).
5. Attendant in the 7th Jeddah Cardiovascular imaging and Interventions Symposium held on 2007 at Jeddah, KSA (16 CME hours).
6. Attendant in the 8th Jeddah Cardiovascular imaging and Interventions Symposium held on 2008 at Jeddah, KSA (17 CME hours).
7. Attendant in the 10th KFAFH International Cardiac Symposium held on 2008 at Jeddah, KSA (12 CME hours).
8. Attendant in the 7th ICC Cardiovascular Conference held on 2008 at Jeddah, KSA (12 CME hours).

Educational Courses:

1997- Educational Echocardiographic Course (4 days) organized by Egyptian Medical Syndicate and held in Al-Hussein university hospital.
2001- European Course of Heart Failure (2days) organized by European Society of cardiology (Luxur, Egypt) (12 EBAC hours)
2005- Fellowship in Thoraxcenter, Erasmus University, Rotterdam- Netherland: from October 2005 till June 2006.
2006- 10th European Symposium of Ultrasound Contrast Imaging (2days): Rotterdam, The Netherlands (12 EBAC hours).
2006- Cardiology and Vascular Medicine: Update and Perspective (3 days): organized by European Society of cardiology (Rotterdam-The Netherlands) (12 EBAC hours)
2006- First European Course on 3D Echocardiography (2days) Rotterdam, The Netherlands (12 EBAC hours).
2007- Basic Cardiac Life Support (BCLS), Saudi Heart association affiliated to the American Heart Association, Jeddah, Saudi Arabia (4 CME hours)
2007- Advanced Cardiac Life Support (ACLS), Saudi Heart association affiliated to the American Heart Association, Jeddah, Saudi Arabia (12 CME hours)
2008- Echocardiography course during the 7th ICC Cardiovascular Conference held on 2008 at Jeddah, KSA (4 CME hours).

Scientific Award:

- Fellowship in the European Society of Cardiology (since 2009).
- Fellowship in the Egyptian Society of Cardiology (since 2000).
- Fellowship in the Egyptian Echocardiography Working Group
- Scientific Reviewer for the submitted manuscripts in Heart (since 2005)
- Scientific Reviewer for the submitted manuscripts in Cardiology. (since 2005)
- Scientific Reviewer for the submitted manuscripts in Journal of Catheterization and cardiovascular Intervention (since 2006)
- Scientific Reviewer for the submitted manuscripts in European Journal of Echocardiography (since 2008)
- Scientific Reviewer for the submitted manuscripts in British Medical Journal (BMJ) (since 2008)

Publications

Original Articles

1. **Anwar MA**, Nosir Y**,** El-Sayed M. Mitral valvuloplasty by metalic valvulotome: two years clinical and echocardiographic follow up. *Egyptian Heart Journal* 2006;58(1):115-119.
2. **Anwar AM**: Assessment of Mitral Valve Morphology in Mitral Stenosis with a New Real-Time Three-Dimensional Echocardiographic Score. *Egyptian Heart Journal* 2007; 59(1):
3. **Anwar AM**: Long-term follow up of percutaneous mitral commissurotomy by metallic valvulotome. *Egyptian Heart Journal* 2007; 59(1):
4. **Anwar AM**, Geleijnse ML, Soliman OI, Nemes A, Ten Cate FJ. Left Atrial Frank Starling Law Assessed by Real-Time Three-Dimensional Echocardiographic Left Atrial Volume Changes. *Heart*. 2007; 93(11):1393-1397.
5. **Anwar AM**, Soliman OI, Geleijnse ML, Nemes A, Vletter WB, Ten Cate FJ.Assessment of left atrial volume and function by real-time three-dimensional echocardiography. *Int J Cardiol*. 2007
6. **Anwar AM**, Geleijnse ML, Soliman OI, McGhie JS, Nemes A, ten Cate FJ. Evaluation of rheumatic tricuspid valve stenosis by real-time three-dimensional echocardiography. *Heart*. 2007;93(3):363-4.
7. **Anwar AM**, Geleijnse ML, Soliman OI, McGhie JS, Frowijn R, Nemes A, van den Bosch AE, Galema TW, Ten Cate FJ. Assessment of normal tricuspid valve anatomy in adults by real-time three-dimensional echocardiography. *Int J Cardiovasc imaging*.2007; 23(6):717-724.
8. **Anwar AM**, Soliman OI, Nemes A, van Geuns RJ, Geleijnse ML, Ten Cate FJ.Value of assessment of tricuspid annulus: real-time three-dimensional echocardiography and magnetic resonance imaging. *Int J Cardiovasc Imaging*. 2007; 23(6):701-705.
9. **Anwar AM**, Soliman OI, Ten Cate FJ, Nemes A, McGhie JS, Krenning BJ, van Geuns RJ, Galema TW, Geleijnse ML.True mitral annulus diameter is underestimated by two-dimensional echocardiography as evidenced by real-time three-dimensional echocardiography and magnetic resonance imaging. *Int J Cardiovasc Imaging*. 2007; 23(5): 541-7.
10. **Anwar AM**, Soliman O, van den Bosch AE, McGhie JS, Geleijnse ML, ten Cate FJ, Meijboom FJ.Assessment of pulmonary valve and right ventricular outflow tract with real-time three-dimensional echocardiography. *Int J Cardiovasc Imaging*. 2007;23(2):167-75.
11. **Anwar AM**, Soliman O, Geleijnse ML, Michels M, Vletter W, Nemes A, Ten Cate FJ. Assessment of Mitral Annulus Size and Function by Real-Time Three-Dimensional Echocardiography in Cardiomyopathy: Comparison With Magnetic Resonance Imaging. *J Am Soc Echocardiogr 2007*; 20(8): 941-8.
12. **Anwar AM**, Soliman O, Nemes A, Krenning BJ, van Geuns R, Geleijnse ML, Ten Cate

FJ. Assessment of Left Atrial Ejection Force in Hypertrophic Cardiomyopathy Using Real-Time Three-Dimensional Echocardiography. *J Am Soc Echocardiogr 2007;20(6):744-748*

13. **Anwar AM**, Soliman O, Geleijnse ML, Nemes A, Ten Cate FJ. An integrated approach to determine left atrial volume, mass and function in hypertrophic cardiomyopathy by two-dimensional echocardiography. *Int J Cardiovas Imaging* 2007.
14. El-Sayed MA, **Anwar AM**. Comparative study between various methods of percutaneous transvenous mitral commissurotomy (Metallic vavotome, Inoue balloon and double balloon techniques) VID study. Journal of Interventional Cardiology 2000;13(%):357-364.
15. Nemes A, **Anwar AM**, Caliskan K, Soliman OI, van Dalen BM, Geleijnse ML, Ten Cate FJ. Evaluation of left atrial systolic function in noncompaction cardiomyopathy by real-time three-dimensional echocardiography. *Int J Cardiovasc Imaging.* 2007
16. Nemes A, **Anwar AM**, Caliskan K, Soliman OI, van Dalen BM, Geleijnse ML, Ten Cate FJ. Non-compaction cardiomyopathy is associated with mitral annulus enlargeent and functional impairment: A real-tie three-dimensional echocardiographic study. *J Heart Valve Dis* 2008;17:31-35
17. Abu Saif HS, Allam SR, Abu-El-Magd AH, Abdel-Magid AM, **Anwar AM.** Assessment of effects of ductus arteriosus on complications of respiratory distress syndrome in neonates. *Al-Azhar Journal of Pediatrics* 2002;5 (1):183-193.
18. Mostafa M M, **Anwar AM**, Rizk A, Ramzy AA, Gazar A, Kamal E. Effect of thrombolytic therapy on QT dispersion in patients with acute myocardial infarction. *Al-Azhar Medical J* 2005; 34(2):277-282.
19. Soliman OI, Knaapen P, Geleijnse ML, Dijkmans PA, **Anwar AM**, Nemes A, Michels M, Vletter WB, Lammertsma AA, Ten Cate FJ. Assessment of Intra- and Extra-Vascular Mechanisms of Myocardial Perfusion Abnormalities in Obstructive Hypertrophic Cardiomyopathy by Myocardial Contrast Echocardiography. *Heart*. 2007; 93: 1204 - 1212.
20. Nemes A, Caliskan K, Geleijnse ML, Soliman OI, **Anwar AM**, Ten Cate FJ.Alterations in aortic elasticity in noncompaction cardiomyopathy. *Int J Cardiovasc Imaging* 2007
21. Nemes A, Geleijnse ML, Krenning BJ, Soliman OI, **Anwar AM**, Vletter WB, Ten Cate FJ. Usefulness of ultrasound contrast agent to improve image quality during real-time three-dimensional stress echocardiography. *Am J Cardiol*. 2007 15;99(2):275-8.
22. Soliman OI, Theuns DA, Geleijnse ML, **Anwar AM,** Nemes A, Caliskan K, Vletter WB, Jordaens LJ, Cate FJ.Spectral pulsed-wave tissue Doppler imaging lateral-to-septal delay fails to predict clinical or echocardiographic outcome after cardiac resynchronization therapy. *Europace*. 2007;9(2):113-8.
23. Nemes A, Galema TW, Geleijnse ML, Soliman OI, Yap SC, **Anwar AM,** ten Cate FJ.Aortic valve replacement for aortic stenosis is associated with improved aortic distensibility at long-term follow-up. *Am Heart J*. 2007;153(1):147-51.

24. Nemes A, Soliman OI, Geleijnse ML, **Anwar AM**, van der Beek NA, van Doorn PA, Gavaller H, Csajbok E, Ten Cate FJ.Increased aortic stiffness in glycogenosis type 2 (Pompe's disease). *Int J Cardiol*. 2007; 120(1): 138-41.
25. Nemes A, Geleijnse ML, Soliman OI, Anwar AM, Vletter WB, ten Cate FJ.Real-time three-dimensional echocardiography for regional evaluation of aortic stiffness. *Eur J Echocardiogr*. 2007;8(2):161-2.
26. Soliman OI, Krenning BJ, Geleijnse ML, Nemes A, Bosch JG, van Geuns RJ, Kirschbaum SW, **Anwar AM**, Galema TW, Vletter WB, Ten Cate FJ. Quantification of Left Ventricular Volumes and Function in Patients with Cardiomyopathies by Real-time Three-dimensional Echocardiography: A Head-to-Head Comparison Between Two Different Semiautomated Endocardial Border Detection Algorithms.*J Am Soc Echocardiogr 2007;* 20(9): 1042-9.
27. Soliman OI, Theuns DA, Ten Cate FJ, **Anwar AM**, Nemes A, Vletter WB, Jordaens LJ, Geleijnse ML. Baseline predictors of cardiac events after cardiac resynchronization therapy in patients with heart failure secondary to ischemic or nonischemic etiology. *Am J Cardiol* 2007; 100(3): 464-9.
28. Nemes A, Geleijnse ML, Soliman OI, **Anwar AM**, Vletter WB, ten Cate FJ.Real-time three-dimensional echocardiography for regional evaluation of aortic stiffness. *Eur J Echocardiogr*. 2007;8(2):161-2.
29. Soliman OI, Krenning BJ, Geleijnse ML, Nemes A, van Geuns RJ, Baks T, **Anwar AM,** Galema TW, Vletter WB, Ten Cate FJ A Comparison between QLAB and TomTec Full Volume Reconstruction for Real Time Three-Dimensional Echocardiographic Quantification of Left Ventricular Volumes. *Echocardiogr* 2007; 24(9): 967-74.

Case Reports

1. Nemes A, Geleijnse ML, Soliman OI, **Anwar AM**, Vletter WB, ten Cate FJ.Real-time three-dimensional echocardiography for regional evaluation of aortic stiffness. Eur J Echocardiogr. 2007;8(2):161-2.
2. **Anwar AM**, Nosir YF, Ajam A, Mushtaq M, Alaa N, Chamsi-Pasha H. Multivalvular infective endocarditis in a tetralogy of Fallot. Echocardiography 2008;25(1):88-90.
3. **Anwar AM**, Nosir YF, Ajam A, Galal AN, Asjmeg A, Chamsi-Pasha H. Partial anomalous pulmonary venous connection associated with Lutembacher's syndrome. Echocardiography 2008;25(4):436-39.
4. **Anwar AM**, McGhie JS, Meijboom F, Ten Cate FJ Double orifice mitral valve by real-time three-dimensional echocardiography. Eur J Echocardiogr, 2008;9(5):731-732.
5. **Anwar AM**, Attia WM, Nosir YF, El-Amin AM Unusual bileaflet tricuspid valve by real time three-dimensional echocardiography. Echocardiography 2008; 25(5): 534-536.

6. Chamsi-Pasha M AR, **Anwar AM**, Nosir YF, Ajam A, Al-Sibai MA, Chamsi-Pasha H Pseudomyxoma peritonei mimicking right-sided heart failure. Eur J Radiol 2008;67(1):e9-e11
7. Al-Nasser I, **Anwar AM**, Alqiriaqri A, Chamsi-Pasha MAR, Nosir YFM, Ajam A, Chamsi-Pasha H. Bicaval obstruction complicating right atrial tuberculoma: the diagnostic value of cardiovascular MR. JCMR 2008;10:60-62.
8. Chamsi-Pasha MA, **Anwar AM**, Nosir YF, Abukhudair W, Ashmeg A, Chamsi-Pasha H. Right atrial myxoma associated with an atrial septal defect by real-time three-dimensional echocardiography. Eur J Echocardiogr. 2009;10(2):362-364.
9. Chamsi-Pasha MAR, **Anwar AM**, Nosir YF, Chamsi-Pasha H "Hanging by a thread" left ventricular thrombus in an asymptomatic solider. Saudi Med J 2009;30(3):1296-1298.
10. Chamsi-Pasha MA**, Anwar AM**, Al-Nasser I, Nosir YF, Ajam A, Chamsi-Pasha H. Imaging of ventricular septal tumor in an asymptomatic adolescent using multiple modalities. Echocardiography 2009;26(5):581-585
11. **Anwar AM**, Nosir YF, Chamsi-Pasha H. Real-time three-dimensional echocardiographic assessment of inferior vena caval thrombosis. Eur J Echocardiogr. 2009;

Abstracts

1. **Anwar AM**, Kholief HA. Acute left ventricular functional changes after successful mitral valvuloplasty. 28th International Congress Golden Jubilee of the Egyptian Society of Cardiology (Cairo 19-23 2001).
2. **Anwar AM**, Allam A. Comparison of residual ischemia following PCI or CABG as detected by stress myocardial perfusion imaging. 28th International Congress Golden Jubilee of the Egyptian Society of Cardiology (Cairo 19-23 2001).
3. **Anwar AM**, Allam A. Value of stress ECG for detection of significant ischemia post revascularization compared with myocardial perfusion imaging. 4th International conference of Nuclear Cardiology (2002)
4. **Anwar AM**, Soliman IIO, van den Bosch AE, McGhie JS, Geleijnse ML, ten Cate FJ, Meijboom FJ. Assessment of pulmonary valve and right ventricular outflow tract by real-time three-dimensional echocardiography. 4th annual European Paediatric Cardiology meeting (Bazil. Switzerland 23rd – 26th June 2006):
5. **Anwar AM**, Soliman IIO, Geleijnse ML, Ten Cate FJ. Starling law and left atrium: Real-time three-dimensional echocardiography. 17th Annual Scientific Sessions of American Society of Echocardiography: (Baltimore 3rd –7th July 2006) *J Am Soc Echocardiogr* 2006;19(5):631
6. **Anwar AM**, Soliman IIO, Mcghie J, Geleijnse ML, Nemes A, Ten Cate FJ. Left atrial volume and function assessed by real-time three-dimensional transthoracic echocardiography. 17th Annual Scientific Sessions of American Society of Echocardiography: (Baltimore 3rd –7th July 2006).*J Am Soc Echocardiogr* 2006;19(5):609

7. **Anwar AM**, Soliman IIO, McGhie JS, ten Cate FJ. Double orifice mitral valve by real-time three-dimensional echocardiography. 17th Annual Scientific Sessions of American Society of Echocardiography: (Baltimore 3rd –7th July 2006).
8. **Anwar AM**, Soliman IIO, Geleijnse ML, ten Cate FJ. Effects of cardiac resynchronization therapy on cardiac remodeling. Annual Scientific Sessions of American Heart Failure Society 2006. *J Card Fail*.12(6):Suppl 1:S65.
9. **Anwar AM**, Soliman IIO, Geleijnse ML, McGhie JS, Nemes A, ten Cate FJ. Assessment of tricuspid valve annulus size and shape with real-time three-dimensional echocardiography. XXVIII Congress of the European Society of Cardiology. (2006). *Eur Heart J* 2006;27 Suppl 1:707
10. **Anwar AM**, Soliman IIO, Nemes A, Geleijnse ML, Vletter WB, ten Cate FJ. Assessment of left atrial function; A real-time 3D Echocardiography study. 10th Euro Echo meeting (6-9 December 2006, Prague). *Eur J Echocardiogr*. 7;Suppl 1:S97-S98.
11. **Anwar AM**, Allam A, Shawky I, Kholiefy A, Abdel-Wahab M. Al-Azhar score: a new treadmill scoring system to diagnose coronary artery disease. 8th International conference of Nuclear Cardiology (May 2007, Prague).
12. El-Sayed MA, **Anwar AM,** El-Hawwary SA, El-Amin AM. Comparative study between various methods of percutaneous transvenous mitral commissurotomy (Metallic vavotome, Inoue balloon and double balloon techniques) VID study. XXIInd Congress of the European Society of Cardiology. (Amsterdam-The Netherlands 26-30 August 2000).
13. Soliman OI, Geleijnse ML, **Anwar AM**, Nemes A, Vletter WB, ten Cate FJ.Adenosine Myocardial Contrast Echocardiography versus Positrone Emission Tomography in Assessment of Microvascular Dysfunction in hypertrophic Cardiomyopathy Patients**.** 17th Annual Scientific Sessions of American Society of Echocardiography: (Baltimore 3rd –7th July 2006), *J Am Soc Echocardiogr* 2006;19(5):668.
14. Nemes A**,** Geleijnse ML Vletter WB**,** Soliman IIO, **Anwar AM**, Krenning B, ten Cate FJ.The use of an ultrasound contrast agent is mandatory during real-time 3D stress echocardiography. XXVIII Congress of the European Society of Cardiology (2006). *Eur Heart J*2006;27 Suppl 1:714
15. Soliman IIO, knaapen P, Geleijnse ML **Anwar AM**, Nemes A**,** ten Cate FJ. Adenosine myocardial contrast echocardiography versuspositron emission tomography in assessment of microvascular dysfunction in hypertrophic cardiomyopathy patients. XXVIII Congress of the European Society of Cardiology. (2006). *Eur Heart J*2006;27 Suppl 1:847
16. Soliman IIO, Geleijnse ML **Anwar AM**, Nemes A**,** Vletter WB, ten Cate FJ. Reproducibility of real-time three-dimensional echocardiographic quantification of left ventricular volume using two commercially available software system. XXVIII Congress of the European Society of Cardiology. (2006). *Eur Heart J*2006;27 Suppl 1:858.
17. Soliman IIO, Geleijnse ML, **Anwar AM**, Nemes A, Vletter WB, ten Cate FJ. Regional left ventricular systolic function in hypertrophic cardiomyopathy evaluated by real-time three-

dimensional echocardiography. 10th Euro Echo meeting ((6-9 December 2006, Prague). *Eur J Echocardiogr*. 7;Suppl 1:S213.

18. Soliman IIO, Geleijnse ML, **Anwar AM**, Nemes A, Vletter WB, ten Cate FJ. Regional left ventricular systolic function in dilated cardiomyopathy: A real-time three-dimensional echocardiographic study. 10th Euro Echo meeting ((6-9 December 2006, Prague). *Eur J Echocardiogr*. 7;Suppl 1:S97.
19. Nemes A , Galema TW, Geleijnse ML, Soliman IIO**, Anwar AM**, Yap SC, ten Cate FJ. Aortic valve replacement for aortic stenosis is associated with improved aortic distensibility at long-term follow up. 10th Euro Echo meeting ((6-9 December 2006, Prague). *Eur J Echocardiogr*. 7;Suppl 1:S116.
20. Soliman IIO, Geleijnse ML, **Anwar AM**, Nemes A, Vletter WB, ten Cate FJ. Early echocardiographic predictors of long-term outcome after cardiac resynchronization therapy by combined systolic and diastolic parameters (Role of Tei index and E/e ratio). 10th Euro Echo meeting (6-9 December 2006, Prague). *Eur J Echocardiogr*. 7;Suppl 1:S8.
21. Soliman IIO, krenning BJ, Geleijnse ML, Nemes, A **Anwar AM**, Van Geuns R-J, Kirschbaum SW, Vletter WB, Galema TW, ten Cate FJ. Accuracy of endocardial border tracking algorithms for real-time three-dimensional echocardiographic quantification of left ventricular volumes. XXIX Congress of the European Society of Cardiology. (2007). *Eur Heart J* 2007;28 Suppl 1:488.